



**Preparation of Polysulfone and Polyethylene Membrane and  
Surface Modification by Plasma and UV Radiation for  
Oxygen/Nitrogen and Carbon dioxide/Methane  
Gas Separation.**

**Sutthisa Konruang**

**A Thesis Submitted in Fulfillment of the Requirements for the  
Degree of Doctor of Philosophy in Physics**

**Prince of Songkla University**

**2014**

**Copyright of Prince of Songkla University**

**Thesis Title** Preparation of Polysulfone and Polyethylene Membrane and Surface Modification by Plasma and UV Radiation for Oxygen/Nitrogen and Carbon dioxide/Methane Gas Separation.

**Author** Miss Sutthisa Konruang

**Major Program** Physics

---

**Major Advisor :**

.....  
 (Assoc. Prof. Dr. Thawat Chittrakarn)

**Examining Committee :**

.....Chairperson  
 (Assoc. Prof. Dr. Poonpong Boonbrahm)

**Co-advisor :**

.....  
 (Assoc. Prof. Dr. Pikul Wanichapichart)

.....  
 (Assoc. Prof. Dr. Thawat Chittrakarn)

.....  
 (Dr. Suksawat Sirijarukul)

.....  
 (Dr. Suksawat Sirijarukul)

.....  
 (Assoc. Prof. Dr. Wirote Youravong)

The Graduate School, Prince of Songkla University, has approved this thesis as fulfillment of the requirements for the Phd of Science Degree in Physics

.....  
 (Assoc. Prof. Dr. Teerapol Srichana)

Dean of Graduate School

This is to certify that work here submitted is the result of the candidate's own investigation. Due acknowledgement has been made of any assistance received.

.....Signature

(Assoc. Prof. Dr. Thawat Chittrakarn)

Major Advisor

.....Signature

(Miss Sutthisa Konruang)

Candidate

I hereby certify that this work has not been accepted in substance for any degree, and is not being currently submitted in candidature for any degree.

.....Signature

(Miss Sutthisa Konruang)

Candidate

ชื่อวิทยานิพนธ์	การเตรียมเยื่อพอลิเมอร์พอลิซัลโฟนและพอลิเอทิลีน และการปรับปรุงผิวด้วยเทคนิคทางพลาสมาและรังสีอัลตราไวโอเลตสำหรับการแยกแก๊สออกซิเจน/ไนโตรเจน และ คาร์บอนไดออกไซด์/มีเทน
ผู้เขียน	นางสาวสุทธิษา ก้อนเรือง
สาขาวิชา	ฟิสิกส์
ปีการศึกษา	2552

### บทคัดย่อ

การทดลองนี้ได้เตรียมแผ่นกรองจากพอลิซัลโฟนและพอลิเอทิลีนด้วยเทคนิคการเปลี่ยนเฟส และการกัดรอยทางนิวเคลียร์ ตามลำดับ จากนั้นได้ทำการปรับปรุงผิวของแผ่นกรองด้วยรังสียูวี และพลาสมาของแก๊สอาร์กอน เพื่อศึกษาผลของการปรับปรุงผิวต่อสมบัติในการซึมผ่านและการแยกแก๊สของเมมเบรน โดยใช้แก๊สออกซิเจน ไนโตรเจน คาร์บอนไดออกไซด์ และ มีเทน กรณีของแผ่นกรองพอลิซัลโฟน พบว่าการปรับปรุงผิวของแผ่นกรองด้วยรังสียูวี และพลาสมาของแก๊สอาร์กอนให้ผลการคล้ายกัน คือค่าการซึมผ่านของออกซิเจนลดลง ขณะที่ค่าการซึมผ่านของไนโตรเจน คาร์บอนไดออกไซด์ และมีเทน เพิ่มขึ้น เนื่องจากการปรับปรุงผิวทำให้เกิดหมู่ฟังก์ชันที่มีขั้ว เช่น คาร์บอนิล และไฮดรอกซิลบนผิวแผ่นกรอง หมู่ฟังก์ชันที่มีขั้วเหล่านี้ทำปฏิกิริยากับโมเลกุลของแก๊สที่มีขั้วได้ดีเนื่องจากเกิดปฏิกิริยาสองขั้ว-ขั้ว ระหว่างโมเมนต์สองขั้วของเมมเบรนและโมเมนต์ขั้วของแก๊ส ดังนั้นไนโตรเจนและมีเทน ซึ่งมีค่าสภาพการเกิดขั้วได้สูง และ คาร์บอนไดออกไซด์ซึ่งมีทั้งค่าสภาพการเกิดขั้วได้และค่าโมเมนต์ขั้วสูง จึงผ่านได้แผ่นกรองได้ดีกว่า แก๊สออกซิเจนที่มีค่าสภาพการเกิดขั้วได้และค่าโมเมนต์ขั้วต่ำ. ส่งผลให้ค่าการเลือกของ  $O_2/N_2$  ลดลง และ  $CO_2/CH_4$  เพิ่มขึ้น สำหรับแผ่นกรองพอลิเอทิลีนพบว่าการปรับปรุงผิวด้วยพลาสมาของแก๊สอาร์กอนมีผลต่อสมบัติที่ผิวของแผ่นกรองมากกว่ารังสียูวี จากการศึกษาผลของเงื่อนไขในการกักขายรอยพบว่า การซึมผ่านของแก๊สทั้งสี่ชนิดเพิ่มขึ้นเมื่อความเข้มข้นของสารละลาย, เวลา และอุณหภูมิที่ใช้ในการกักขายรอยเพิ่มขึ้น แต่การปรับปรุงผิวด้วยพลาสมาไม่มีผลอย่างมีนัยสำคัญต่อการซึมผ่านของแก๊ส ซึ่งแสดงว่าความมีขั้วของแก๊สและหมู่ฟังก์ชันที่มีขั้วของเมมเบรนไม่ส่งผลต่อการซึมผ่านของแก๊ส แต่การซึมผ่านของแก๊สนั้นเป็นผลจากความดันและขนาดโมเลกุลของแก๊สแต่ละชนิด นอกจากนี้ยังพบว่าค่าการเลือกของ  $O_2/N_2$  และ  $CO_2/CH_4$  ลดลงเมื่อความเข้มข้นของสารละลาย และเวลาที่ใช้ในการกักขายรอยเพิ่มขึ้น ขณะที่อุณหภูมิที่ใช้ในการกักขายรอยไม่มีผลต่อค่าการเลือกของแก๊ส

**Thesis Title** Preparation of Polysulfone and Polyethylene Membrane and Surface Modification by Plasma and UV Radiation for Oxygen/Nitrogen and Carbon dioxide/Methane Gas Separation.

**Author** Miss Sutthisa Konruang

**Major Program** Physics

**Academic Year** 2009

### Abstract

Polysulfone and polyethylene membranes were prepared by phase inversion and nuclear track etching method, respectively. The effect of surface modification by UV irradiation and Ar plasma treatment on gas separation property of membrane was studied. Permeability and selectivity of gases including O<sub>2</sub>, N<sub>2</sub>, CO<sub>2</sub> and CH<sub>4</sub> were examined. For polysulfone membranes, the similar results were obtained by UV irradiation and Ar plasma treatment. Compared with untreated membranes, O<sub>2</sub> permeation decreased while permeation of N<sub>2</sub>, CH<sub>4</sub> and CO<sub>2</sub> was increased. Polar functional groups such as carbonyl and hydroxyl were introduced on the surface of hydrophobic PSF membrane by UV irradiation. These polar functional groups have an affinity for polar gas due to dipole–quadrupole interactions. Therefore, N<sub>2</sub> and CH<sub>4</sub> which high polarizability and CO<sub>2</sub> which high polarizability and high quadrupole moment leads to more permeation. The smaller permeation of O<sub>2</sub> which low polarizability and low quadrupole moment was obtained. This lead to O<sub>2</sub>/N<sub>2</sub> selectivity decreases while the CO<sub>2</sub>/CH<sub>4</sub> selectivity increases after UV irradiation and Ar plasma treatment. For polyethylene membranes, Ar plasma treatment more affected surface property of PE while UV irradiation lightly affects. The effect of conditions for chemical processes was also studied. The results shown that the gases permeance of O<sub>2</sub>, N<sub>2</sub>, CO<sub>2</sub> and CH<sub>4</sub> increased with increasing concentration of etchant, etching time and etching temperature. However, Ar plasma treatment did not have any effect on the gases permeance. This indicated an affinity of polar gas and polar functional groups of membranes were not present. Therefore, the gas permeation caused by the different of molecular sizes of gases and pressure. Moreover, the O<sub>2</sub>/N<sub>2</sub> and CO<sub>2</sub>/CH<sub>4</sub> selectivity decreased when concentration of

etchant and etching time increased. For etching temperature, membranes cannot separate these gases.

## Acknowledgement

I wish to express special thanks to my advisors, Associate Professor Dr. Thawat Chittrakarn, Associate Professor Dr. Pikul. Wanichapichart and Dr. Suksawat Sirijarukul, who provides the guidance and fruitful discussion throughout the course of this work.

I would like to express my thanks to Associate Professor Dr. Wirote Youravong and Associate Professor Dr. Poonpong Boonbrahm, the thesis committee, for providing useful comments and suggestions during the thesis examinations.

I would like to express my thanks to the National Research University Project of Thailand's Office of the Higher Education Commission for financial support.

I would like to express my thanks to the Thailand Center of Excellence in Physics and membrane science and technology research center for the use of the equipment facilities.

I would like to express my thanks to Wichian Ratanatongchai for his valuable guidance and helpful throughout this research. I would like to express my thanks to the Office of Atomic Energy for Peace Thailand for the use of the equipment facilities.

I would like to thank Ruen Tong Jarean Service Limited Partnership for supporting polyethylene resin. I would also like to thank Mr. Chalad Yueanyao who developed plasma system and helped me in the part of plasma treatment.

Finally, I would like to thank my family and my friend for their contributed support and encouragement throughout this entire research work.



## Contents

	<b>Page</b>
Abstract (Thai)	v
Abstract (English)	vi
Acknowledgement	viii
Contents	ix
List of Tables	x
List of Figures	xi
List of Papers and Proceedings	xvi
Reprints were made with permission from the submitted manuscript	xvii
Chapter 1 Introduction	1
Chapter 2 Theory and literature reviews	4
Chapter 3 Experimental	28
Chapter 4 Result and Discussion	36
Chapter 5 Conclusion	80
References	83
Appendix	87
Vitae	119

## List of Tables

<b>Tables</b>		<b>Page</b>
Table 2.1	Test of the fissionability of four nuclides.	16
Table 2.2	A comparison of structural, physical, and electronic parameters of gas molecules.	27
Table 2.3	Some polar groups of importance attraction.	27
Table 4.1	The compositions of polymer solutions.	37
Table 4.2	The composition of PSF membranes according to the PSF content.	40
Table 4.3	The thicknesses of the skin layers.	42

## List of Figures

<b>Figure</b>		<b>Page</b>
Figure 2.1	Schematic diagram of the basic membrane gas separation process.	5
Figure 2.2	Schematic diagrams of asymmetric membranes (a) and polysulfone asymmetric membrane prepared by phase inversion method (b).	6
Figure 2.3	Molecular transport through membranes can be described by a flow through permanent pores (a) or by the solution-diffusion mechanism (b).	6
Figure 2.4	Separation of methane and carbon dioxide from gas mixtures and pure gas with cellulose acetate membranes.	9
Figure 2.5	Diagram of the prepare track-etch membranes; Step 1: The thin film is irradiated by particles in a nuclear reactor. Step 2: The latent tracks were etched into uniform, cylindrical pores.	12
Figure 2.6	Nuclepore (polycarbonate) nucleation track membrane.	13
Figure 2.7	Schematic diagram of etched pore geometry.	14
Figure 2.8	The stage of typical fission process, according to the collective model of Bohr and Wheeler.	15
Figure 2.9	The potential energy at various stages in the fission process.	16
Figure 2.10	The distribution by mass number of the fission fragment that were found when many fission events of $^{235}\text{U}$ were examined.	17
Figure 2.11	The ion explosion spike mechanism for track formation in inorganic solids.	18

## List of Figures (Cont.)

<b>Figure</b>		<b>Page</b>
Figure 2.12	Chain scissions that can be induced by UV irradiation of polysulfone.	22
Figure 2.13	The locations for oxidation on the polysulfone backbone by plasma treatment.	24
Figure 3.1	Uranium screen composed of Ammonium diurate $[(\text{NH}_4)_2\text{U}_2\text{O}_7]$ .	30
Figure 3.2	The particle discriminators limit the angle of incident which fission fragments strike the thin PE film.	31
Figure 3.3	Schematic diagram of latent track in the PE film for using the particle discriminator at thickness 5 mm.	31
Figure 3.4	Position of thermal column at the nuclear reactor.	31
Figure 3.5	UV ray source (VILBER LOURMAT, VI-215.MC).	32
Figure 3.6	Plasma systems develop by Mr. Chalad Yueanyao.	33
Figure 3.7	Gas membrane permeation testing unit. (1) Gas and pressure gauge (2) Feed gas (3) Membrane cell (4) Retentate (5) Bubble flow meter (6) Permeate.	34
Figure 4.1	SEM micrographs of the surface (left) and the cross-sections (right) of the membranes prepared from 20% PSF; (a) 20% PSF: 80% DMF, (b) 20% PSF: 40% DMF: 40% DMAC and (c) 20% PSF: 80% DMAC.	38
Figure 4.2	SEM micrographs of surface (a) and cross-sections (b) of asymmetric membranes prepared from polymer solution consist of 20% PSF, 60% DMAC and 20% AC.	39
Figure 4.3	SEM micrographs of the membranes cross-section prepared by different polymer concentrations; (a) PSF 19%, (b) PSF 22% and (c) PSF 25%; (1) $\times 1,000$ and (2) $\times 5,000$ .	41

### List of Figures (Cont.)

<b>Figure</b>		<b>Page</b>
Figure 4.4	The dielectric property of PSF membranes.	42
Figure 4.5	Comparing water contact angles of PSF membranes irradiation by 254 and 312 nm UV ray wavelengths.	43
Figure 4.6	Variation of water contact angles on the treated membranes by the UV ray with 312 nm wavelength vs. storage time.	44
Figure 4.7	FTIR spectra of the untreated and the treated membrane by two UV ray wavelengths, 254 and 312 nm for 3 membranes; (a) PSF 19%, (b) PSF 22% and (c) PSF 25%.	47
Figure 4.8	Surface free energy of UV-ray irradiation polysulfone membrane with the increase in polymer concentration; (a) surface free energy, (b) polar component and (c) dispersive component.	48
Figure 4.9	AFM images of untreated (a) and treated membranes (b) by UV ray.	49
Figure 4.10	Comparison of O <sub>2</sub> (a), N <sub>2</sub> (b), CO <sub>2</sub> (c), and CH <sub>4</sub> (d) permeation through the untreated and treated membrane by UV ray.	53
Figure 4.11	Selectivity of the untreated and treated membrane by UV ray for O <sub>2</sub> /N <sub>2</sub> (a) and CO <sub>2</sub> /CH <sub>4</sub> (b).	54
Figure 4.12	Comparison of FTIR spectra of the untreated and the treated membrane by UV ray; (a) PSF 19%, (b) PSF 22% and (c) PSF 25%.	56
Figure 4.13	Water contact angles of the treated PSF membranes by Ar plasma treatment for 1-20 min.	58

## List of Figures (Cont.)

<b>Figure</b>		<b>Page</b>
Figure 4.14	The water contact angle as a function of the storage time for the PSF19% (a), PSF22% (b) and PSF25% (c) modified by Ar plasma for 1-20 min.	59
Figure 4.15	Comparison of O <sub>2</sub> (a), N <sub>2</sub> (b), CO <sub>2</sub> (c), and CH <sub>4</sub> (d) permeation through the untreated and treated membrane by UV ray.	62
Figure 4.16	Selectivity of the untreated and treated membrane by UV ray for O <sub>2</sub> /N <sub>2</sub> (a) and CO <sub>2</sub> /CH <sub>4</sub> (b).	63
Figure 4.17	SEM micrographs of the PE film; (a) surface and (b) cross-section.	64
Figure 4.18	Water contact angles of the untreated and the treated film by the UV irradiation with 312 nm wavelength for 3-24 hr.	65
Figure 4.19	Water contact angles of the PE file treated by Ar plasma for 1-20 min.	66
Figure 4.20	Water contact angle as a function of the storage time for the PE film treated by Ar plasma for 1-20 min.	66
Figure 4.21	FTIR spectra of PE films in the range from 600 cm <sup>-1</sup> to 4000 cm <sup>-1</sup>	68
Figure 4.22	FTIR spectra of PE films in the range from 3100 cm <sup>-1</sup> to 3500 cm <sup>-1</sup> (a) and 1600 cm <sup>-1</sup> to 1700 cm <sup>-1</sup> (b).	68
Figure 4.23	Graph of permeation of O <sub>2</sub> (a), N <sub>2</sub> (b), CO <sub>2</sub> (c), and CH <sub>4</sub> (d) vs. concentration of etchant for the untreated and treated membrane by Ar plasma.	72
Figure 4.24	Graph of permeation of O <sub>2</sub> (a), N <sub>2</sub> (b), CO <sub>2</sub> (c), and CH <sub>4</sub> (d) vs. etching time for the untreated and treated membrane by Ar plasma.	74

## List of Figures (Cont.)

<b>Figure</b>		<b>Page</b>
Figure 4.25	Graph of permeation of O <sub>2</sub> (a), N <sub>2</sub> (b), CO <sub>2</sub> (c), and CH <sub>4</sub> (d) vs. etching temperature for the untreated and treated membrane by Ar plasma.	76
Figure 4.26	Graph of selectivity vs. concentration of etchant for the untreated and treated membrane by Ar plasma; (a) O <sub>2</sub> /N <sub>2</sub> and (b) CO <sub>2</sub> /CH <sub>4</sub> .	77
Figure 4.27	Graph of selectivity vs. etching time for the untreated and treated membrane by Ar plasma; (a) O <sub>2</sub> /N <sub>2</sub> and (b) CO <sub>2</sub> /CH <sub>4</sub> .	76
Figure 4.28	Graph of selectivity vs. etching temperature for the untreated and treated membrane by Ar plasma; (a) O <sub>2</sub> /N <sub>2</sub> and (b) CO <sub>2</sub> /CH <sub>4</sub> .	79

# Chapter 1

## Introduction

### 1.1 Background

Currently, membrane technology have been used in various applications, including metal industries for metal recovery and pollution control, food and biotechnology industries for separation and purification, chemical process industries for organic material separation, gas separation and recycle chemicals, and medical industries such as artificial organs and blood fractionation [1, 2]. Six major membrane processes used in these application are microfiltration, ultrafiltration, nanofiltration and reverse osmosis, electro dialysis, gas separation and pervaporation [3]. Membranes gas separation is a relatively new technology and has many advantages, including low capital investment, ease of operation, installation and scaling, good weight and space efficiency, minimal associated hardware and utility requirements, no moving parts, flexibility, low environmental impact and reliability [4]. Generally, the processes can be operated under normal conditions without the phase change, which requires a lot of energy. Therefore, membrane technology can reduce energy consumption and costs of separation processes [1, 5].

Nowadays, gas separation membranes are widely used for  $O_2/N_2$  and  $CO_2/CH_4$  separation [3, 5]. Oxygen and nitrogen are the primary components of the air - 21% oxygen and 78% nitrogen, having abundant supply in the atmosphere. The nitrogen applications for production the blankets for safety use and controlled atmosphere and transportation for the preservation of perishable foods. The majorities of membrane applications for oxygen enrichment are for medical oxygen productions and the improvement of industrial combustion efficiency [6]. Generally, increasing concentration of carbon dioxide ( $CO_2$ ) in the atmosphere is a major contributor to the global warming. Not only being released from vehicles,  $CO_2$  is also commonly found in natural gas streams, biogas, flue gas from fossil fuel combustion, and product of coal gasification [7].  $CO_2$  is classified as an acid gas, similar to  $H_2S$  and  $SO_2$ . Pipeline specifications for natural gas usually require  $CO_2$  concentrations below 2%. The



separation of CO<sub>2</sub> from CH<sub>4</sub> is important in many industrial processes such as natural gas processing, biogas upgrading, oil recovery enhancement and landfill gas purification [7-9]. CO<sub>2</sub> is removed from the gas streams before compressing and delivering. Since CO<sub>2</sub> reduces the calorific value and makes the gas stream to become acidic and corrosive, this then reduces gas compression [1, 7, 9]. Gas separation processes by membranes show more advantage in capital cost and power consumption in comparison with traditional processes such as adsorption or cryogenics [2]. Therefore, gas separation membranes are considered for CO<sub>2</sub>/CH<sub>4</sub> and O<sub>2</sub>/N<sub>2</sub> separations.

There have been several studies conducted due to the lack of membranes with high permeability and high selectivity in membrane-based gas separation processes [3]. However, despite a lot of new polymers developed, only a few polymeric membranes are commercially available [10]. Thus, the surface modification of available membranes has gained much attention, and various modification methods have been reported, including plasma treatment [11, 12], UV-ray irradiation [13, 14], ozone treatment [15] and gamma-ray irradiation [16, 17]. Among these, plasma treatment and UV-ray irradiations have been widely studied as a simple, versatile, and relatively cheap means for modifying the surface properties of polymer membranes [10, 18]. The plasma processes can alter the physico-chemical properties of the polymer surface. It improves polymer wettability, permeability, conductivity, adhesion or biocompatibility [19]. UV irradiation causes crosslinking and chain scission of polymeric membrane. These processes lead to shaping the transport properties of the modified membrane. In addition, UV irradiation of the membrane is usually conducted in the presence of hydrophilic monomers [20].

In this study, polysulfone and polyethylene membrane are prepared with phase inversion and nuclear-tracked etching technique, respectively. Membrane surface are modified by plasma treatment and UV-ray irradiation, in order to investigate its effects on CO<sub>2</sub>/CH<sub>4</sub> and O<sub>2</sub>/N<sub>2</sub> separations.

## **1.2 Objectives of research**

1. To prepare polysulfone and polyethylene membrane by phase inversion and nuclear track etching technique, respectively.
2. To instigated the membranes selectivity of  $O_2/N_2$  and  $CO_2/CH_4$
3. To modified membrane surface by UV-ray irradiation and plasma treatment.

## **Chapter 2**

### **Theory and literature reviews**

There are many processes for gas separation such as absorption into a liquid, adsorption on a solid, chemical conversion to another compound, condensation and permeation through a membrane. Among these processes, membranes separation processes has certain advantages over other methods because it can be operated under normal conditions without the phase change, Therefore, energy consumption and costs of separation processes were reduced. In addition, the membrane separation process is based on the mass transfer rate through the membrane, not the phase equilibrium and the mechanical separation. Therefore, the additive materials such as the extractor and the adsorber which as the potential pollutants are not required. So this process is environmental friendly [1, 4, 5].

#### **2.1 Membrane gas separation process**

Membrane gas separation process is based on the difference in rates of permeation through a thin membrane barrier. The rate of permeation for each component dependent on the characteristics of the component, the characteristics of the membrane, and the partial pressure differential of the gaseous component across the membrane. When membrane surface were forced with pressure, the gas dissolved in the polymer to a higher concentration at higher pressure side. Then the gas diffuses through the other side of membrane. This process is driven by concentration and pressure gradient. The basic process of membrane gas separation is illustrated in Figure 2.1.[4, 21, 22]

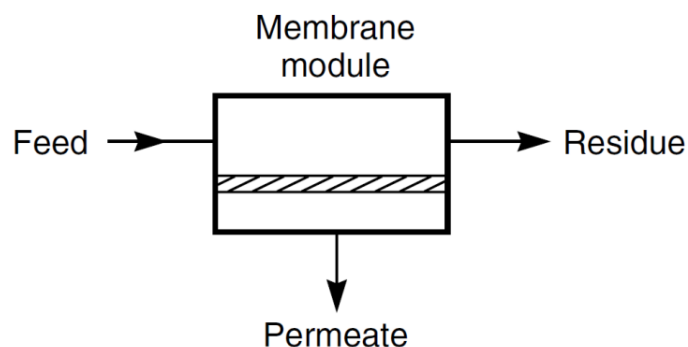


**Figure 2.1** Schematic diagram of the basic membrane gas separation process [22].

## 2.2 Mechanisms for gas separation

Performance of membrane for gas separation process depends on permeability and selectivity of membrane. High permeability membrane leads to higher productivity whereas high selectivity membrane leads to more efficient separations and higher recovery. Moreover, membranes with simultaneously high values of selectivity and permeability would lead to the most economical gas separation processes [23]. However, an inverse relationship generally occurs between the permeability and selectivity. The asymmetric membrane was suitable for gas separation because of its high permeability and selectivity [3]. The structure of asymmetric membrane was shown in Figure 2.2. It consists of a very thin and dense skin layer (labeled 1) supported on a relatively thick and porous sublayers (labeled 3). The skin layer normally presence surface pores or defects (labeled 2). The skin as the actual selective barrier, while the sublayer only as a mechanical support for the skin, with slight effects on separation [23].

Generally, the transport of gases through a dense polymeric membrane is described by the solution-diffusion mechanism. This mechanism is based on the solubility of specific gases within the membrane and their diffusion through the dense membrane matrix. Therefore, the separation is based on physical-chemical interaction between the various gas species and the polymer, which determines the differences in permeability of gas in the membrane polymeric matrix [24].

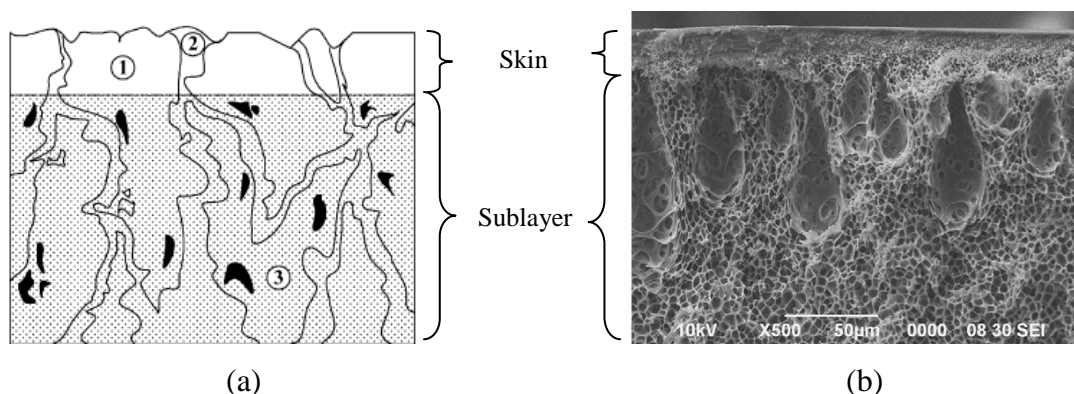


**Figure 2.2** Schematic diagrams of asymmetric membranes (a) [23] and polysulfone asymmetric membrane prepared by phase inversion method (b) [25].

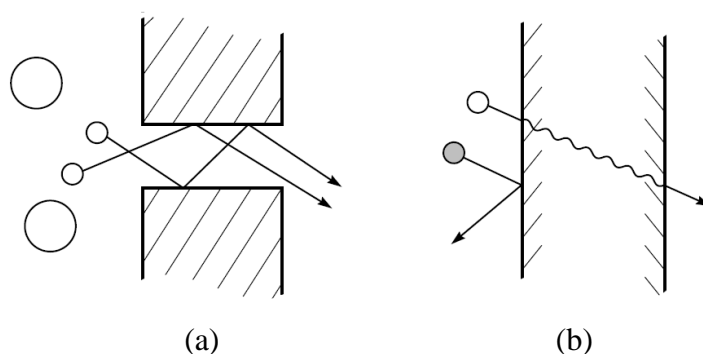


**Figure 2.3** Molecular transport through membranes can be described by a flow through permanent pores (a) or by the solution-diffusion mechanism (b) [22].

The solution-diffusion mechanism consists of three steps: (1) the absorption or adsorption of the gas at the upstream boundary, (2) the solution of the gas into the membrane, and the diffusion of the gas through the membrane, and (3) the desorption of the gas on the other side. These mechanisms represent Henry's law and Fick's first law of diffusion and can be stated as follows: [4, 22]

$$C_i = S_i p_i \quad \text{Henry's law} \quad (2.1)$$

$$J_i = -\frac{D_i dC_i}{dx} \quad \text{Fick's law} \quad (2.2)$$

Where:  $C_i$  = concentration of i in the membrane ( $\text{m}^3(\text{STP})/\text{m}^3$ )  
 $J_i$  = steady state flux of i ( $\text{m}^3(\text{STP})/\text{m}^2.\text{s}$ )  
 $S_i$  = solubility coefficient of i ( $\text{m}^3(\text{STP})/\text{m}^3.\text{Pa}$ )  
 $D_i$  = diffusivity coefficient of i ( $\text{m}^2/\text{s}$ )  
 $p_i$  = partial pressure of i in the gas (Pa)  
 $x$  = distance through active membrane (m)

The gas transport in a dense membrane is represented by two coefficients, e.g. diffusivity coefficient ( $D$ ) and solubility coefficient ( $S$ ). The permeability coefficient ( $P_i$ ) can be expressed as [26]:

$$P_i = D_i \times S_i \quad (2.3)$$

Combining and integrating equations (2.1) and (2.2) over the full membrane thickness across the membrane, yields [4, 27]

$$J_i = \frac{P_i \Delta p_i}{l} \quad (2.4)$$

or

$$\frac{P_i}{l} = \frac{J_i}{\Delta p_i} = \frac{Q_i}{A \Delta p_i} \quad (2.5)$$

Where:  $P_i$  = permeability coefficient of i ( $\text{m}^3(\text{STP})\text{m}/\text{m}^2.\text{s}.\text{Pa}$ )  
 $\frac{P_i}{l}$  = permeance ( $\text{m}^3(\text{STP})/\text{m}^2.\text{s}.\text{Pa}$ )  
 $\Delta p_i$  = the pressure difference across the membrane (Pa)  
 $l$  = membrane skin thickness (m)  
 $Q_i$  = flow rate of permeate of component of i ( $\text{m}^3(\text{STP})/\text{s}$ )  
 $A$  = surface area of membrane ( $\text{m}^2$ )

The selectivity ( $\alpha_{ij}$ ) is an indication of a membrane's ability to separate species i and j. It is defined as [3, 26]:

$$\alpha_{ij} = \frac{P_i}{P_j} = \left( \frac{D_i}{D_j} \right) \left( \frac{S_i}{S_j} \right) = \frac{(P/l)_i}{(P/l)_j} \quad (2.6)$$

where  $D_i/D_j$  and  $S_i/S_j$  represent the diffusivity selectivity and the solubility selectivity, respectively.

Diffusivity selectivity is strongly influenced by the size difference between the gas molecules, normally represented by their kinetic diameters, whereas solubility selectivity is controlled by the relative condensability of the gas molecules and the affinity between the gas molecules and the polymer matrix. The condensability was indicated by critical temperature ( $T_c$ ) [26].

In some case, the molecules size cannot exist, for example, polar or quadrupolar gases (e.g.  $\text{CO}_2$ ,  $\text{H}_2\text{S}$ ,  $\text{H}_2\text{O}$ , etc.) diffuse in polymer matrices that either promote aggregation of penetrants for strong and favorable interactions with the gases, such as  $\text{CO}_2$  diffusion in amine-containing polymers. However, in many cases, such strong interaction effects were not present, and diffusion coefficients of gases should depended on gas molecules size [21].

The selectivity calculated from the ratio of pure gas permeabilities is the ideal selectivity, an intrinsic property of the membrane material. In some case, the gases in a mixture do not interact strongly with the membrane material so that the selectivity from pure gas and the mixed gas will be equal, for example  $\text{O}_2$  and  $\text{N}_2$ . However, in the case of  $\text{CO}_2$  and  $\text{CH}_4$  mixture,  $\text{CO}_2$  is sufficiently absorbed by the membrane to increase the  $\text{CH}_4$  permeability far above the pure gas  $\text{CH}_4$  permeability value. As a result the selectivity's measured with gas mixtures are much lower than those calculated from pure gas data as show in Figure 2.4. Pure gas selectivities are much more commonly reported in the literature than gas mixture data due to they are easier to measure [22].

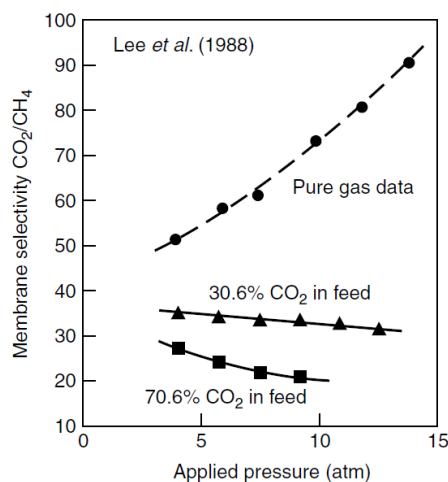


**Figure 2.4** Separation of methane and carbon dioxide from gas mixtures and pure gas with cellulose acetate membranes [22].

### 2.3 Preparation of polymeric membrane

There are several methods of membranes preparation and these include sintering, leaching, phase inversion and track etching method [28]. Currently, most of the commercial membranes are produced by phase inversion methods mainly because of its simplicity, flexible production scales lead to maintain the low cost of production. For track etching method, it is occasionally used for the fabrication of membranes. The polymer film is subjected to high energy particle radiation (metal ions) applied to the material, followed by etching in acid or an alkaline bath. The membrane porosity is mainly determined by the duration of radiation. While the pore size is determined by the etching time and temperature [2]. Due to track etched membranes for gas separation are few so this method is interested. Consequently, this research prepared polysulfone and polyethylene membranes using phase inversion and track etching method.

#### 2.3.1 Phase inversion method

The phase inversion can be described as a changing a one-phase homogeneous polymer solution into two separate phases. A liquid polymer solution is precipitated into two phases are a solid, polymer-rich phase that forms the matrix of



the membrane and a liquid, polymer-poor phase that forms the membrane pores. This precipitation of the cast liquid polymer solution to form the asymmetric membrane can be achieved in several ways such as thermally induced phase separation (TIPS), controlled evaporation of solvent from three component systems, precipitation from the vapor phase and immersion precipitation (IP). However, IP are the most commonly employed methods in the fabrication of industrial asymmetric membranes due to the simplicity of its process. However, ultrathin and defect-free asymmetric membranes can be prepared by dry/wet phase inversion process. The casting solution consists of a polymer dissolved in a mixture of a more volatile solvent and a less volatile solvent. In dry step, the volatile more solvent evaporates first. The loss of the volatile solvent leads to the formation of the top skin layer of the membrane. This step can be observed from turbidity in the top skin layer region. Then, the membrane is immersed in a coagulation bath containing a non-solvent, which is a wet-phase separation step. The exchange of the solvent in polymer solution with the non-solvent from the coagulation bath results in the phase separation. In this step, the bulk of the membrane structure is formed and the remaining solvents and non-solvents in film are extracted [2, 22, 29]. Most of the PSF membranes are also produced by this method because of its ease of dissolution in common organic solvents. In addition, as an amorphous polymer, the phase separation behaviour of a polysulfone polymer is simpler than a semi-crystalline polymer such as poly (vinylidene fluoride) (PVDF) polymer.

Research and development of PSF membranes prepared using phase inversion process have been interested by a number of researchers, focusing on the effect of various preparation conditions on membrane morphology and performance. For example, Lee et. al., (2000) [30] fabricated polysulfone membranes by a wet/wet phase inversion technique. In two non-solvent baths, iso-propanol (IPA) was used in the first bath and water was used in the second. They revealed that the skin layer thickness was determined by changing the immersion time of the first IPA bath. It increased from about 2  $\mu\text{m}$  to about 13  $\mu\text{m}$  as immersion times increased from 10 sec to 80 sec, which lead to the  $\text{O}_2$  permeability decreasing and  $\text{O}_2/\text{N}_2$  selectivity increasing. The selectivity of  $\text{O}_2/\text{N}_2$  of a membrane immersed to first IPA bath during 80 sec obtained up to about 6.0. Ismail et. al., (2003) [27] studied the effects of

membranes coating with a silicone polymer on asymmetric polysulfone membrane structure and  $O_2/N_2$  and  $CO_2/CH_4$  gas separation performance. Asymmetric polysulfone membrane prepared by phase inversion method. The component dope solution was used 22% (w/w) polysulfone, 31.8% (w/w) DMAc, 31.8% (w/w) THF, and 14.4% (w/w) ethanol. Water was used in the coagulation bath. The solutions were mixed under temperature of 60 °C for 8-10 h until the polymeric solution become homogeneous. The polymer solution was cast on a clean glass. After evaporation step of 5 s, the membranes were immersed in the quench medium (wet phase inversion). The coating was applied by flooding the membrane skin layer surface with 3% w/w solution of the silicone in n-hexane for 15 min. After coating, the membranes were placed in an oven at 60 °C for 4 h to allow curing prior the gas permeation testing. They found that  $O_2/N_2$  and  $CO_2/CH_4$  selectivity of the uncoated membrane were 4.01 and 19.48, respectively. For the coated membrane, the selectivity of  $O_2/N_2$  and  $CO_2/CH_4$  were approximately 6.72 and 32.63, respectively. This suggested that silicone rubber had successfully plugged the pores that were present at the membrane skin layer or repaired the membranes imperfections. Moreover, Madaeni and Moradi (2011) [29] found that  $O_2/N_2$  selectivity as a function of casting thickness. The selectivity was improved from 3 to 10 by increasing the casting thickness from 280 to 350  $\mu\text{m}$ . The selectivity enhancement may be explained on the basis of membrane structure. Increasing of casting thickness lead to an increment in the thickness of the skin layer. The thicknesses of the established skin layers were 1.1 and 8.3  $\mu\text{m}$  for the membranes with the casting thicknesses of 280 and 350  $\mu\text{m}$ . The membrane with thicker skin layer provides higher resistance against passing gas leading to permeance decreasing. When oxygen permeance was declined, selectivity was improved.

They prepared asymmetric polysulfone membranes using a mixture of a more volatile solvent (THF) and less volatile solvent (NMP) instead of one single nonvolatile solvent. They found that the skin layer is thicker and less defects. They explain a volatile solvent can rapidly evaporate from the outermost surface of the membrane during polymer casting, which results in higher polymer concentration in the upper layer of the membrane. Delayed liquid–liquid demixing was induced, and as a result, a denser membrane skin with few pores or defects was prepared. Acetone is a

more volatile solvent with has boiling point 56 °C, while boiling point of THF is 66 °C. It mean acetone more rapidly evaporate than THF so that it is possible to prepared asymmetric membranes with dens skin layer using acetone [25, 30-32]. Madaeni et. al., (2004) [31] found that addition of acetone in to polymeric solution consist of PSF and DMAc cause a decline in flux and an improvement in the retention of protein. In the same condition, Aryanti et. al., (2013) [32] reported humic acid rejection increase with acetone concentration increase. This is confirmed that acetone could improve dense membrane.

### 2.3.2 Track etching method

Track etching method consists of two-step preparation process, namely, irradiation and chemical etching as illustrated in Figure 2.5. In irradiation, latent tracks were produced in the thin polymer film to be transformed into porous membranes. These tracks are much more susceptible to chemical attack than the base polymer material. In chemical etching step, the film is passed through a solution that etches the polymer. The film is preferentially etched along the sensitized nucleation tracks, thereby forming pores. Their pore size, shape and density are determined by the etching time and exposure time of the film to radiation [22, 33].

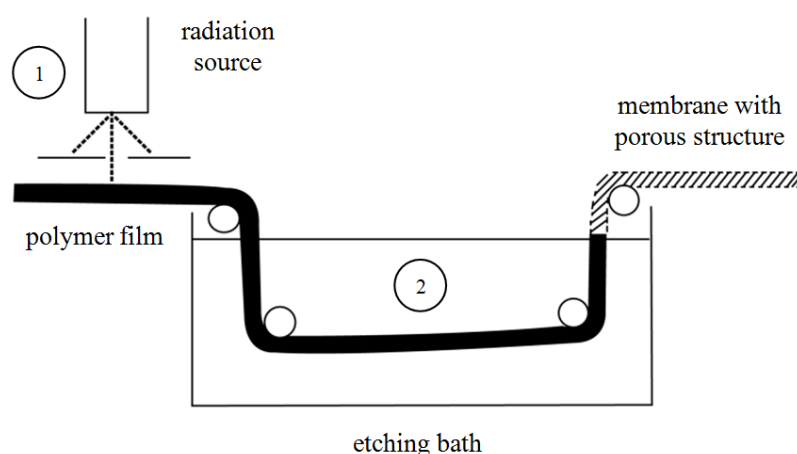


**Figure 2.5** Diagram of the prepare track-etch membranes [28];

Step 1: The thin film is irradiated by particles in a nuclear reactor.

Step 2: The latent tracks were etched into uniform, cylindrical pores.

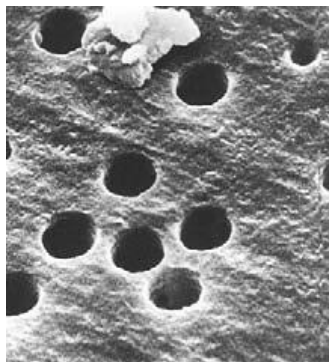


**Figure 2.6** Nuclepore (polycarbonate) nucleation track membrane [22].

### 2.3.2.1 Irradiation

The massive particles pass through the film, breaking polymer chains and damaging polymer molecules, thus producing latent tracks. There are two basic methods of producing latent tracks. The first method is ion beams from accelerators. The accelerators provide beams of higher intensities. The energies of accelerated ions are a few MeV per nucleon. The beams can be pulsing or continuous. The advantages of the accelerator tracking method are no radioactive contamination of the material when the ion energy is below the Coulomb barrier, all tracks show the same etching properties, higher energy of particles can perforate thicker film, better for producing high-density track arrays, particles heavier than fission fragments can be used, it is easier to control the impact angle and produce arrays of parallel tracks. However, the disadvantages of the accelerator tracking method are usually lower stability of the particle flux from an accelerator and a higher cost of irradiation [33].

The second method is the irradiation with fragments from the fission of heavy nuclei such as californium or uranium. In initiates the fission of  $^{235}\text{U}$ , the uranium target was exposed to a neutron flux from a nuclear reactor. The fission fragments have an almost isotropic angle distribution. Therefore, to create an array of latent tracks penetrating the thin film, a collimator is usually used. The advantages of the fission fragment tracking are good stability of a particle flux in time, a non-parallel particle flux can the production of membranes with a high porosity and relatively low cost. However, the limitations of the method are caused by the contamination of the tracked film with radioactive products so that cooling of the

irradiated material is needed, a limited range of the fission fragments lead to thickness limiting of the membrane, limitations of creating various angle distributions of pore channels and fragments of different masses and energies manufacture tracks with different etching properties [33].

### 2.3.2.2 Chemical etching

Chemical etching is a process which latent track was enlarged lead to pore formation. The damaged zone of a latent track was removed and transformed into a hollow channel during this process. It is the determination stage of pore size and pore shape. The pore geometry was described with two parameters, the bulk etch rate  $V_B$  and the track etch rate  $V_T$  (Figure 2.7). The conical pore shape is transformed into a cylindrical one at  $V_T > V_B$ . The cylindrical pore shape was produced from the conical pore shape at  $V_T > V_B$ . The bulk etch rate depends on the material, etchant composition and temperature. While the track etch rate depends on a much greater number of factors such as sensitivity of the material, irradiation conditions, post-irradiation conditions and etching conditions. The irradiation conditions include parameters of the bombarding particle, atmosphere and temperature. The variations of the etchant composition, component concentrations and temperature lead to the track to bulk etch rate ratio in a very wide range. The changing the temperature during etching can be used to increase or decrease the etch rate ratio due to activation energy of the track etching process often differs from that of the bulk etching. Another parameter is the size of the damaged zone that dissolves at a different rate compared with that for the bulk material [33].

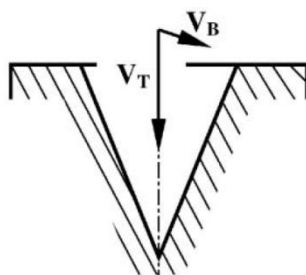


**Figure 2.7** Schematic diagram of etched pore geometry [33].

### 2.3.3 Nuclear fission reaction

A Nuclear fission reaction take place when various heavy nuclei are bombarded by neutrons, new radioactive elements are produced. Niels Bohr and John Wheeler described nuclear fission reaction based on the model between a nucleus and charged liquid drop. When high mass nucleus such as  $^{235}\text{U}$ , absorbs a thermal neutron as show in Figure 2.8 (a). The potential energy of neutron is transformed into internal excitation energy of the nucleus, which  $^{235}\text{U}$  become to  $^{236}\text{U}$ , as show in Figure 2.8 (b). This excitation energy is equal to the binding energy ( $E_n$ ) of the neutron in that nucleus. It result to nucleus behaving like an oscillating charged liquid, which develop a short neck and will being to separate into two globs later (Figure 2.8 (c-d)). If the electric repulsion between these two globs enough to break the neck, the two fragment are produced. And some residual excitation energy still carrying lead to flying apart of these fragments (Figure 2.8 (e-f)). Therefore, nuclear fission reaction has occurred [34].

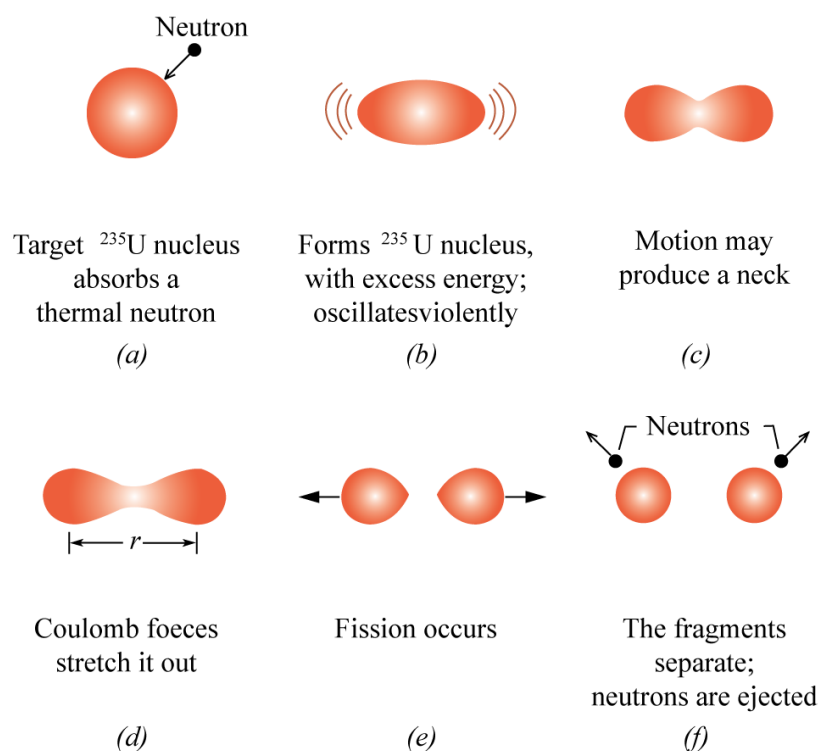


**Figure 2.8** The stage of typical fission process, according to the collective model of Bohr and Wheeler [34].

A graph of the potential energy of the fission nucleus was shown in Figure 2.9, which energy is plotted against distortion parameter ( $r$ ). This parameter is the distance between the centers of fragments when they are far apart [34].

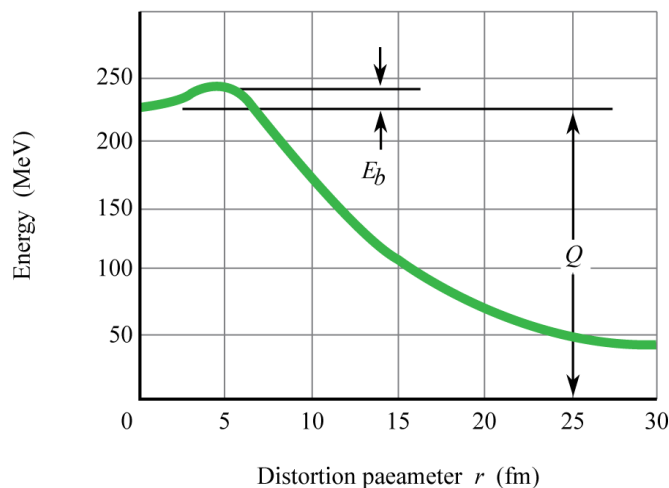


**Figure 2.9** The potential energy at various stages in the fission process [34].

For  $^{235}\text{U}$  and  $^{239}\text{Pu}$ , due to their excitation energy value is higher than barrier height value ( $E_n > E_b$ ), therefore, the fission by absorption of a thermal neutron can occur for these nuclides. For the other two nuclides ( $^{238}\text{U}$  and  $^{243}\text{Am}$ ), the excitation energy value is lower than barrier height value ( $E_n < E_b$ ) lead to not enough energy from a thermal neutron for the excited nucleus to overcome the barrier. However, the nuclides  $^{238}\text{U}$  and  $^{243}\text{Am}$  can be made to fission by absorb an energetic (rather than a thermal) neutron such as fast neutron [34].

**Table 2.1** Test of the fissionability of four nuclides [34].

Target Nuclide	Nuclide Being Fissioned	$E_n$ (MeV)	$E_b$ (MeV)	Fission by Thermal Neutrons?
$^{235}\text{U}$	$^{236}\text{U}$	6.5	5.2	Yes
$^{238}\text{U}$	$^{239}\text{U}$	4.8	5.7	No
$^{239}\text{Pu}$	$^{240}\text{Pu}$	6.4	4.8	Yes
$^{243}\text{Am}$	$^{244}\text{Am}$	5.5	5.8	No

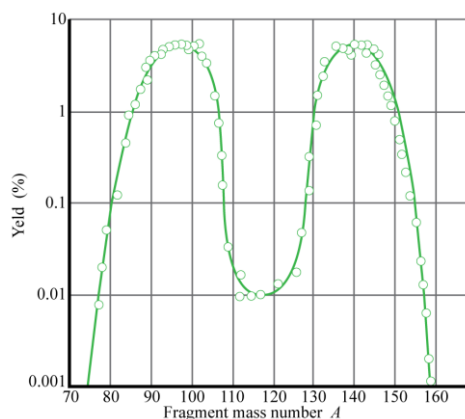
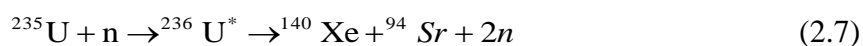


**Figure 2.10** The distribution by mass number of the fission fragment that were found when many fission events of  $^{235}\text{U}$  were examined [34].

When  $^{235}\text{U}$  was bombarded with thermal neutrons, the distribution by mass number of fission fragment produced was shown in Figure 2.8. The most probable mass numbers of fission products were around 95 and 140. Due to a  $^{235}\text{U}$  nucleus absorbs a thermal neutron, a compound nucleus  $^{236}\text{U}$  was produced in an excited state. This nucleus split into two fragments and rapidly emits two neutrons, leaving  $^{140}\text{Xe}$  and  $^{94}\text{Sr}$  as fission fragments. Thus, fission equation for this event is



During the fission of compound nucleus, the number of proton and neutron were conserved.

### 2.3.4 Mechanism [35]

#### 2.3.4.1 Thermal spike

Thermal spike described that a charged particle which passes into material causes intense ionization and excitation along its path. In this region, material is rapidly heated to a high temperature and then rapidly quenched by thermal expansion into the surrounding matrix, lead to the disordering the core material or straining the matrix. For this reason, the path of a charged particle becomes narrow cylinder.



### 2.3.4.2 Ion explosion spike

For ion explosion spike, the interactions with the electrons in the detector lead to the damage of along track in inorganic solids. Due to ionization in material, an array of interstitial ions and vacant lattice sites is produced by the Coulomb energy of the ions, which electrostatically unstable array of adjacent ions which eject one another from their normal sites into interstitial positions. Then elastic relaxation diminishes the acute and local stresses by spreading the stain more widely. This is the creation of long range strains in this step.

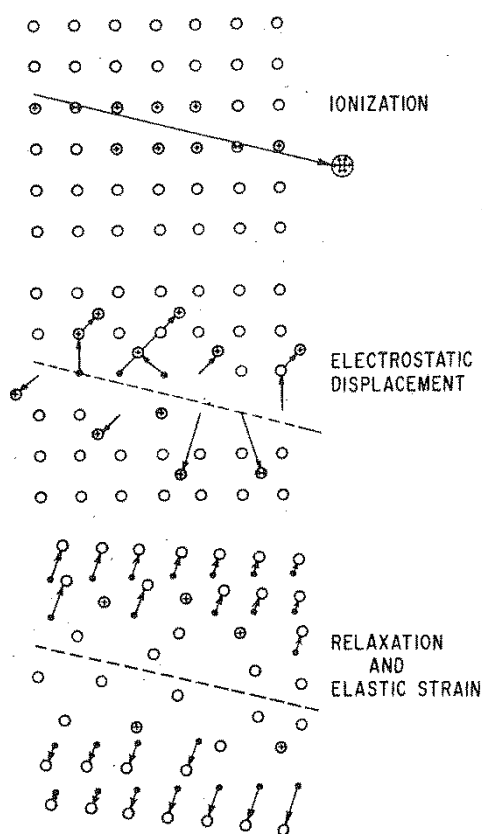


**Figure 2.11** The ion explosion spike mechanism for track formation in inorganic solids [35].

Most of track-etched membrane use ion beams from accelerators for produced latent tracks in the film to be transformed into porous membranes. For example, Vijay et. al., (2004) [36] prepared track-etched membrane from polycarbonate (PC) film. The film were irradiated by  $\text{Si}^{8+}$  ions of 100 MeV and

etched chemically in 6 N NaOH at 60 °C. They found the permeability of H<sub>2</sub> and CO<sub>2</sub> increases rapidly after increases etching time and H<sub>2</sub>/CO<sub>2</sub> selectivity is about 1.25-4. Achary et. al., (2006) [37] reported that deposition of Ti thin film (100–150 nm) on polymer membrane surface which was prepared by C<sup>5+</sup> ion of 60 MeV could restricts the permeation rates for all gases except hydrogen. Consequently, these can be use in the fabrication of devices that are functional for hydrogen purification. Kulshrestha et. al., (2007) [38] could product asymmetric track-etched membrane with Ni<sup>7+</sup> ion of 100 MeV. They reported that the permeability of hydrogen and carbon dioxide increases with increasing etch time. The gas permeability from the ion incidence side (front) is more than that of ion-emergence side (back) due to the shape of the etched track and the gas permeability of the same membrane is greater for hydrogen than for carbon dioxide due the difference of their molecular sizes.

The production of latent tracks in the foils by fragments from the fission of heavy nuclei such as californium or uranium rather lacked. Yamazaki et. al., (1996) [39] prepared membrane with track-etching technique. PC film was irradiated with fragments from the fission of uranium. The thermal neutron flux was about  $2.7 \times 10^{11} \text{ ncm}^{-2}\text{s}^{-1}$ . They found that this method could produced ultrafiltration membranes which has been developed down to a pore size of 15 nm employing a pore density around  $8.0 \times 10^8 \text{ pores cm}^{-2}$ . He et. al., (2006) [40] prepared polypropylene (PP) porous membrane by track-etching technique. PP film was irradiated with fragments from the fission of uranium to form latent tracks, and chemically etched by potassium dichromate and sulfuric acid. They reported that the etching rate of PP was related to the concentration of etching reagent, temperature and time.

In Thailand, there were many research that prepared track-etched membrane which fragment from the fission of <sup>235</sup>U. Beside the advantages described above, this is also availability of a nuclear reactor at the Thailand Institute of Nuclear Technology (Pubic Organization). For example, Kaewsane (2005) [41] reported a successful preparation of track-etched membranes from the 13 μm thick polystyrene (PS) films. The PS film specimen was tracked with fission fragments produced from the nuclear reactor between <sup>235</sup>U from the neutron converter screen and the thermal neutrons from the Thai Research Reactor. The latent tracks were subsequently enlarged by a chemical etchant comprising sulfuric acid and potassium dichromate at

80 °C for 6-10 hours. The average diameter of the pores was generated 1.28  $\mu\text{m}$  to 3.37  $\mu\text{m}$  with the average pore density  $1.33 \times 10^5 \text{ cm}^{-2}$ . The water fluxes increase with increasing of etching time. While Thongphud (2005) [42] prepared track-etched membranes from polycarbonate (PC) and found that using the particle discriminators with increasing thickness the shape of the pores became rounder at the expense of the density of the pores. In the same method, Makphon et. al., (2006) [43] found that the porosity of the PC membranes can be controlled by varying the exposure time in the nuclear reactor and the average pore diameter by varying the etching conditions. The average pore diameter of the prepared membranes ranged from 2.0  $\mu\text{m}$  to 9.5  $\mu\text{m}$  and the highest pore density achieved was 150,000 pores  $\text{cm}^{-2}$ . In addition, It was found that chemical etching also caused a reduction in the film thickness and the water permeability of the track etched PC membranes was found to increase with increasing average pore diameter.

However, production of track-etched membranes by tracking with fission fragments in the nuclear reactor at the Thailand Institute of Nuclear Technology (Pubic Organization) was not gas separation test. Therefore, preparation of track-etched membranes for gas separation with fission fragments was interested.

## **2.4 Surface modification of polymeric membrane**

Recently, polymeric membrane technology has been increasingly attractive to scientists in gas separation task. High gas permeability and selectivity are always desirable for polymeric membranes. In most cases, an increase in gas permeability often causes a decrease in gas selectivity. Asymmetric membranes of a highly selective thin layer on top were known as a high performance membrane type for gas separation [44, 45] due to the selectivity of a membrane relies totally on this extremely thin layer. Therefore, there are two methods about how to obtain a highly selective layer: one is to make the top layer dense and the other is to make a top layer with high affinity to gas molecule [45].

The gas transport property of polymeric membranes depended on physical-chemical interaction between the various gas species and the polymer molecules [24]. Thus, the differences of gas transport do exist in the membrane

material properties, such as dipole moment and gas properties, such as polarizability and quadrupole moment [46]. As mentioned previously, there are several researches reported that polar groups such as carbonyl (CO), hydroxyl (OH), sulfone (SO<sub>2</sub>), and ether (ROR') groups could increased selectivity of CO<sub>2</sub>/nonpolar gas (N<sub>2</sub>, H<sub>2</sub>, C<sub>2</sub>H<sub>6</sub> and CH<sub>4</sub>) [26, 47-49]. Therefore, membrane modification with polarity addition to the surface is of interest to improve the selectivity for gas separation process. There are many techniques to modify the membrane surface such as UV-ray irradiations [13, 14], plasma treatment [11, 12], ozone treatment [15] and gamma-ray irradiations [16, 17]. Among these techniques, UV-ray irradiations and plasma treatment are the two most commonly employed techniques in the surface modification of polymeric membranes.

#### **2.4.1 UV-ray irradiation**

Many studies about the effects of these methods on several types of polymers have been reported. But the information about the effects UV irradiation on microporous PSF membrane especially, is scarce. However, it has been reported that it increased flux and the hydrophilicity of the membranes[13]. Compared with other surface modification techniques such as plasma treatment, ozone treatment and gamma-rays irradiation, UV irradiation has distinct advantages over other techniques due to its simplicity, inexpensive and widespread industrial applications. Most importantly, surface modification occurs mainly on the membrane surface [18].

The reactions taking place in the chain, when irradiated with UV are bond scissions and dissociations of the methyl side groups, either by the formation of a methyl or a hydrogen radical, indicated in Figure 2.12. As end products such as sulfonic acid, ketone and ethenyl groups can be formed [13].

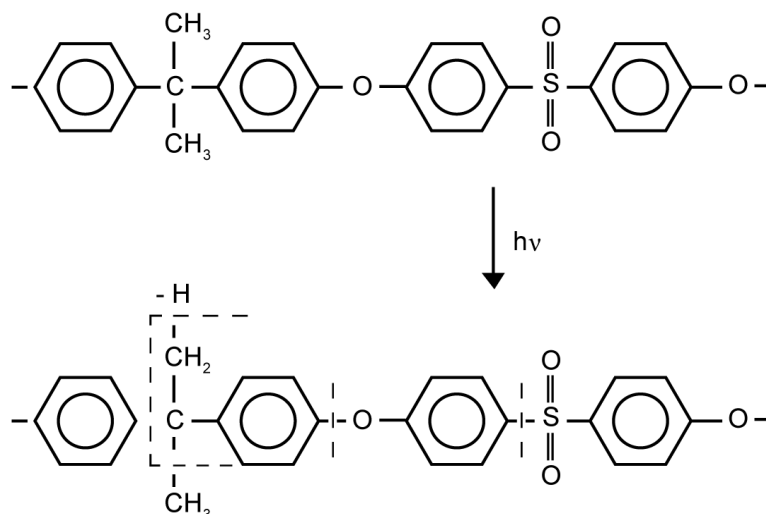


**Figure 2.12** Chain scissions that can be induced by UV irradiation of polysulfone [13].

Nystrom and Jarvinen (1991) reported increases in flux and hydrophilicity of polysulfone (PSF) membranes after UV irradiation [13]. In addition, Hsu et. al., (1993) revealed that UV irradiation on poly trimethylsilyl propyne (PTMSP) membranes resulted in an improvement of  $O_2/N_2$  selectivity from 1.4 to approximately 4 after the treatment [14].

#### 2.4.2 Plasma treatment

Although there are many ways to modified the membranes surface, plasma treatment was one of the most effective and convenient ones. In addition, plasma treatment is also a quite simple and clean process. The plasma processes can alter the physico-chemical properties of the polymer surface lead to improvement of wettability, conductivity, adhesion or biocompatibility of polymer. Moreover, it can increase both gas permeability and selectivity of membranes gas separation process. The plasma treatment can activate the upper molecular layers on the surface, without affecting the bulk of the polymer. The various surfaces could be obtained from a single material by changing parameters of plasma process. However, there is also a lack of permanency resulting from this technique it difficult to control the chemical structure of the plasma treated polymer [15, 19, 45, 50, 51].

There are three basic phenomena affecting membrane properties by plasma treatment [51]:

1. Ablation-etching and reactions giving volatile products lead to increase of pore diameter and porosity.
2. Deposition of polymer film made of plasma gas and/or of volatile products that come from the etched surface, which can result in lower porosity.
3. Modification of the chemical structure of the surface layer result in hydrophilization or hydrophobization depending on plasma conditions with introduction of various functional groups that can be used for immobilization or grafting.

Chen et. al., (1997) modified the surface of a polybutadiene (PB)/polycarbonate (PC) composite membrane by Chloroform ( $\text{CHCl}_3$ ) plasma. They found that the selectivity of the composite membrane was improved after plasma treatment. The selectivity enhancement as a result of the physical structure changing on the membrane surface rather than the chemical effect introduced by chlorine. According to the SEM observation, the surface of the PB/PC membrane became less porous after plasma treatment. Before plasma treatment, an oxygen permeation flux and  $\text{O}_2/\text{N}_2$  selectivity of PB/PC composite membrane is 2.4 GPU and 3.55, respectively. After 40 min treatment by 40 W  $\text{CHCl}_3$  plasma the oxygen permeation flux reduced to 0.3 GPU but the  $\text{O}_2/\text{N}_2$  selectivity increased to 7.5 [45]. Then, Chen et. al., (1998) reported that the  $\text{O}_2$  permeability of the untreated polyurethane (PU) membrane was 0.875 GPU and the  $\text{O}_2/\text{N}_2$  selectivity was 2.6. After ethylenediamine (EA) plasma treatment, the gas permeability decreased to 0.375 GPU but the  $\text{O}_2/\text{N}_2$  selectivity increased to 3.1. The decrease in gas permeability was probably as a result of the cross linking effect on the treated surface. Due to cross-linking result in the reduction of free volume and flexibility of polymer chains. Based on the concept of solution-diffusion model, there might be two possible reasons for the increase in membrane selectivity. Those were the size-sieving effect caused by the surface cross-linking and the increase in oxygen solubility caused by the incorporation of ethylenediamine [52]. Steen et. al., (2001) [50] found that  $\text{H}_2\text{O}$  plasma treatment could modify the hydrophilicity of asymmetric PSF membranes, which confirmed by contact angle measurement. XPS analysis of treated membranes demonstrates the  $\text{CH}_x$

percentage decreases but percentages of C-O and C-O<sub>x</sub> groups increase relative to the untreated material. As there are no C-O<sub>x</sub> groups present in the untreated material, these functional groups must be introduced by the plasma treatment. These results indicated that the increase in hydrophilicity for H<sub>2</sub>O plasma-treated membranes is a result of the formation of these covalently bound hydrophilic functional groups. They offer there are three other locations for oxidation on the polymer backbone as represented in Figure 2.13. For example, oxidation at position 1 yields a ketone functionality. Additionally, oxidation at position 2 yields an aldehyde, which can be further oxidized to yield a carboxylic acid group. Finally, oxidation at position 3 resulting in sulfate-like groups.

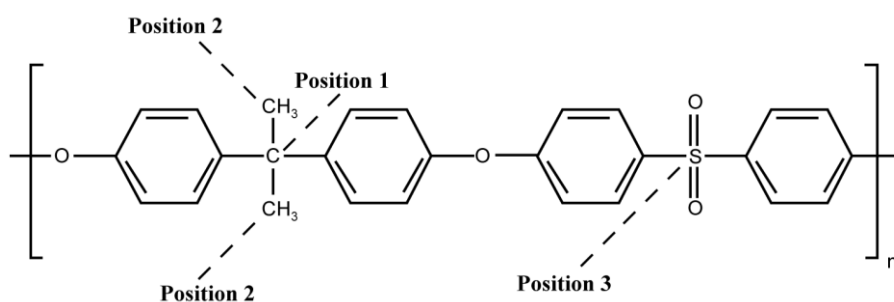


**Figure 2.13** The locations for oxidation on the polysulfone backbone by plasma treatment [50].

Bryjak et. al., (2002) [19] studied the effect of NH<sub>3</sub> and NH<sub>3</sub>/Ar plasma on PSF membranes. Results of contact angle, FTIR-ATR and X-ray photoelectron spectroscopy showed that both plasmas introduced hydrophilic, nitrogen- and oxygen-containing moieties on the polymer surface and that NH<sub>3</sub>/Ar plasma was more efficient. Contact angle method was used for evaluate surface tension and both its components (polar and dispersive components) of modified PSF membranes. Results showed that increase of membranes surface hydrophilicity, which observed from increase of polar components of surface tension. From the FTIR-ATR and X-ray photoelectron spectroscopy, the spectrum for untreated PSF membranes shows only two peaks such as bonds C-C and C-O. While the spectrum of NH<sub>3</sub> and NH<sub>3</sub>/Ar plasma modified surfaces appears the third peak, which is assumed to be characteristic for C=O and N-C=O bonds. Therefore, the grafting of ammonia to the

surface can cause an additional increase of N-C bonds. Kim et. al., (2002) [53] [53] investigated the changing from hydrophobicity to hydrophilicity in PSF membranes by oxygen plasma treatment. They found the contact angles of water for O<sub>2</sub> plasma treated PSF membranes decreased with plasma treatment time increased since polar functional groups were introduced on the surface of hydrophobic PSF membrane by oxygen plasma treatment. This is related to the increment of polar component of surface free energy in PSF membranes after plasma treatment. Polar functional groups such as hydroxyl, carbonyl, and carboxyl group were confirmed by XPS analysis. Wavhal and Fisher (2005) [54] reported that the hydrophilicity of PSF membranes was enhanced by CO<sub>2</sub> plasma treatment as a result of implantation of hydroxyl, carbonyl, and carboxylic acid polar functional groups. The presence of these groups was confirmed by FTIR and XPS measurements. Wanichapichart et. al., (2009) [55] studied the surface modification of chitosan membranes using Ar plasma. They found that contact angle between water drop and the surface of the membranes reduces from 65°-70° to about 20°-25°, after only 30 s of treatment. The results indicate that membranes increase in hydrophilicity after the plasma treatment. Moreover, results from ATR-FTIR showed a major increase in the absorption spectra of carbonyl (C=O) and methyl (C-H) functional groups. This result is consistent with the changes in hydrophilicity measurement using contact angle measurements.

Lin and Freeman (2004) [26] studied the effect of polar ether linkages in poly (ethylene oxide) (PEO) on gas transport and illustrated by comparing transport properties in poly (ethylene oxide) (PEO) with those in polyethylene (PE). They found that PEO exhibits CO<sub>2</sub> permeability coefficient of 12 Barrers, and CO<sub>2</sub>/N<sub>2</sub> pure gas selectivities of 48. In contrast, at similar conditions, the permeability of PE to CO<sub>2</sub> is 13 Barrers, but the CO<sub>2</sub>/N<sub>2</sub> selectivity is only 13. This is qualitatively consistent with the notion that polar, basic ether linkages interact favorably with acidic penetrants such as CO<sub>2</sub>, thus increasing CO<sub>2</sub> sorption. Zhang et. al., (2013) [7] reported that the CO<sub>2</sub> is more permeable than CH<sub>4</sub> due to the larger condensability. Polymers containing polar groups, such as ether groups, have an affinity for CO<sub>2</sub> due to dipole-quadrupole interaction. Therefore, polymer membranes containing polar segments have been applied to CO<sub>2</sub>/CH<sub>4</sub> separation. Due to the CO<sub>2</sub> molecule has high polarizability and a high quadrupole moment, with help the CO<sub>2</sub> molecule to



permeate through the membrane by dipole-quadrupole interactions between the membranes polar segments and CO<sub>2</sub> molecule [26, 56]. Koros (1985) suggested that the solubility selectivity for the CO<sub>2</sub>/CH<sub>4</sub> separation increases as the mass density of polar carbonyl or sulfone groups in the polymer increases [47]. Bondar et. al., (1999) studied gas sorption in a copolymer containing polyether segments. They found that solubility selectivity of CO<sub>2</sub>/nonpolar gases (CO<sub>2</sub>/N<sub>2</sub> and CO<sub>2</sub>/H<sub>2</sub>) increases with increasing concentration of polar ether groups in these copolymers [48]. Lin and Freeman (2004) [26] studied the effect of polar ether linkages in poly (ethylene oxide) (PEO) on gas transport compared to the transport properties with those in polyethylene (PE). They found that the CO<sub>2</sub>/C<sub>2</sub>H<sub>6</sub> solubility selectivity is 0.35 in PE, but in more polar PEO, the CO<sub>2</sub>/C<sub>2</sub>H<sub>6</sub> solubility selectivity is 3.1. This result suggested that CO<sub>2</sub> has favorable interactions with the polar ether groups in PEO. Sadeghi et. al., (2009) [49] investigated the CO<sub>2</sub>, CH<sub>4</sub> and N<sub>2</sub> transport properties in a composite membrane of polybenzimidazole (PBI) and silica. They found the solubility of condensable gases (CO<sub>2</sub> and CH<sub>4</sub>) will be increased due to the silica content in the polymer matrix since the number of polar OH groups in the polymer matrix will also be increased. Moreover, they found the strong correlation between the solubility coefficients and condensability of the gases, as well as the diffusion coefficient of the penetrants and their kinetic diameter [21]. Electrical properties of gases and polar functional groups of polymers were shown in Table 2.1 and 2.2, respectively.

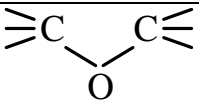
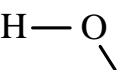
These research illustrate that plasma treatment could incorporate the varieties of polar functional groups such as hydroxyl, carbonyl and carboxylic group on membranes surface leading to the enhancement of the hydrophilicity of the treated membranes. The membranes hydrophilicity was analyzed by contact angle method, which could evaluate polar components of surface free energy. Moreover, these polar functional groups were confirmed by FTIR and XPS analysis. However, the most of plasma treated membranes were applied to reduced protein fouling and increased water flux due to their hydrophilicity property, for example Bryjak et. al., (2002) [19], Kim et. al., (2002) [11], Wavhal and Fisher (2005) [54] and Wanichapichart et. al., (2009) [55]. Therefore, the membranes surface modification using plasma treatment for gas separation was interesting because polar functional groups affect the

enhancement of the electrochemical properties of membranes [12], which could increment affinity between the gas molecules and the membranes. Finally, the selectivity was improved.

**Table 2.2** A comparison of structural, physical, and electronic parameters of gas molecules [7, 57, 58].

Parameters	O <sub>2</sub>	N <sub>2</sub>	CH <sub>4</sub>	CO <sub>2</sub>
Kinetic diameter [Å]	3.34	3.68	3.82	3.30
Dipole moment [D]	0	0	0	0
Quadrupole moment $10^{40} \theta$ [Cm <sup>2</sup> ]	1.3	4.7	0	13.4
Polarizability $\alpha$ [ $10^{-40} \text{ J}^{-1} \text{ C}^2 \text{ m}^2$ ]	1.75	1.97	2.89	2.93
Critical temperature T <sub>c</sub> [K]	154.6	126.2	190.6	304.2
Structure	linear	linear	tetrahedral	Linear

**Table 2.3** Some polar groups of importance attraction [6].

Polar groups	Dipole moment (Debye Unit)	Polar groups	Dipole moment (Debye Unit)
H—C	0.4	H—F	1.9
H—S	0.9	$\geq\text{C}=\text{NH}$	2.5
	0.9	$\geq\text{C}=\text{O}$	2.5
H—Cl	1.1	$\geq\text{C}=\text{S}$	3.0
H—O 	1.6	$-\text{C}\equiv\text{N}$	3.8

## **Chapter 3**

### **Experimental**

#### **3.1 Preparation of polysulfone membranes by phase inversion method**

##### **3.1.1 Materials**

Polysulfone (PSF: Udel P-3500) supplied by Solvay (China). N,N-dimethylacetamide (DMAc), N,N-dimethylformamide (DMF) and Acetone (Ac) were used as solvents for PSF membrane and supplied by Sigma-Aldrich Co. (USA) and Guangdong Guanghua Chemical Factory Co., Ltd. (China), respectively. Tap water was used as a coagulation medium.

##### **3.1.2 Preparation of polysulfone membranes**

Membranes were prepared by phase-inversion process. Polymeric solution in this study consisted of PSF resin was dried in an oven at 80 °C for 24 h to remove humidity before being used. Polysulfone (PSF) was dissolved in solutions with different compositions under 60 °C for 24 h. Each polymeric solution was placed in an ultrasonic water bath to remove air bubbles before cast on a clean glass plate at an ambient atmosphere (25 °C and 85% relative humidity). In dry step, the solvent was allowed to evaporate in atmosphere for about 5 s. Then, the membranes were immersed in the coagulation bath at 25 °C and left for 24 h. The wet membranes were dried at room temperature for 24 h before being used.

## **3.2 Preparation of polyethylene membranes by track etching method**

### **3.2.1 Materials**

Polyethylene (PE, Linear low-density polyethylene : LLDPE) was supplied by Ruen Tong Jarean Service Limited Partnership. Toluene and Sodium hydroxide (NaOH) were supplied by MERCK-Schuchardt. Distilled water was used for washing the film.

### **3.2.2 Preparation of polyethylene film**

Polyethylene resin was dissolved in toluene solution under temperature of 90 °C for 1 h until the polymeric solution become homogeneous. The precisely prepared polymeric solution of 2% of PE at the control volume was immediately poured on a clean glass plate and was dried in the oven at 60 °C for 30 min. After that, the film was immersed in a 2 N NaOH solution for 30 min. at room temperature to extract it from a glass plate. The film was washed and soaked in distilled water for 24 h and the obtained wet film was dried at room temperature for 24 h.

### **3.2.3 Preparation of polyethylene membranes**

For production of latent track on PE film, yellow cake or ammonium diurate ( $(\text{NH}_4)_2\text{U}_2\text{O}_7$ ) (Figure 3.1) was used as fission plates to generate fission fragments when being bombarded by thermal neutrons. Thermal neutrons from thermal column of Thai Research Reactor-1/Modification1 (TRR-1/M1), located at the Office of Atomic Energy for Peace (OAEP), Thailand, were used for this study. Nuclear fission reaction between  $^{235}\text{U}$  nucleus and thermal neutron caused the high energy fission fragments with uncertainly direction as show in Figure 3.2. Therefore, the particle direction discrimination was determined. The polyethylene gratings with 5 mm thickness were used.

A  $2 \times 7 \text{ cm}^2$  PE film was laid side by side with a fission plate, composed, mainly of yellow cake and the grating was placed between yellow cake and PE film and as show in Figure 3.3. Then specimen was filled in thermal column of the TRR-1/M1 reactor as show in Figure 3.4. The membranes were irradiated with fission fragments from nuclear reactions of  $^{235}\text{U}$  and thermal neutrons for 60 s.

The conditions effect of chemical processes on gas permeation was study. Chemical etching enlarged the latent tracks formed during the tracking step into pores. The irradiated PE films were etched in  $\text{K}_2\text{Cr}_2\text{O}_7$  in  $\text{H}_2\text{SO}_4$  (40% W/W) solutions having initial concentrations of 0.5, 1, 2 and 3 N. The etching time and temperature were also varied as 1, 3, 5 and 10 min and as 25, 40, 50 and 60 °C, respectively).

- To study the concentration effect, PE film was etched in 0.5-3 N  $\text{K}_2\text{Cr}_2\text{O}_7$  in  $\text{H}_2\text{SO}_4$  (40% W/W) at 25 °C for 1 min.

- To study the etching time effect, PE film was etched in 2 N  $\text{K}_2\text{Cr}_2\text{O}_7$  in  $\text{H}_2\text{SO}_4$  (40% W/W) at 25 °C for 1-10 min.

- To study the etching temperature effect, PE film was etched in 2 N  $\text{K}_2\text{Cr}_2\text{O}_7$  in  $\text{H}_2\text{SO}_4$  (40% W/W) at 25-60 °C for 10 min.



**Figure 3.1** Uranium screen composed of Ammonium diurate  $[(\text{NH}_4)_2\text{U}_2\text{O}_7]$ .

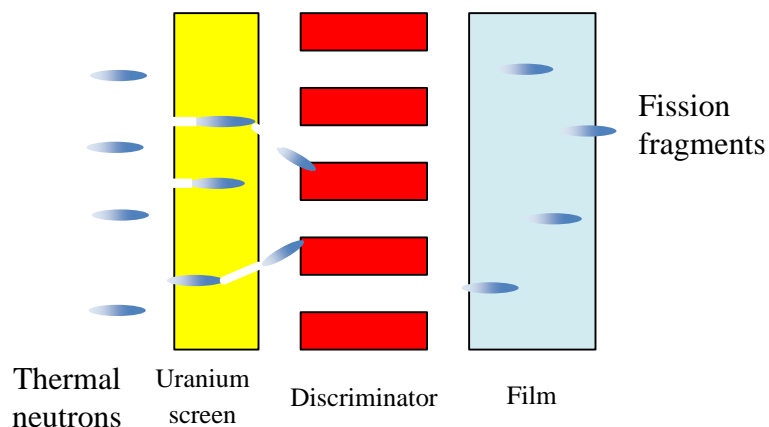


**Figure 3.2** The particle discriminators limit the angle of incident which fission fragments strike the thin PE film.

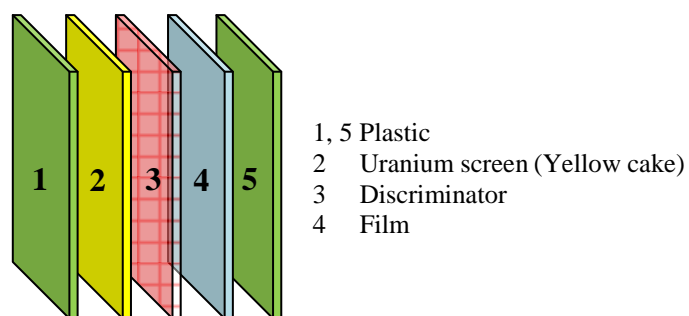


**Figure 3.3** Schematic diagram of latent track in the PE film for using the particle discriminator at thickness 5 mm.

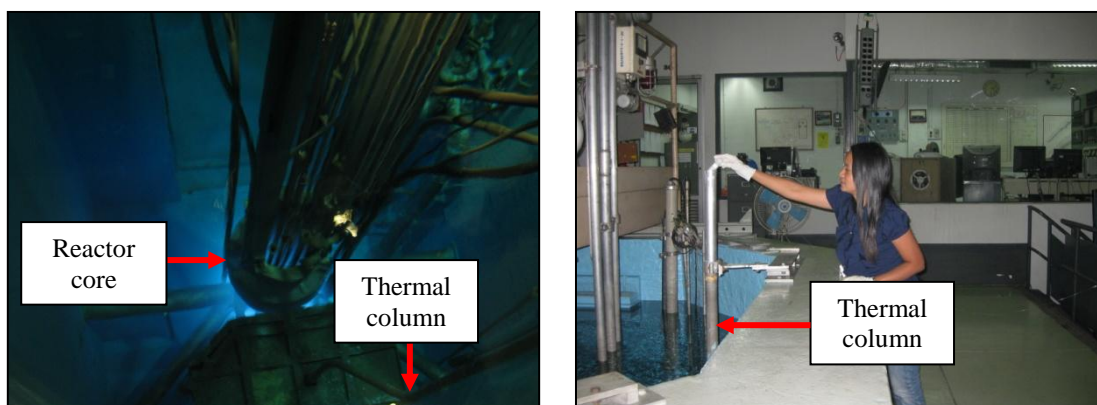


**Figure 3.4** Position of thermal column at the nuclear reactor.

### 3.3 Modification of membranes surface by UV-ray irradiation

The UV ray source (VILBER LOURMAT, VI-215.MC) with 254 and 312 nm wavelength and 2000 and 360  $\mu\text{w}/\text{cm}^2$  power, respectively, was used for the membranes treatment. The exposure area was 20  $\text{cm}^2$ . Three square pieces of polysulfone and polyethylene membranes with approximate area 2  $\text{cm}^2$  were irradiated by UV ray source (VILBER LOURMAT, VI-215.MC) in air at room temperature. The distance between the source and sample holder was constant at 3 cm. Membranes were exposed for surface modification in varied times such as 3, 6 and 12 h at atmosphere. The control (0 h) was placed in the box without humidity.



**Figure 3.5** UV ray source (VILBER LOURMAT, VI-215.MC).

### 3.4 Modification of membranes surface by plasma treatment

Polysulfone and polyethylene membranes were modified by Ar Plasma in dc discharge. DC plasma generation chamber was a cylindrical vacuum chamber, made of stainless, of internal diameter 25.5 cm and height 38.1 cm with two electrodes. The membrane piece was placed on anode to receive the plasma uniformly. The front face of membrane piece was exposed to same intensity of plasma by keeping it at 2 cm from cathode. Initially, the system was evacuated to a pressure of  $6.7 \times 10^{-2}$  mbar and Ar gas was purged into the chamber until pressure was raised to  $2.5 \times 10^{-1}$  mbar. Plasma power was adjusted to 15 W. The treatment time was varied from 1-20 min.

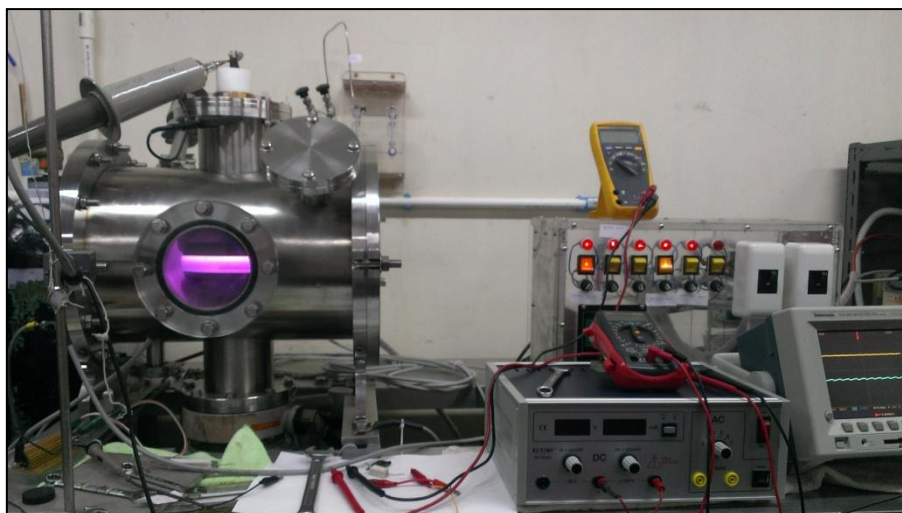


**Figure 3.6** Plasma systems develop by Mr. Chalad Yueanyao.

### **3.5 Gas permeation measurement**

The performance of PSF membranes were evaluated by two parameters: the permeance ( $P/l$ ) and the selectivity ( $\alpha$ ). Gas permeation measurements were conducted by using a gas permeation unit as shown in Figure 3.7. PSF membranes were cut into circle area of  $3.14 \text{ cm}^2$  and mounted in the gas permeation unit. The testing temperature was room temperature ( $25 \text{ }^\circ\text{C}$ ). The testing pressure was controlled from 3 to 8 bar and the testing gases were  $\text{O}_2$ ,  $\text{N}_2$ ,  $\text{CO}_2$  and  $\text{CH}_4$ . The feed gas was fed into the up-side and the permeating gas was at the down-side of the membrane. The gas flow rate ( $Q$ ) was determined by bubble flow meters. The pure gas permeance ( $P/l$ ) and the selectivity ( $\alpha$ ) of the membrane were calculated by equation 2.5 and 2.6, respectively. Each membrane was determined 3 times for each gas and the results were presented in average.



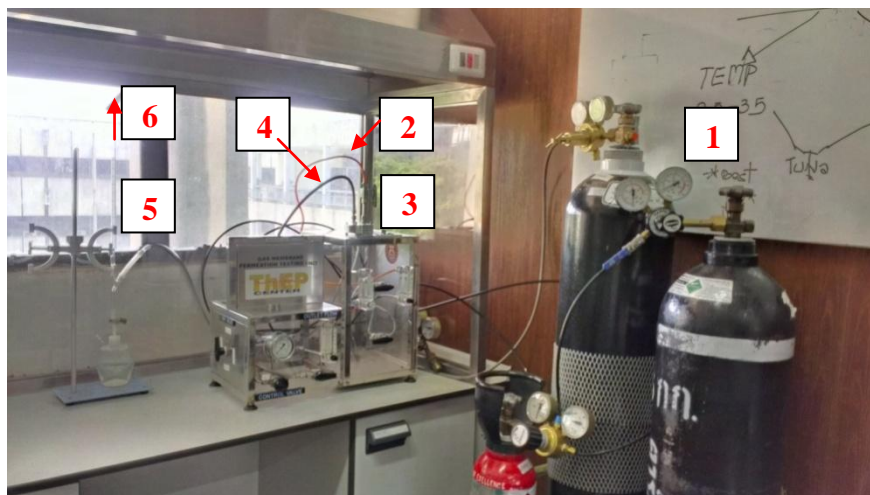


**Figure 3.7** Gas membrane permeation testing unit. (1) Gas and pressure gauge (2) Feed gas (3) Membrane cell (4) Retentate (5) Bubble flow meter (6) Permeate.

### 3.6 Membrane characterization

#### 3.6.1 Water contact angle

Water contact angle of membranes was measured using a contact angle device (Dataphysics, OCA 15 EC, Germany). Static contact angles of 10  $\mu\text{l}$  water were measured on the membranes. Each contact angle was measured three times at different positions of each membrane sample and an average value was calculated.

#### 3.6.2 Surface free energy

The contact angles of formamide and ethylene glycol were measured by contact angle device (Dataphysics, OCA 15 EC, Germany). Contact angle measurements were used to estimate the changes in the surface energy with image analysis software (SCA20). The surface energy measurement can classify the polar properties of treated and untreated membranes. The polar properties of membranes affected membranes selectivity performance.

### 3.6.3 Dielectric constant

Dielectric constant of the membrane was determined by using Precision LRC meter (Agilent 4258A) at frequencies from 75 kHz to 30 MHz with 1 MHz steps. Dielectric constant was calculated using equation  $\epsilon = C_p/C_0$ , where  $C_p$  is the capacitance measured using an LCR meter and the  $C_0$  is the vacuum capacitance. The latter was calculated using equation  $C_0 = \epsilon_0 A/t$ , where  $A$  and  $t$  are the cross-sectional area of the electrode and thickness of the sample, respectively.  $\epsilon_0$  is the permittivity of vacuum, equivalent to  $8.85 \times 10^{-12}$  F/m [12].

### 3.6.4 Membrane surface

The structure and morphology of membrane was determined with scanning electron microscope (SEM : FEI-Quanta 400). The samples were first frozen in liquid nitrogen and fractured for cross-sections analysis. After that the samples were gold-coated using a sputtering coater before scanning. Moreover, the membrane surface topography was observed using an atomic force microscope (AFM) operated in the tapping-mode scanning.

### 3.6.5 FTIR spectra

Fourier Transform Infrared Spectrometer (FTIR : Bruker, EQUINOX 55) was used to investigate functional groups of the membrane chemistry. The membrane was scanned at 400-4000  $\text{cm}^{-1}$  wave numbers.

## **Chapter 4**

### **Result and Discussion**

#### **4.1 Preparation of asymmetric polysulfone membranes**

Among many methods, phase separation was the common method for fabrication of flat sheet asymmetric membranes [25]. There are several researches which prepared asymmetric polysulfone membranes using tetrahydrofuran (THF) as a more volatile solvent such as Ismail et. al., (2003) [27] and Aroon et. al., (2010) [25]. They found that the skin layer is thicker and less defects. This was due to a volatile solvent can rapidly evaporate from the outermost surface of the membrane during polymer casting, which results in higher polymer concentration in the upper layer of the membrane lead to delayed liquid-liquid demixing and as a result, a dense skin layer with less defects and pin-holes was prepared [25].

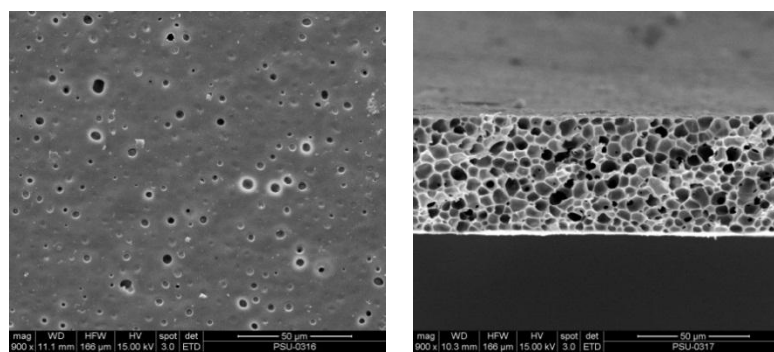
Acetone is a more volatile solvent with has boiling point 56 °C, while boiling point of THF is 66 °C [59]. It mean acetone more rapidly evaporate than THF so that it is possible to prepared asymmetric membranes with dense skin layer using acetone [25, 31, 32, 60]. Madaeni et. al., (2004) [31] found that addition of acetone in to polymeric solution consist of PSF and DMAc cause a decline in flux and an improvement in the retention of protein. In the same condition, Aryanti et. al., (2013) [32] reported humic acid rejection increase with acetone concentration increase. This is confirmed that acetone could improve dense membrane. In this study, asymmetric polysulfone membranes were prepared using acetone and DMAc as more volatile solvent and less volatile solvent, respectively. For study acetone effect on membranes structure, membranes were prepared without acetone follow by 4.1.1. After that, acetone was added in polymer solution follow by 4.1.2. Finally, both results were compared together.

#### 4.1.1 Effect of solvent

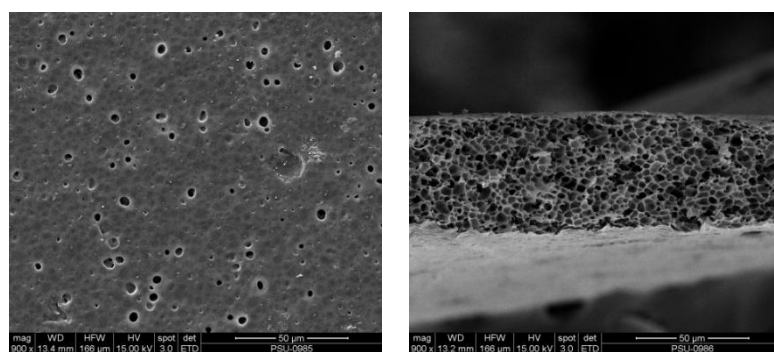
The 20% of polysulfone (PSF) was dissolved in different compositions of solutions as shown in Table 4.1. The SEM micrographs of surface layer and cross-sections of membranes prepared from various rates of solvent pairs (DMF : DMAc) were shown in Figure 4.1. All these fabricated membranes consist of spongy like substructure and no distinctive skin layer was formed. The membrane surface prepared under all conditions also illustrate defect. Therefore, difference of solvent is not significantly affects membranes structures. The asymmetric membrane was suitable for gas separation because of its high permeability and selectivity [3]. The structure of asymmetric membrane consists of a very thin and dense skin layer supported on a relatively thick and porous sublayers. The skin as the actual selective barrier, while the sublayer only as a mechanical support for the skin, with slight effects on separation [23]. Therefore, the membranes which prepared without a more volatile are unsuitable for gas separation.

**Table 4.1** The compositions of polymer solutions.

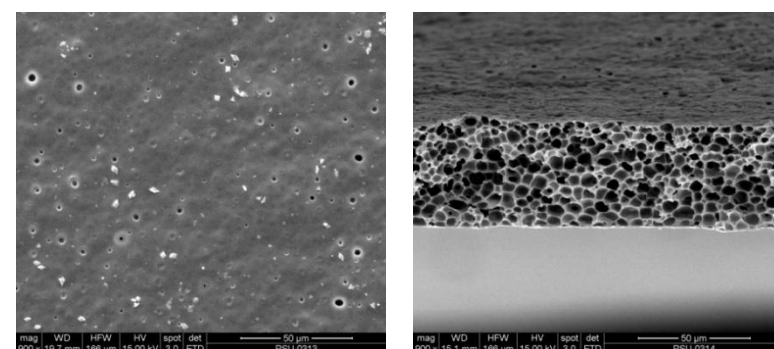
PSF (wt.%)	DMF (wt.%)	DMAc (wt.%)
20	80	-
20	40	40
20	-	80



(a)



(b)



(c)

**Figure 4.1** SEM micrographs of the surface (left) and the cross-sections (right) of the membranes prepared from 20% PSF; (a) 20%PSF: 80%DMF, (b) 20%PSF: 40%DMF: 40%DMAC and (c) 20%PSF:80%DMAC.

#### 4.1.2 The effect of volatile nonsolvent

Normally, quantity of PSF for prepare flat sheet membrane is 14%-22% [29]. There are many researches use DMAc as a solvent for PSF [29, 31, 32]. For fabricate the dense skin layer and free defect surface, THF usually was used as more volatile solvent. For this study, membranes were prepared from PSF (20% wt/wt), DMAc (60% wt/wt) and AC (20% wt/wt) using as more volatile solvent. The morphology of the membrane is generally very different from the membrane cast from a dope without Acetone (Figure 4.1) as shown in Figure 4.2. Acetone enables the fabrication of skin layer with less defects and pin-holes. Besides, it also changes the morphology of the membranes supporter from sponge-like to finger-like structure. This method produced asymmetric membranes, which suitable for gas separation [3]. This was in accordance with result determined by Aroon et. al., (2010) [25], although they used THF as a volatile solvent instead.

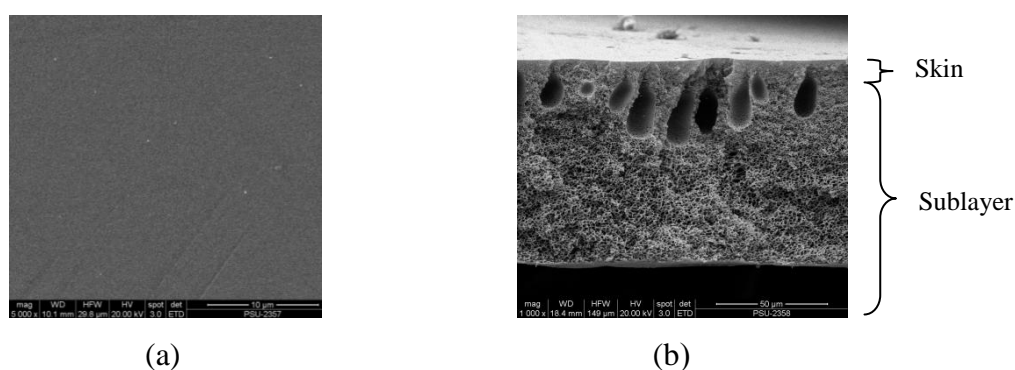


**Figure 4.2** SEM micrographs of surface (a) and cross-sections (b) of asymmetric membranes prepared from polymer solution consist of 20%PSF, 60%DMAc and 20%AC.

### 4.1.3 The effect of polymer concentration

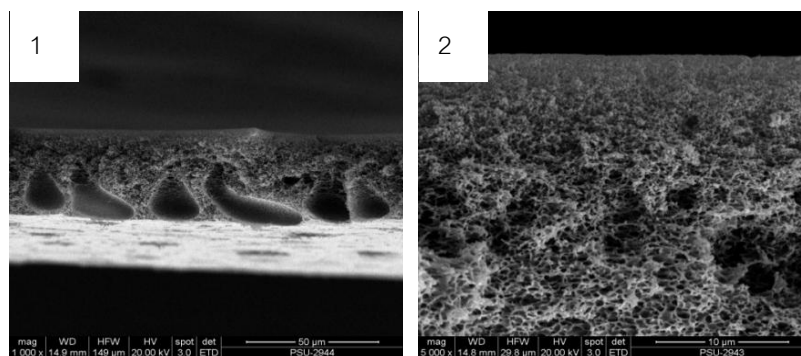
Asymmetric polysulfone flat sheet membranes were prepared by casting using solution consisting of polysulfone (polymer), DMAc (less volatile solvent) and acetone (more volatile solvent) of various concentrations (Table 4.2), while the ratio of DMAc and acetone was fixed at 2:1 (wt/wt).

The formation of dense skin layer and a sponge-like support with less macrovoid at higher polymer concentration are shown in Figure 4.3. The thicknesses of the skin layers are 2.4, 3.5 and 8.3  $\mu\text{m}$  for polymer concentrations of 19%, 22%, and 25%, respectively, and shown in Table 4.3. The formation of this structure is due to higher resistance for exchange of solvent and nonsolvent for more concentrated polymer. Therefore, a delayed liquid–liquid phase demixing is developed and hence a membrane skin with few pores or defects and denser support will be formed [29]. However, some macrovoids are still present.

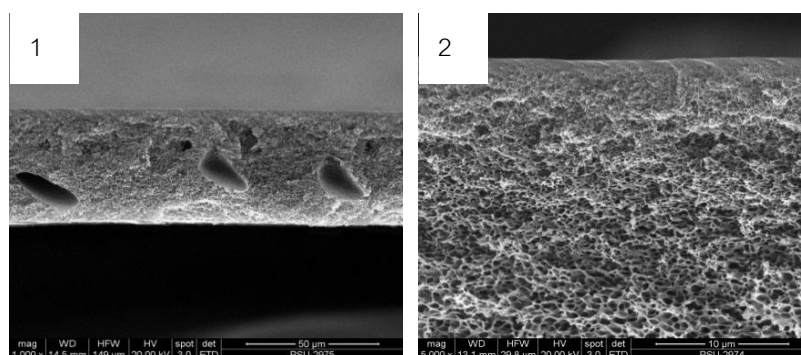
**Table 4.2** The composition of PSF membranes according to the PSF content.

Samples	PSF (wt.%)	DMAc (wt.%)	Ac (wt.%)
PSF19%	19	54	27
PSF22%	22	52	26
PSF25%	25	50	25

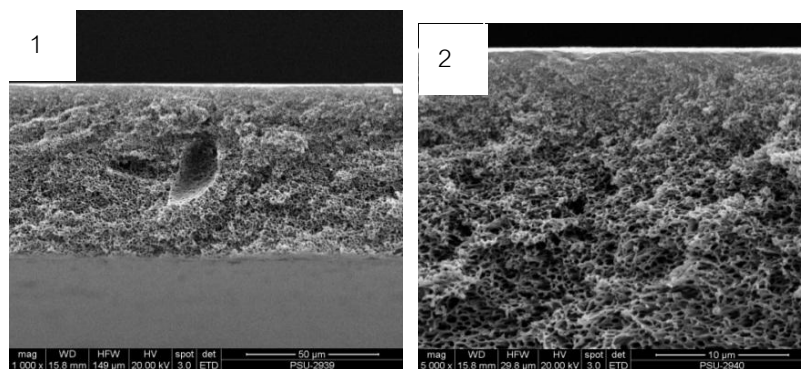
\*The ratio of DMAc and Ac was fixed at 2:1 (wt/wt)



(a)



(b)



(c)

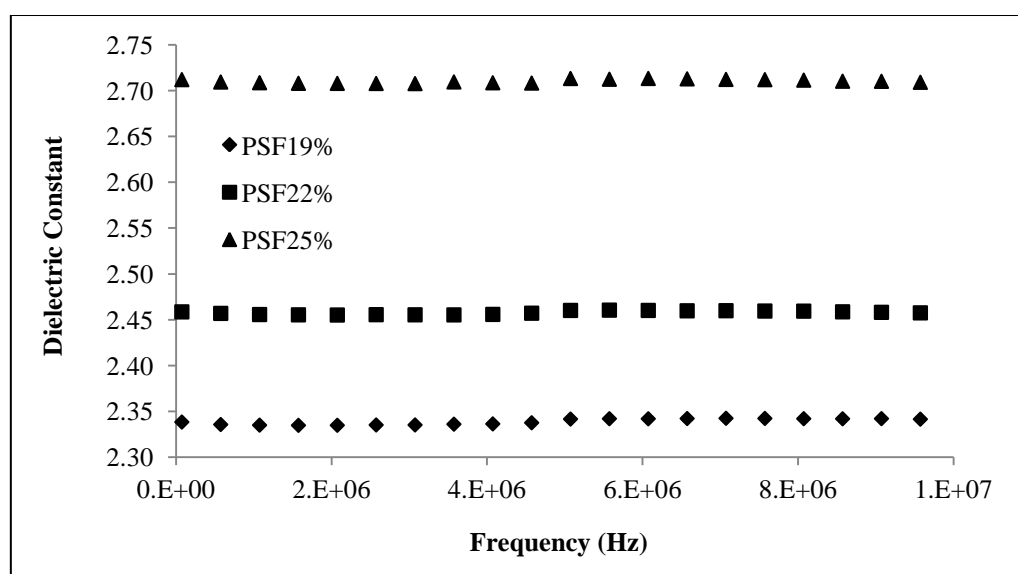
**Figure 4.3** SEM micrographs of the membranes cross-section prepared by different polymer concentrations; (a) PSF 19%, (b) PSF 22% and (c) PSF 25%; (1)  $\times 1,000$  and (2)  $\times 5,000$ .



**Table 4.3** The thicknesses of the skin layers.

Samples	Skin layers are ( $\mu\text{m}$ )
PSF19%	2.4 $\pm$ 0.3
PSF22%	3.5 $\pm$ 0.2
PSF25%	8.3 $\pm$ 0.4

To check on the effect due polymer concentrations, the membrane dielectric constant was investigated. Figure 4.4 shows that the dielectric constant of membranes is independent of the frequencies. Among the three polymer concentrations, the smallest and the greatest dielectric values belong to membrane PSF 19% and membrane PSF 25%, respectively. In fact, that membrane with a greater void volume would exhibit a smaller dielectric value, as described by Jaleh et. al., [12, 61]. This implies that the former concentration larger void volume and the reverse are smaller for the latter. This could be verified by the SEM micrograph in Figure 4.3.

**Figure 4.4** The dielectric property of PSF membranes.

## 4.2 Modification of asymmetric polysulfone membranes by UV-ray irradiation

### 4.2.1 The effect of UV-ray irradiation on contact angles

Measuring water contact angles was the simplest method for determining the hydrophilicity of the film surface. Water contact angle of PSF membranes was measured immediately after the UV ray treatment and shown in Figure 4.5 in comparison to the untreated ones. The untreated membranes have contact angles about  $71^{\circ}$  to  $76^{\circ}$  (irradiation time is 0 h as shown in Figure 4.5). However, those of the treated membranes reduced greatly after UV ray irradiation. In addition, the 312 nm UV wavelength reduced water contact angles of the treated membranes greater than the 254 nm wavelength. The contact angles reduced from  $71^{\circ}$ – $76^{\circ}$  to about  $15^{\circ}$ – $18^{\circ}$ , after 6 h of 312 nm ray treatment and being stable about  $10^{\circ}$ – $12^{\circ}$  after 12 h of the treatment. For 254 nm wavelength, they were about  $52^{\circ}$ – $59^{\circ}$  after 6 h treatment and became stable about  $52^{\circ}$ – $56^{\circ}$  after 12 h treatment. The results indicate that the UV ray treatment increased the hydrophilicity of PSF membranes. However, variation of polymer concentration from 19% to 25% did not significantly affect the hydrophilicity of the treated membranes.

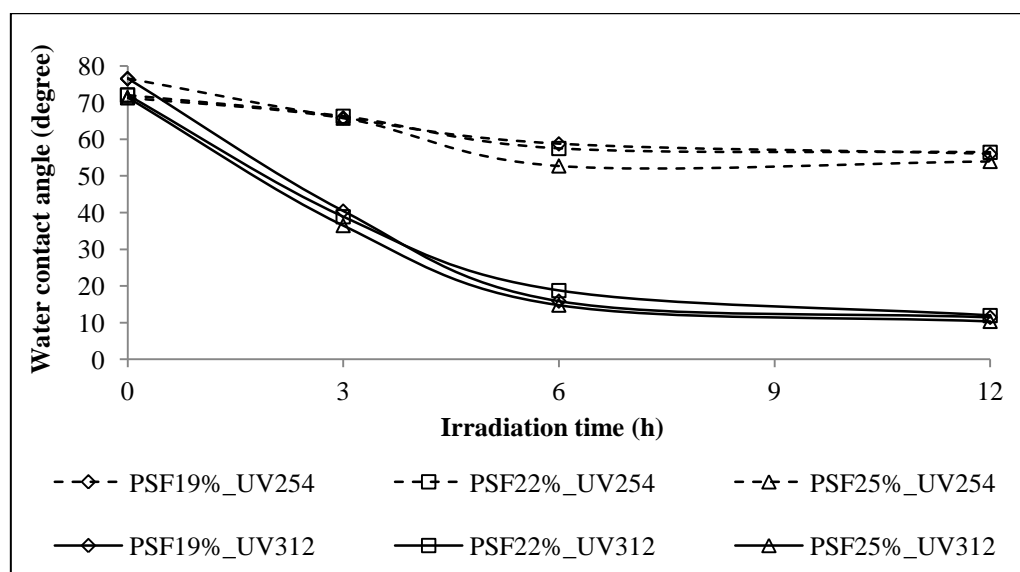


**Figure 4.5** Comparing water contact angles of PSF membranes irradiation by 254 and 312 nm UV ray wavelengths.

To test whether the effect from UV irradiation was permanent, further experiment was carried out on the treated membrane by measuring water contact angle after several periods of times. The treated membrane by the UV ray with 312 nm wavelength was selected for this study because this condition showed a very distinctive reduction of water contact angle. Changes in water contact angle with time was observed and shown in Figure 4.6. The contact angle for the treated membranes increased rapidly up to 1 week. They increased from 30° to 70°, from 25° to 35° and from 15° to 25° while the irradiation time was increased to 3, 6 and 12 h, respectively. Then they increased slowly during 1-2 weeks. It relatively stables after 3 weeks of storage time. At 3 h of irradiation, the water contact angle increased nearly equal to the untreated membranes within 2-4 weeks after the irradiation. It indicated that hydrophilicity gained by short irradiation time is not stable; the effect can be smaller and even disappear completely, namely “hydrophobic recovery” [62]. However, hydrophobic recovery decreased when irradiation time increased. Moreover, the polymer concentration affect water contact angle slightly at the same irradiation time.

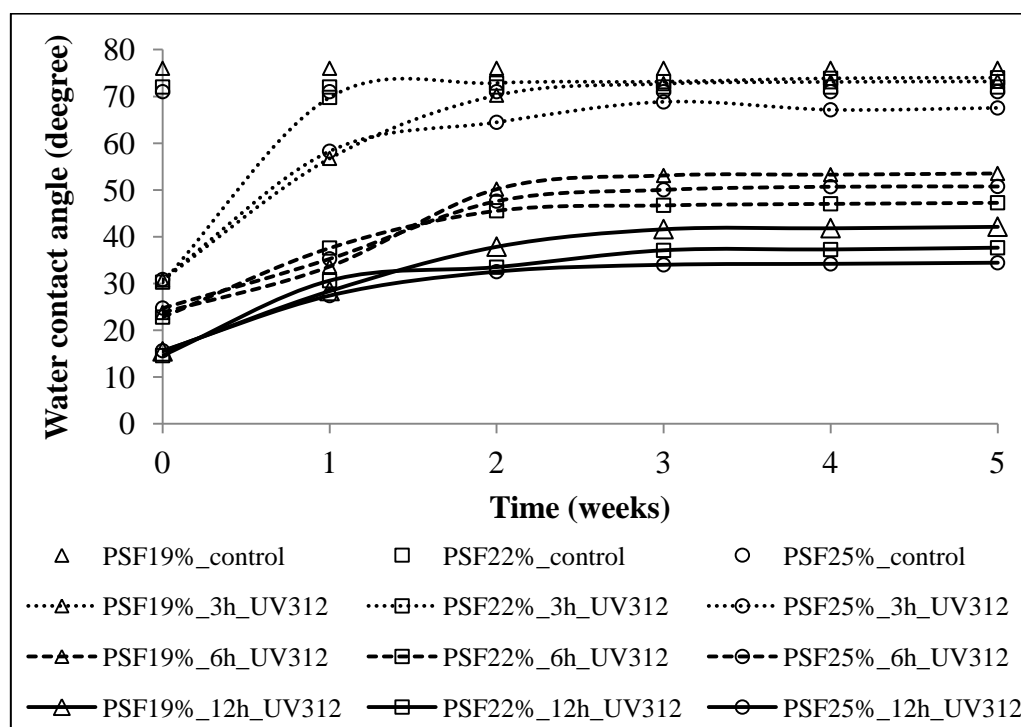
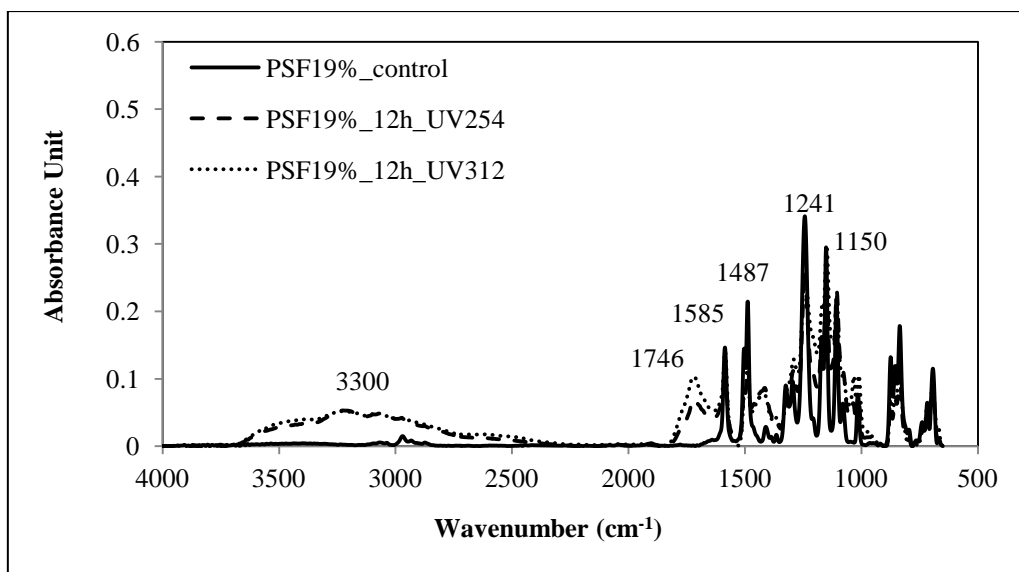


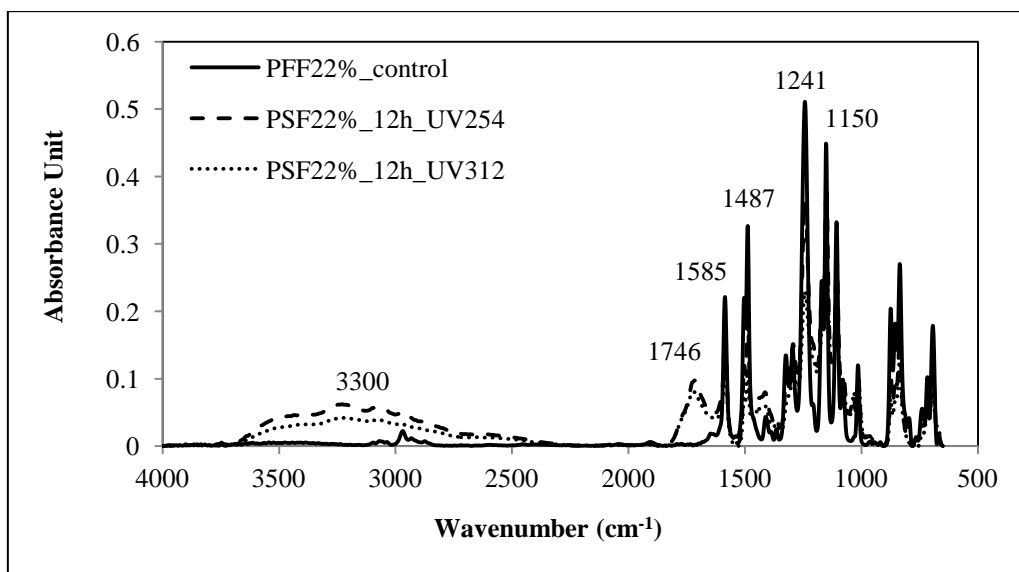
**Figure 4.6** Variation of water contact angles on the treated membranes by the UV ray with 312 nm wavelength vs. storage time.

#### 4.2.2 The effect of UV-ray irradiation on chemical structure

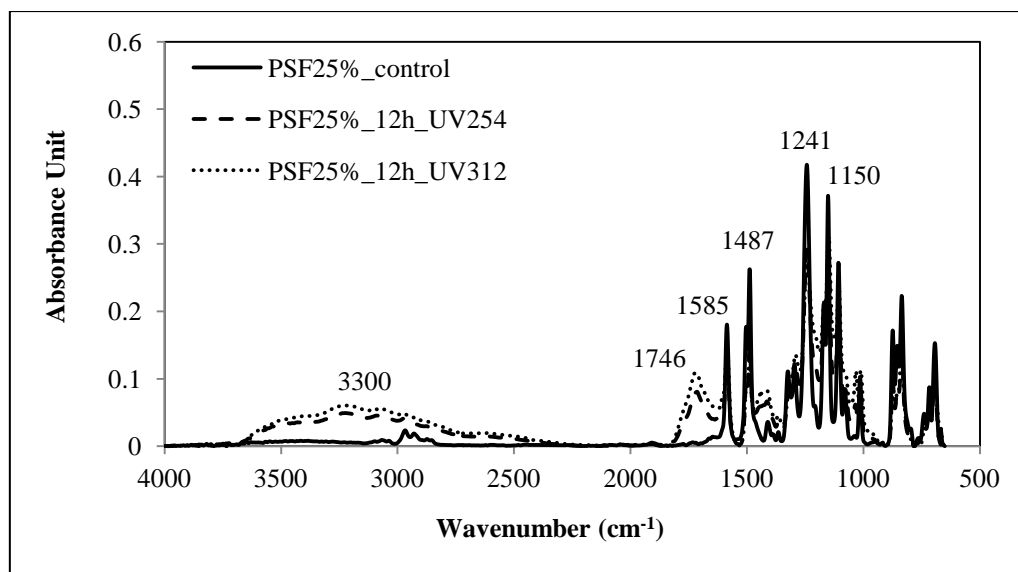
The treated film by UV ray with 254 and 312 nm wavelengths for 12 h was selected for this study because the contact angle shows minimum value at this condition. The FTIR spectra of the treated membranes were shown in Figure 4.7, compared to the untreated membranes. Based on the spectral change, the result show that variation of PSF has same effect on membrane functional groups. The PSF consists of a backbone made up of diaryl sulfone (Ar-SO<sub>2</sub>-Ar), diaryl ether (Ar-O-Ar) groups showed strong bands at 1150 and 1241 cm<sup>-1</sup>, respectively. The bands at 1487 and 1585 cm<sup>-1</sup> belong to the vibration of the aromatic (C=C) in PSF molecule [27]. However, the intensities of the peak at 1150, 1241, 1487 and 1585 cm<sup>-1</sup> decreased after UV ray treatment, while new broad peaks arose around 3300 cm<sup>-1</sup> and near 1746 cm<sup>-1</sup>. The peaks appeared around 3300 and 1746 cm<sup>-1</sup> are ascribed to the stretching vibration of hydroxyl (-OH) group and carbonyl (C=O) group, respectively. The appearance of the peaks around 3300 and 1746 cm<sup>-1</sup> by UV ray treatment indicates that the carbons in methyl group and in benzene ring of PSF were attacked and oxidized by UV ray to form carbonyl (C=O) group and hydroxyl (-OH) group. This is accordance with result determined by Choi et. al., (2003) [15], although they used ozone treatment instead. These functional groups were polar [11], resulting in an increase of the hydrophilic property of the membrane. In addition, it was found that the UV ray with 312 nm wavelength affected carbonyl and hydroxyl functional group of the treated membranes more than 254 nm wavelength. This result was consistent with the changes in hydrophilicity determinations using contact angle measurements.



(a)



(b)



(c)

**Figure 4.7** FTIR spectra of the untreated and the treated membrane by two UV ray wavelengths, 254 and 312 nm for 3 membranes; (a) PSF 19%, (b) PSF 22% and (c) PSF 25%.

#### 4.2.3 The effect of UV-ray irradiation on surface free energy

To confirm polar segments of the membrane, its surface properties were examined by contact angle measurement of formamide and ethylene glycol (Dataphysics, OCA 15 EC, Germany). The results were shown in Figure 4.8. For the treated membrane, it was found that surface free energy increased from 31-36 to 83-84 mN/m and polar component increased from 4-13 to 82-84 mN/m after . However, dispersive component decreased from 18-31 to 0.8-0.9 mN/m. Therefore, surface free energy increased mainly due to the increase of polar component. This result was consistent with surface modification of PSF membrane by oxygen plasma treatment of Kim et. al., (2002) [11]. This indicates UV induces the polar component to membranes surface. Moreover, the result shows that variation of PSF has same effect. Polymer concentrations affect the bulk of membrane while the surface free energy only measure on the surface. Therefore, polymer concentrations not affect polar component.

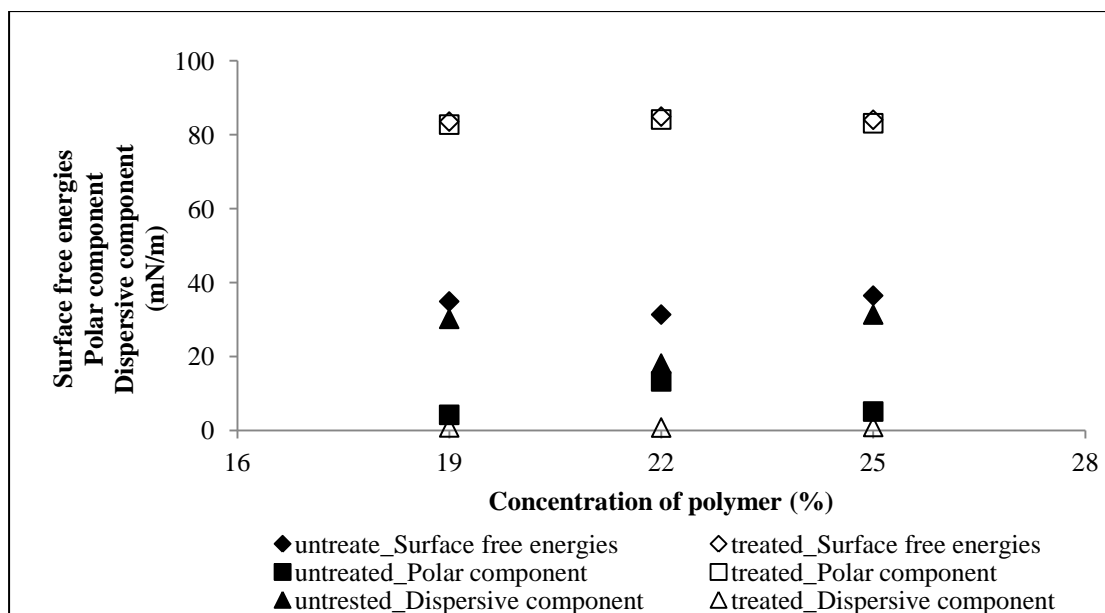
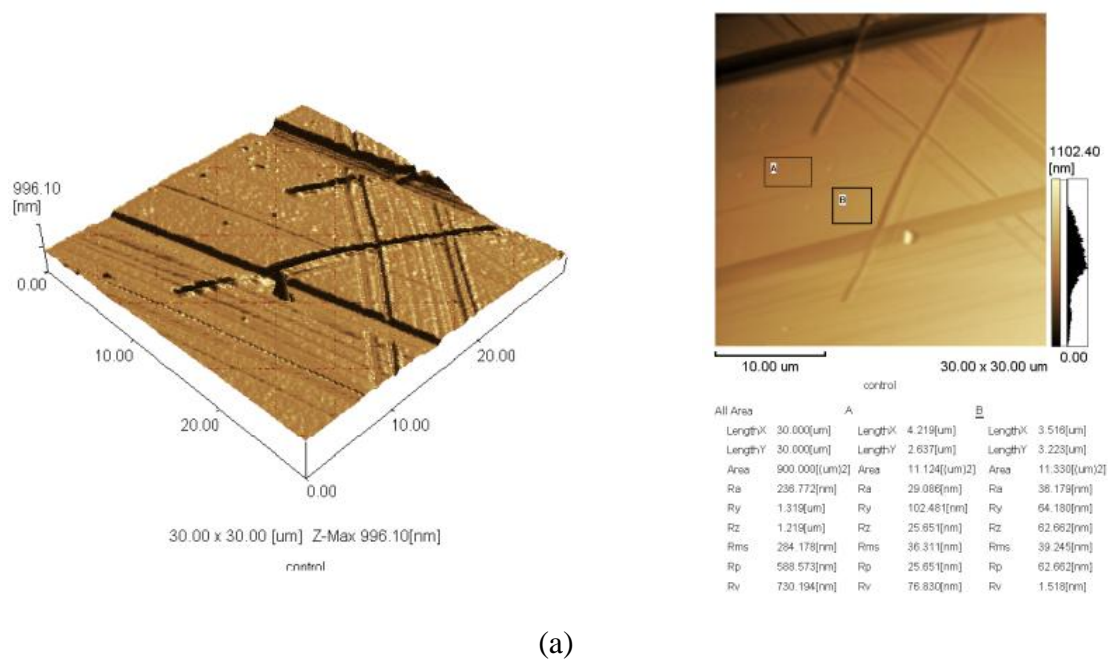


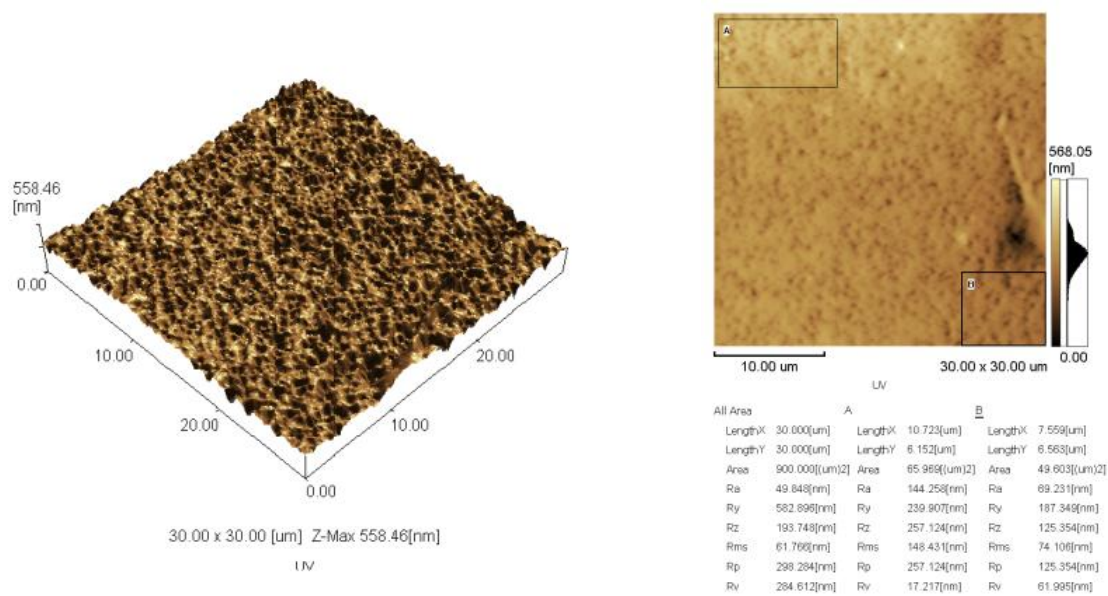
**Figure 4.8** Surface free energy of UV-ray irradiation polysulfone membrane with the increase in polymer concentration; (a) surface free energy, (b) polar component and (c) dispersive component.

#### 4.2.4 The effect of UV-ray irradiation on membranes surface

The hydrophilicity of membranes depend both the chemical groups at the polymer surface and the surface roughening [63]. The membrane surface topography was observed using an atomic force microscope (AFM). The AFM scanning found the membrane surface roughness increased significantly after the UV irradiation compared with the control, as shown in Figure 4.9. The reactions taking place in the chain, when irradiated with UV are bond scissions and dissociations of chain. Therefore, the surface roughening can be formed [13]. It may be supported the increasing hydrophilicity of polysulfone membranes due to this surface roughness enhanced water absorption [55].



(a)



(b)

**Figure 4.9** AFM images of untreated (a) and treated membranes (b) by UV ray.



#### 4.2.5 The effect of UV-ray irradiation on gas separation

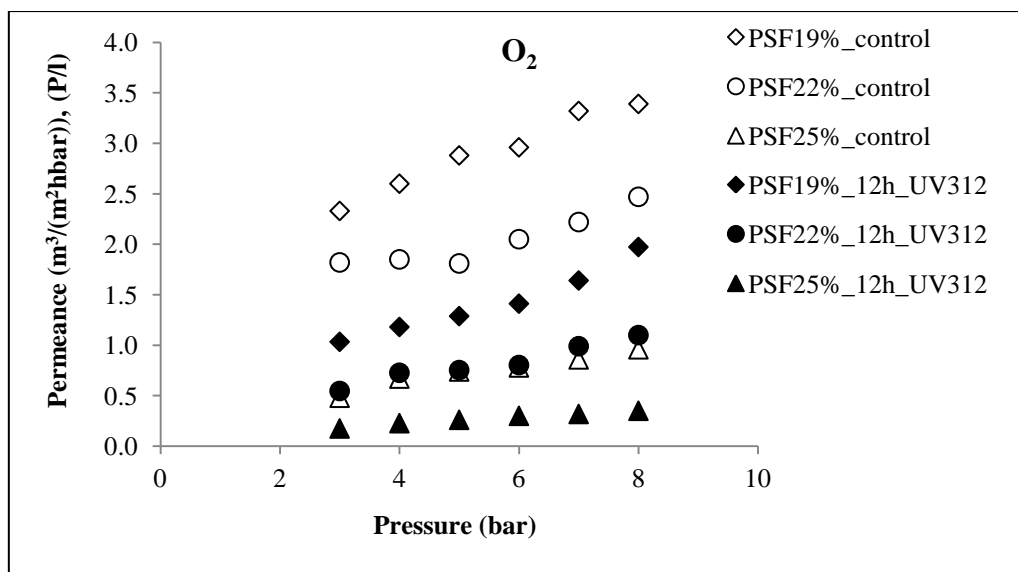
From contact angle result, the 12 h UV irradiation was the optimum condition due to it gave the lowest water contact angle. So that the 12 h UV treated membranes was selected for this study. The permeance of four gases through the untreated and treated membrane at different polymer concentration was investigated using equation (2.5), and illustrated in Figure 4.10. The result showed that O<sub>2</sub> permeation was decreased while permeation of N<sub>2</sub>, CH<sub>4</sub> and CO<sub>2</sub> was increased after UV irradiation. The permeation of N<sub>2</sub>, CH<sub>4</sub> and CO<sub>2</sub> were increased about 1.8, 2.6 and 4.2 times of the untreated membranes, respectively, while the permeation of O<sub>2</sub> was decreased about 2.5 times of the untreated membrane. Based on the principle of solution-diffusion mechanisms, solution parameter was controlled by affinity between the gas molecules and the polymer matrix [26]. In this case, membrane containing polar moieties have an affinity for N<sub>2</sub>, CH<sub>4</sub> and CO<sub>2</sub> due to dipole–quadrupole interaction [56]. UV irradiation improved polar group such as hydroxyl and carbonyl groups on membrane surface which confirmed by FTIR analysis. Therefore, the highly polar groups in the treated membranes should be more attractive to CO<sub>2</sub>, N<sub>2</sub>, and CH<sub>4</sub> because the CO<sub>2</sub> molecule has high quadrupole moment and polarizability, while the N<sub>2</sub> and CH<sub>4</sub> have high polarizability (Table 2.2) leads to more permeance. However, the O<sub>2</sub> has low quadrupole moment and polarizability lead to a repellant from polar membrane and hence smaller gas permeation was evidenced. This result was according to Klepac et. al., (2014) [64]. They explained the formation of carbonyl and carboxyl groups lead to increment of polarity of the chains. This contributes to the changes in permeability of nonpolar gases, like oxygen. Their research indicated the decrease in O<sub>2</sub> permeability with formation of carbonyl and carboxyl groups using polyethylene membranes treat by gamma ray [64].

In addition, solution parameter also depended condensability which was indicated by critical temperature ( $T_c$ ) whereas diffusion parameter was strongly influenced by the size of gas molecules, represented by their kinetic diameters (Table 2.2) [26]. This reason affected the untreated membranes because the molecular size of O<sub>2</sub> smaller than N<sub>2</sub> and its critical temperature hither than N<sub>2</sub>, hence O<sub>2</sub> permeance is

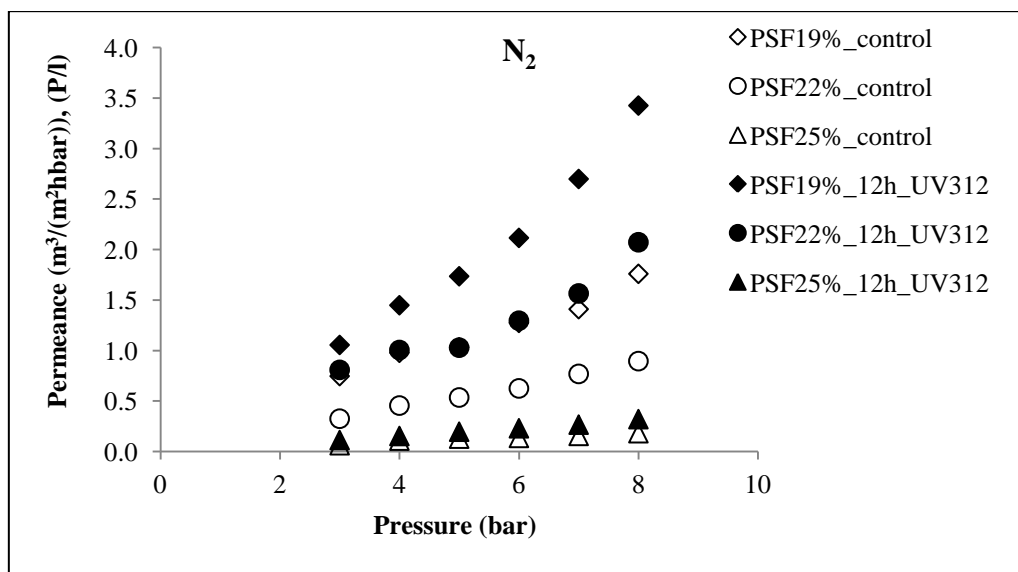
higher than  $N_2$  in the same condition. For the same reason,  $CO_2$  permeance is higher than  $CH_4$  [7, 26, 29, 57].

These permeations affect  $O_2/N_2$  and  $CO_2/CH_4$  selectivity of membranes because selectivity was a proportion of 2 gas permeation following equation 2.6. Therefore,  $O_2/N_2$  and  $CO_2/CH_4$  selectivity were calculated using data from Figure 4.10 (a-b) and Figure 4.10 (c-d), respectively, and shown in Figure 4.11 (a) and Figure 4.11 (b), respectively. The result shown the  $O_2/N_2$  selectivity decreases while the  $CO_2/CH_4$  selectivity increases after UV irradiation. For  $O_2/N_2$  selectivity, the permeance of  $O_2$  through the treated membranes decreases, while that of  $N_2$  increased lead to a decreasing in  $O_2/N_2$  selectivity. In the case of  $CO_2/CH_4$  selectivity, both permeances increase after UV irradiation but  $CO_2$  permeance was greater due to its greater quadrupole moment hence  $CO_2/CH_4$  selectivity was improved.

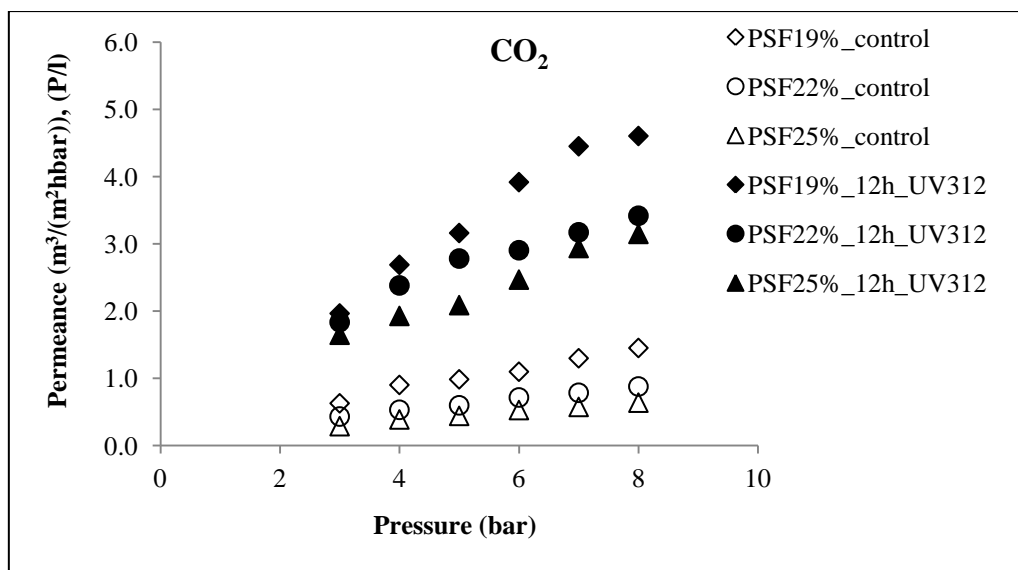
Moreover, it also pointed out that the selectivity increased with increased polymer concentration from 19% to 25%. The effect of polymer concentration of casting solution on gas permeance was reported by Madaeni et. al., (2011) [29] and Ismail and Lai (2003) [65]. They explained the increasing of casting concentration leads to delayed liquid–liquid phase demixing, which was resulted in an increment in the thickness of the skin layer. The membrane with thicker skin layer provides a low value of permeance but a relatively high degree of selectivity for gas separation process. In contrast, casting membranes from a dilute polymer solution produced a thin and porous skin layer, leading to a high value of permeance but a low selectivity. Therefore, PSF 25% illustrated the maximum selectivity for this studied. In addition, the selectivity decreased with increased pressure. The maximum selectivity of  $CO_2/CH_4$  and  $O_2/N_2$  was found at 3 bar. Considering the polymer concentration of 25% and pressure of 3 bar, the maximum of  $CO_2/CH_4$  selectivity was 6.4 which increased about 3 times of the untreated membranes. In contrast, the maximum of  $O_2/N_2$  selectivity was 7.5 belonging to the untreated membranes which was higher than the treated membranes by 4.9 times of the



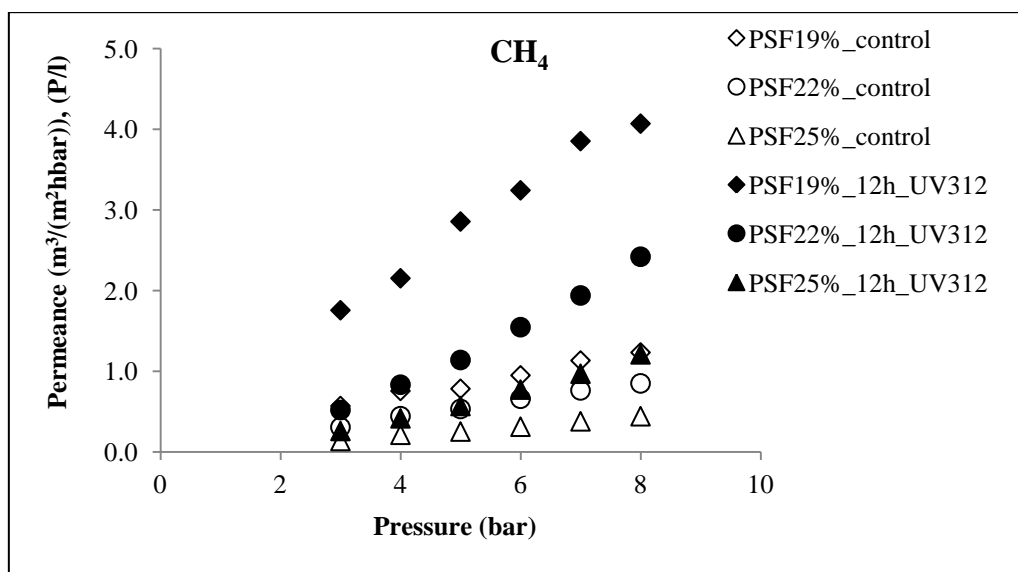
(a)



(b)

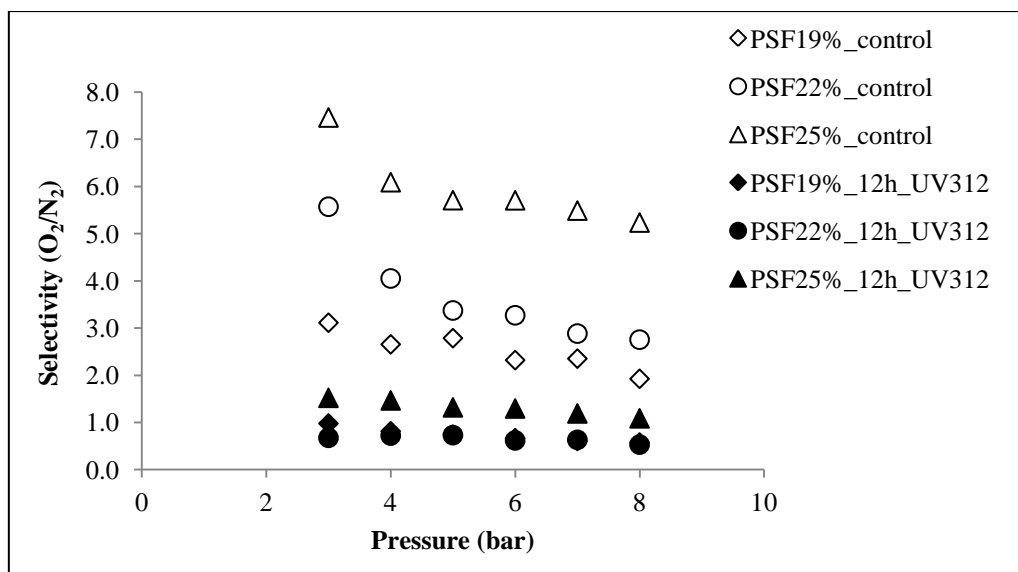


(c)

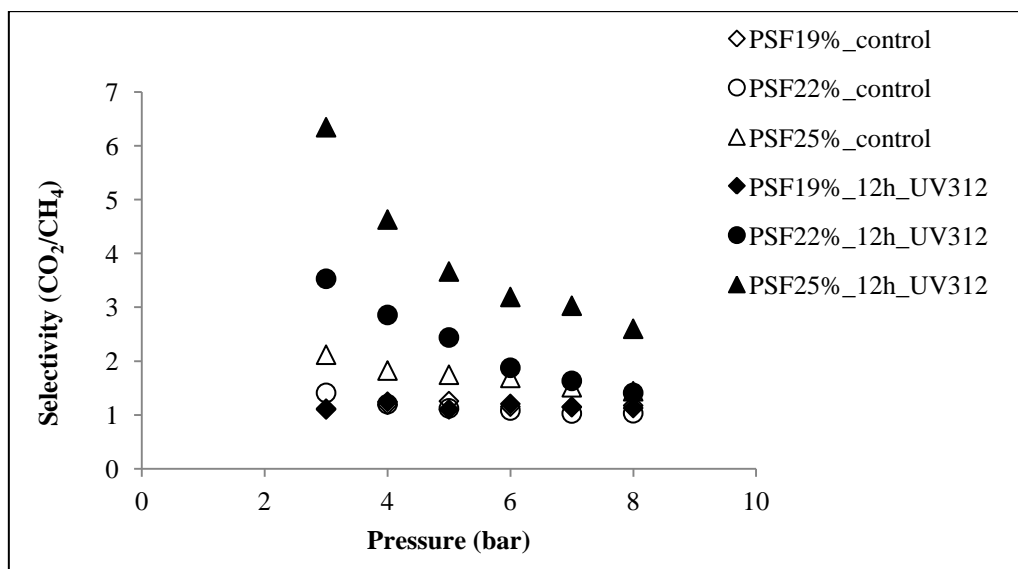


(d)

**Figure 4.10** Comparison of O<sub>2</sub> (a), N<sub>2</sub> (b), CO<sub>2</sub> (c), and CH<sub>4</sub> (d) permeation through the untreated and treated membrane by UV ray.



(a)



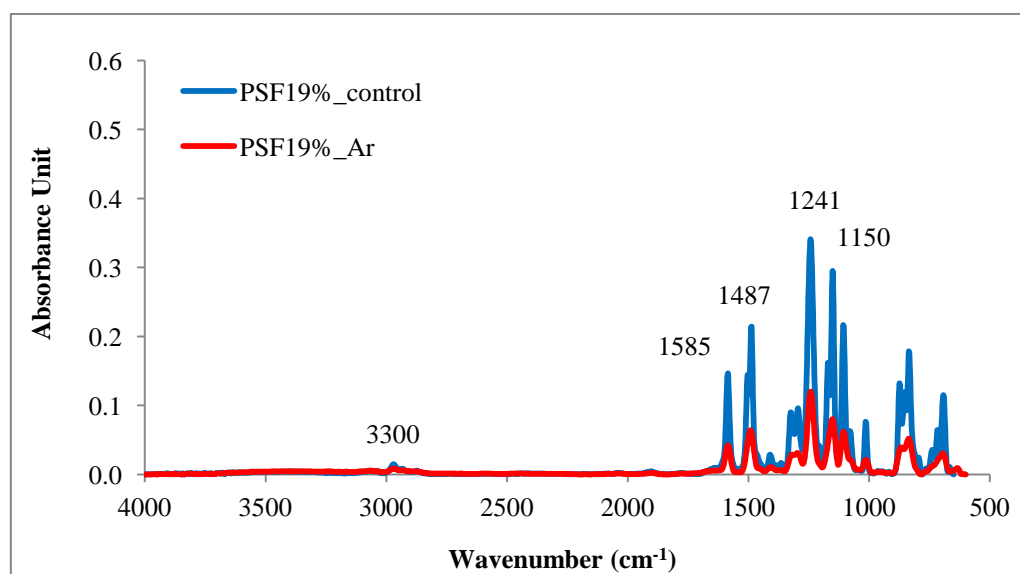
(b)

**Figure 4.11** Selectivity of the untreated and treated membrane by UV ray for  $O_2/N_2$  (a) and  $CO_2/CH_4$  (b).

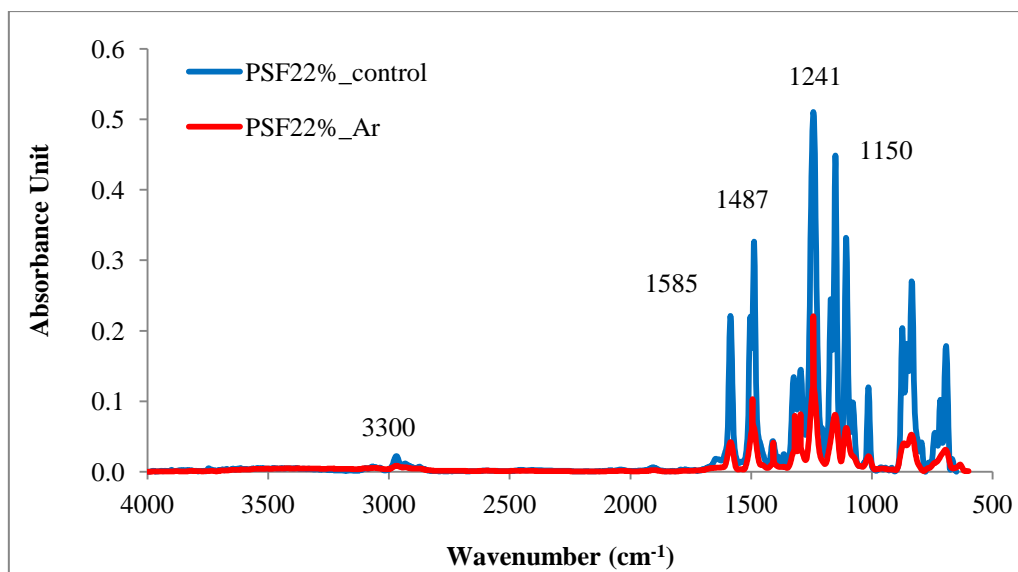
### 4.3 Modification of asymmetric polysulfone membranes by Ar plasma treatment

#### 4.3.1 The effect of Ar plasma treatment on chemical structure

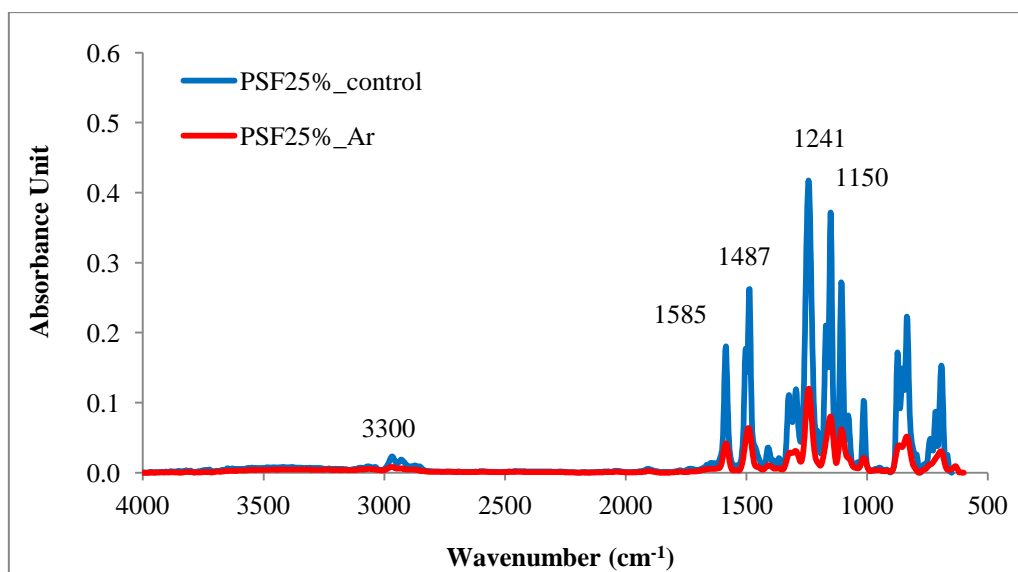
Figure 4.12 shows the FTIR spectra of the treated membranes by Ar plasma for 3 min, compared to the untreated membranes. The result shown that the PSF consists of a backbone made up of diaryl sulfone (Ar-SO<sub>2</sub>-Ar), diaryl ether (Ar-O-Ar) groups showed strong bands at 1150 and 1241 cm<sup>-1</sup>, respectively. The bands at 1487 and 1585 cm<sup>-1</sup> belong to the vibration of the aromatic (C=C) in PSF molecule [27]. However, the intensities of the peak at 1150, 1241, 1487 and 1585 cm<sup>-1</sup> decreased after Ar plasma treatment. PSF was natural hydrophobic. Therefore, it may be decreasing these peaks lead to the increasing hydrophobicity of PSF.



(a)



(b)



(c)

**Figure 4.12** Comparison of FTIR spectra of the untreated and the treated membrane by UV ray; (a) PSF 19%, (b) PSF 22% and (c) PSF 25%.

### 4.3.2 The effect of Ar plasma treatment on contact angle

The dependence of the water contact angle on the treatment time for the membranes treated in Ar plasma at  $2.5 \times 10^{-1}$  mbar are presented in Figure 4.13. For polymer concentrations of 19%-25%, they showed similarly result. The contact angles are rapidly decreasing with values up to  $20^\circ$ - $30^\circ$ , in 3 min of treatment, afterward increases until 5 min and reaching after 5 min a value relatively stable at  $40^\circ$ - $50^\circ$ . However, the highest value is also lower with  $30^\circ$  than the value of the untreated membranes (0 min). The contact angle value depend both the chemical groups at the polymer surface and the surface roughening. These factors cannot be separated from the measurements [63]. Due to Ar is non polymerizing gases, therefore, Ar plasma causes not only ablation of polymeric material but also deposition of degraded particles. Ablation usually occur the higher ratio at the beginning of the plasma treatment process. This treatment resulted in increase of the surface roughness and the wettability. So the contact angles decrease in the early stage of treatment time. After that the particles from degraded membrane skin could be deposited on membrane surface, as a result, decrease of defect or roughness during plasma treatment [51]. Therefore, the contact angles increase for the latter. From FTIR spectra, they indicate the decreasing of hydrophobic peak after treatment. It may be lead to the increasing hydrophobicity of membrane. Therefore, although contact angles increased, they are not equal to the untreated membrane. The results indicate the plasma treatment increase of polysulfone membranes. The maximum hydrophilicity is found in 3 min of treatment.

Variation of water contact angle with storage time was also performed and the result was shown in Figure 4.14. It showed that the water contact angle for the plasma treated membranes increases with the increase of storage time. The water contact angle rapidly increases within 1 week, and then it increases slowly during 2-3 weeks. It relatively stables after 3 weeks of storage time. This was due to hydrophilicity gained by plasma modification not stable. This phenomenon was caused mobility of surface functionalities, or sorption of hydrophobic moieties appearing in laboratory air lead to hydrophobic recovery [62]. However, the treatment



time about 3-5 min was shown minimum hydrophobic recovery. Therefore, polysulfone membrane with Ar plasma treatment time for 3 min was an optimum condition.

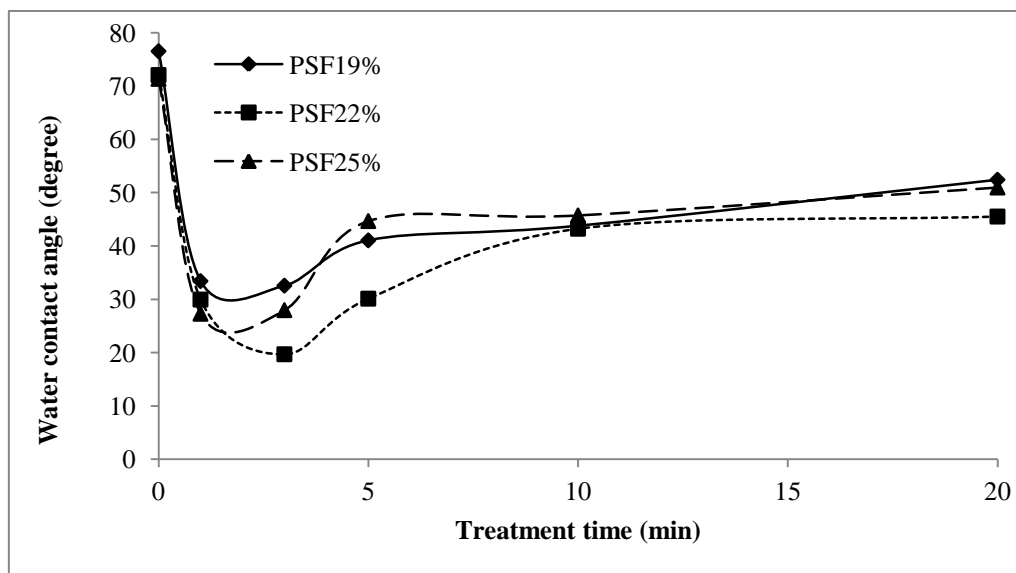
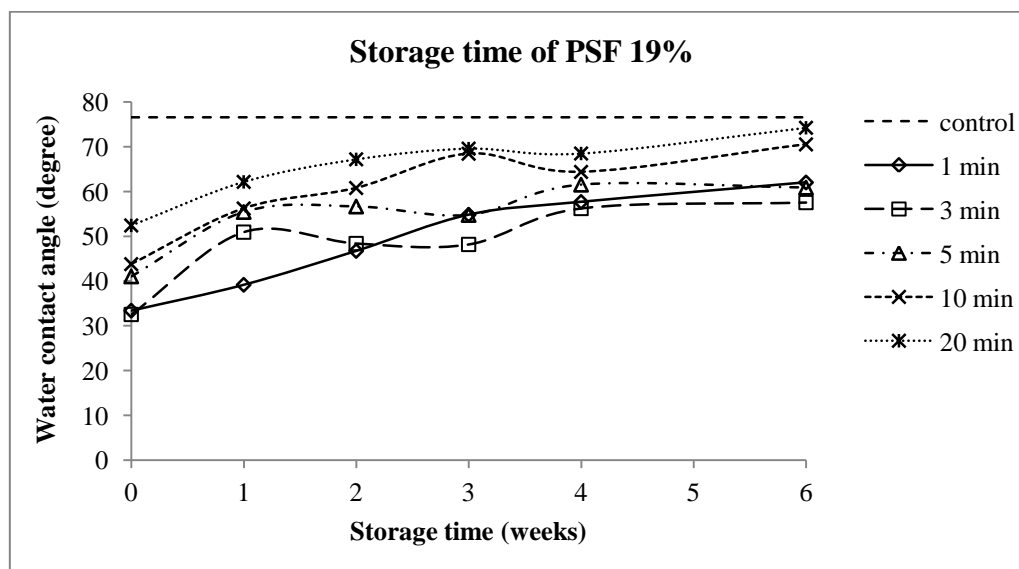
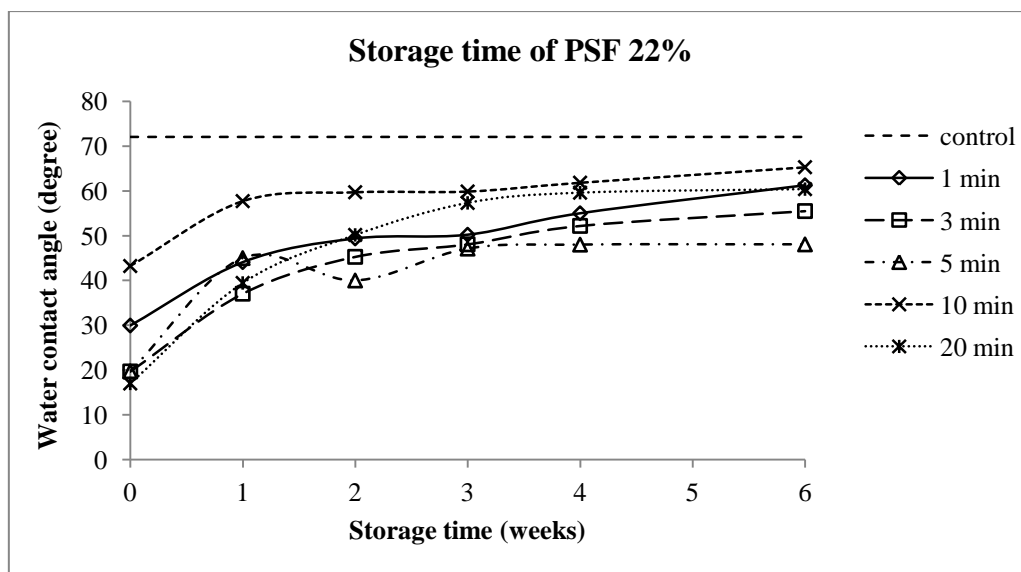


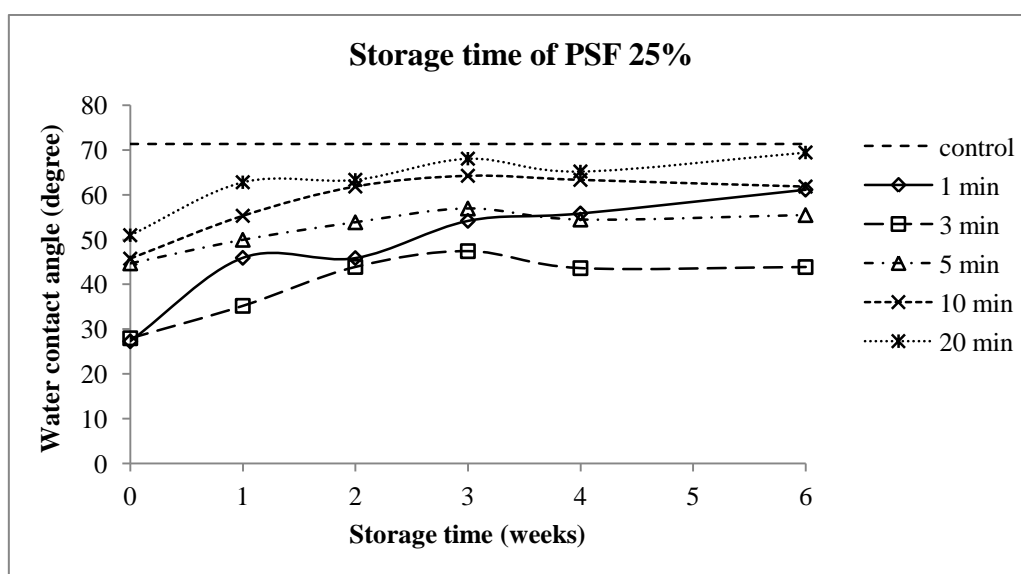
**Figure 4.13** Water contact angles of the treated PSF membranes by Ar plasma treatment for 1-20 min.



(a)



(b)

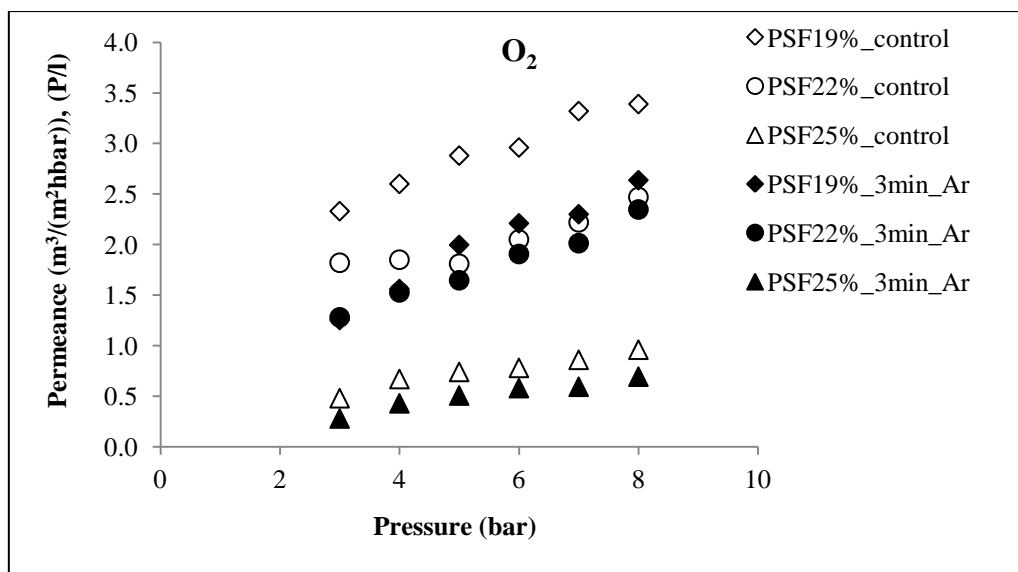


(c)

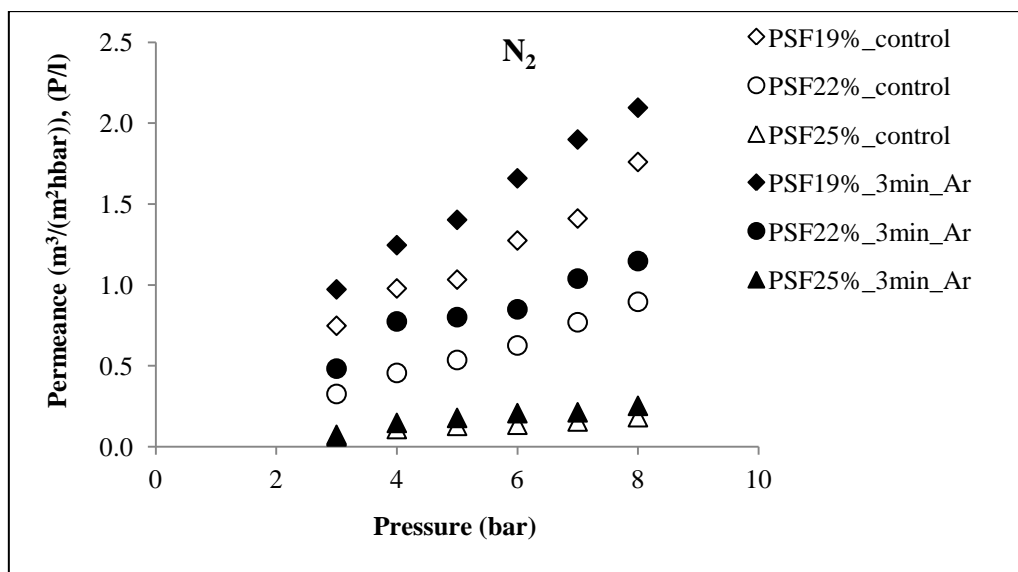
**Figure 4.14** The water contact angle as a function of the storage time for the PSF19% (a), PSF22% (b) and PSF25% (c) modified by Ar plasma for 1-20 min.

### 4.3.3 The effect of Ar plasma treatment on gas separation

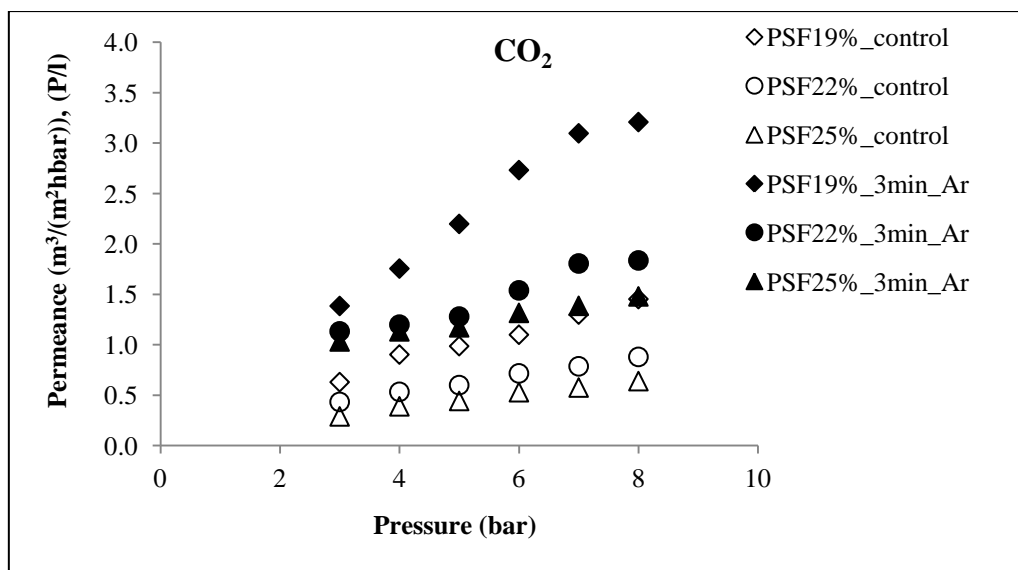
The 3 min Ar plasma treatment membrane was selected for this study because it was the optimum condition which observed by the lowest water contact angle. The permeance and selectivity of four gases through the untreated and treated membrane at different polymer concentration was investigated using same method with UV irradiation. The results were shown in Figure 4.15-4.16. It was noted that Ar plasma treatment effected was similar to UV irradiation but lower. That was decreasing  $O_2$  permeation while permeation of  $N_2$ ,  $CH_4$  and  $CO_2$  were increased after Ar plasma treatment. The permeation of  $N_2$ ,  $CH_4$  and  $CO_2$  were increased about 1.4, 1.8 and 2.4 times of the untreated membranes, respectively, while the permeation of  $O_2$  was decreased about 1.4 times of the untreated membrane. This effect was caused by dipole-quadrupole interaction [56] between polymer matrix and gas molecules, as well as UV irradiation. These permeations affect  $O_2/N_2$  and  $CO_2/CH_4$  selectivity, which was shown in Figure 4.16. The result shown the  $O_2/N_2$  selectivity decreases while the  $CO_2/CH_4$  selectivity increases after Ar plasma treatment. For  $O_2/N_2$  selectivity, the permeance of  $O_2$  through the treated membranes decreases, while that of  $N_2$  increased lead to a decreasing in  $O_2/N_2$  selectivity. In the case of  $CO_2/CH_4$  selectivity, both permeances increase after Ar plasma treatment but  $CO_2$  permeance was greater than  $CH_4$  and hence  $CO_2/CH_4$  selectivity was improved. In addition, the selectivity increased with increasing polymer concentration from 19% to 25%. The PSF 25% illustrated the maximum selectivity for this studied. Although the selectivity decreased with increased pressure, however, the maximum selectivity of  $CO_2/CH_4$  and  $O_2/N_2$  was found at 3 bar. For the polymer concentration of 25% and pressure of 3 bar, the  $CO_2/CH_4$  and  $O_2/N_2$  selectivity of Ar plasma treatment membranes were 4.3 and 3.8, respectively, which increased about 2 times and decreased about 2 times of the untreated membranes, respectively,



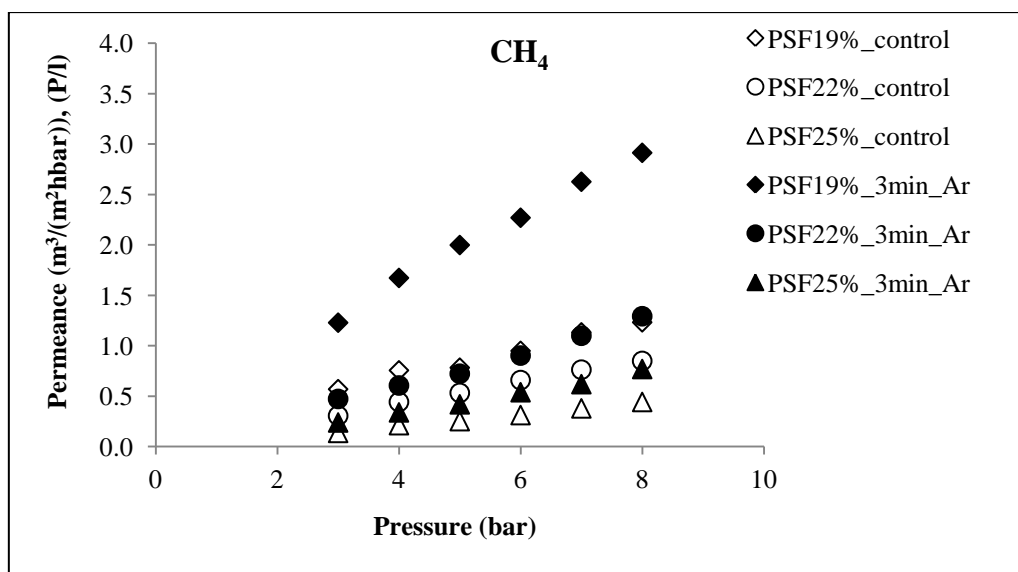
(a)



(b)

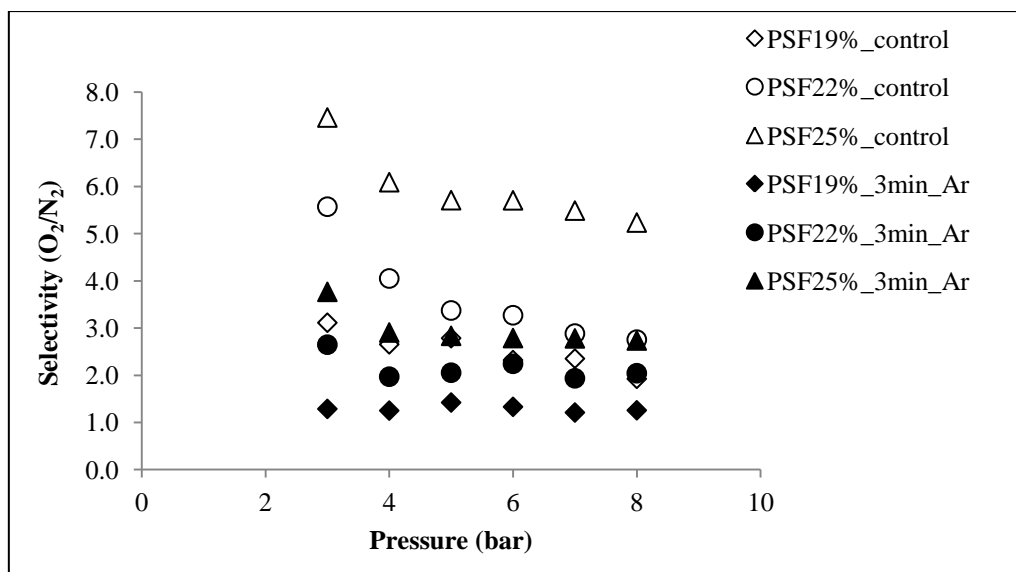


(c)

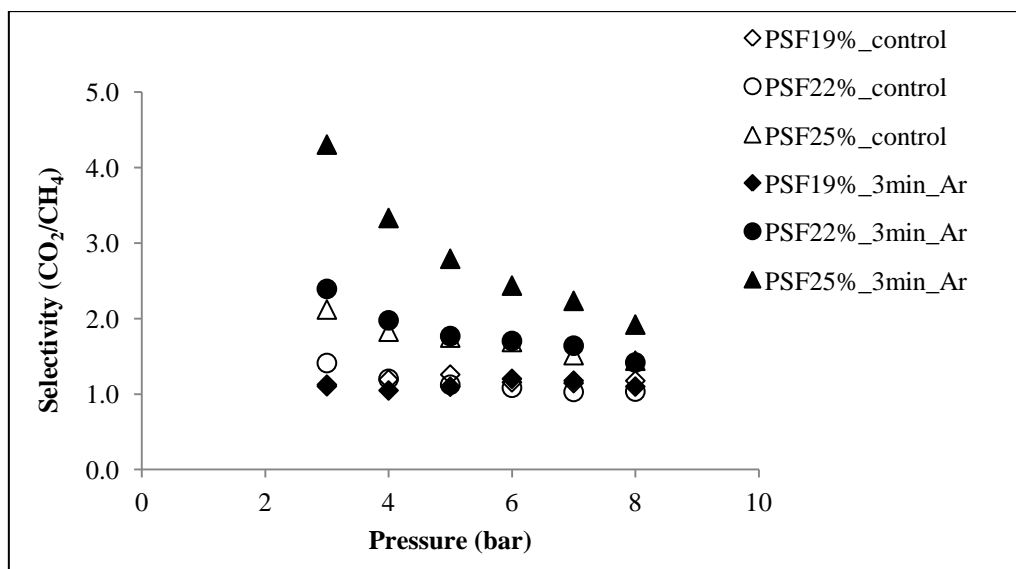


(d)

**Figure 4.15** Comparison of O<sub>2</sub> (a), N<sub>2</sub> (b), CO<sub>2</sub> (c), and CH<sub>4</sub> (d) permeation through the untreated and treated membrane by UV ray.



(a)



(b)

**Figure 4.16** Selectivity of the untreated and treated membrane by UV ray for O<sub>2</sub>/N<sub>2</sub> (a) and CO<sub>2</sub>/CH<sub>4</sub> (b).

#### 4.4 Preparation of polyethylene membranes

SEM micrograph of PE film was shown in Figure 4.17. The result illustrated the evenness of PE film surface. For the cross-section, the SEM micrograph showed the dense structure without distinct pore. The average thickness of film which measured using a thickness gauge (Peacock, Model G-7C, Japan) was about 13 $\mu$ m.

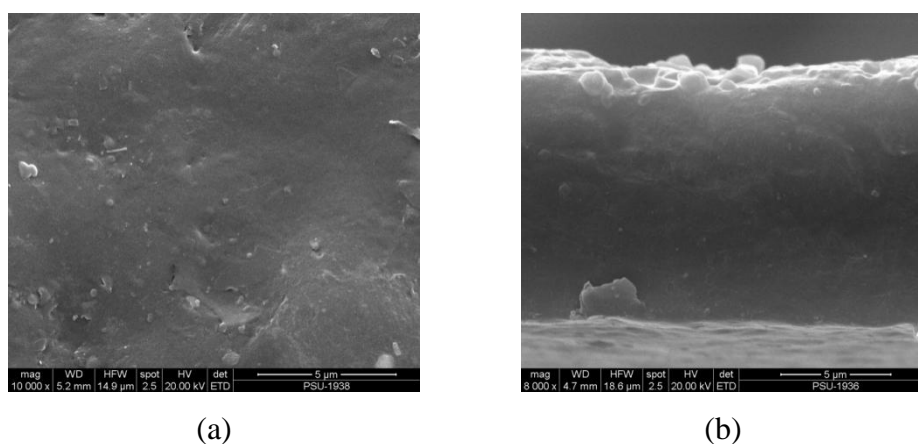


**Figure 4.17** SEM micrographs of the PE film; (a) surface and (b) cross-section.

#### 4.5 Modification of polyethylene film by UV irradiation

##### 4.5.1 The effect of UV irradiation on contact angle

The effect of UV ray with 312 nm wavelength irradiated on water contact angle values was shown in Figure 4.18. The result showed that an average water contact angles of the untreated PE film surface was about 110°. For the treated film, UV ray irradiation hardly affected water contact angle during 3-12 h of irradiation time. However, the water contact angles decreased gently from 105°-83° after UV ray treatment for 12 -18 h and stable at about 80° after 24 h of treatment time. This result indicates the hydrophilicity of PE film increase lightly after UV irradiation at least 24 h. Therefore, this method was unsuitable for PE surface modification

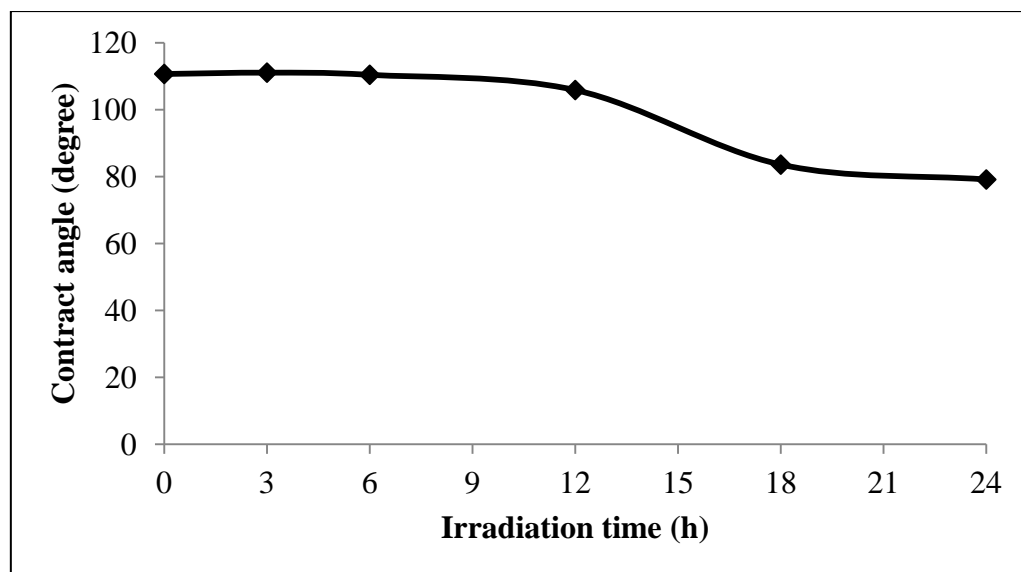


**Figure 4.18** Water contact angles of the untreated and the treated film by the UV irradiation with 312 nm wavelength for 3-24 hr.

#### 4.6 Modification of polyethylene film by Ar plasma treatment

##### 4.6.1 The effect of Ar plasma treatment on water contact angle

The effect of Ar plasma treatment on water contact angle of PE film was measured and shown in Figure 4.19. It was a function of treatment time. The results showed that the water contact angle sharply decrease after 1 min of plasma treatment, and then lightly decrease, reaching after 3 min a value stable at about  $10^\circ$ , which decreased from  $110^\circ$  of the untreated PE film. The results indicate the Ar plasma treatment could increase hydrophilicity of PE film.

Water contact angle variation of PE film treated by Ar plasma with storage time was carried out and the result was shown in Figure 4.20. It showed that the water contact angle increases with the increase of storage time. The water contact angle rapidly increases within 2 week, and then it increases slowly during 3-4 weeks. However, their water contact angle not saturated. This indicated the hydrophilicity not stable. This was caused mobility of surface functionalities, or sorption of hydrophobic moieties appearing in laboratory air lead to hydrophobic recovery [62]. However, the



treatment time about 10 min was shown minimum hydrophobic recovery. Therefore, PE film with Ar plasma treatment time for 10 min was an optimum condition.

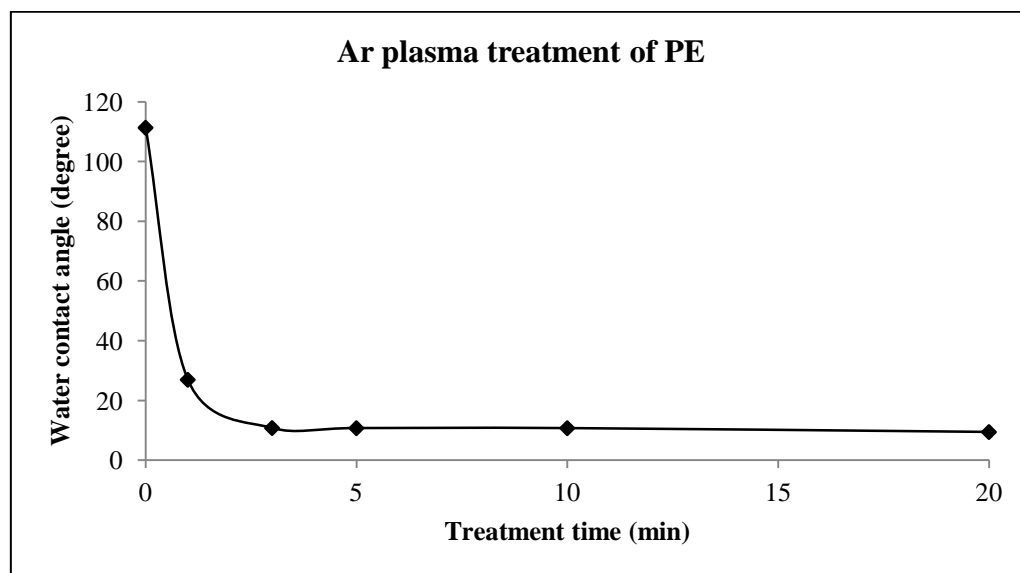


**Figure 4.19** Water contact angles of the PE file treated by Ar plasma for 1-20 min.

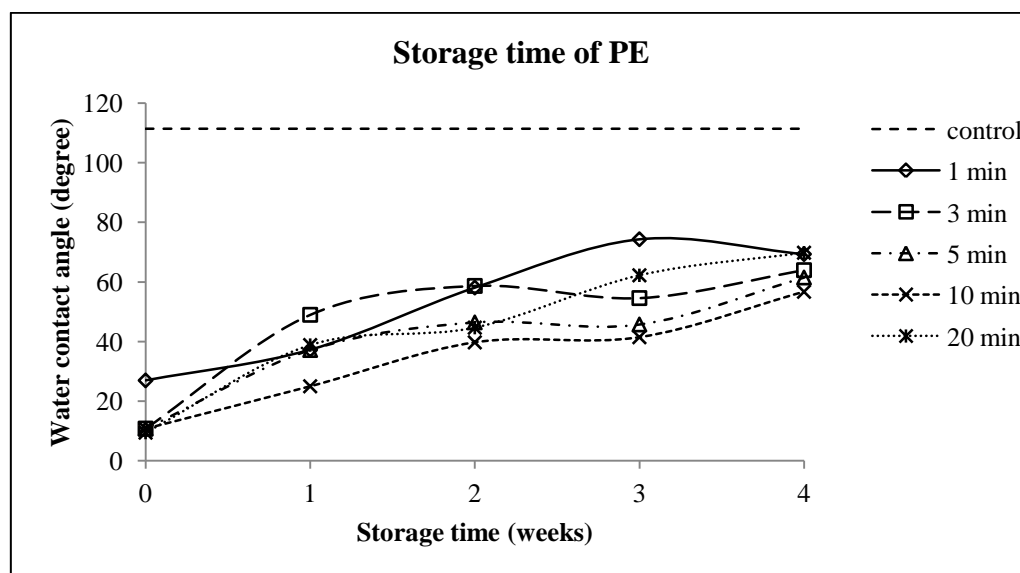


**Figure 4.20** Water contact angle as a function of the storage time for the PE film treated by Ar plasma for 1-20 min.

#### 4.6.2 The effect of Ar plasma treatment on chemical structure

The chemical structures of PE film were characterized by FTIR spectroscopy. The FTIR spectra of the untreated and Ar plasma treated PE was shown in Figure 4.21 and 4.22. A strong absorption was characteristic for the symmetric and non-symmetric stretching of C-H bonds in methyl and methylene groups [64]. The absorption peaks of 2915, 2848, 1468, and 725  $\text{cm}^{-1}$  are attributed to methylene non-symmetry stretch vibration, methylene symmetry stretch vibration, methylene non-symmetry changing angle vibration, and methylene swing in plane vibration, respectively (Figure 4.21) [66, 67]. When the Ar plasma treated PE spectrum was compared with the untreated PE spectrum, these peaks reduced. Moreover, two new broad band occur around 3300  $\text{cm}^{-1}$  and 1500-1747  $\text{cm}^{-1}$  (Figure 4.22), which corresponds to the hydroxyl group (-OH) and the oxygen based groups [67].

After Ar plasma treatment, the low molecular weight chains on the PE surfaces such as C-H and C-C were broken and in turn help in improving the cross linkage density. This results in the reduced methylene stretch vibration because the cross-linking of molecular chains could prevent the stretch vibration. And hence the surface was activated. When plasma treated PE film were exposed to the atmosphere, the plasma activated surface readily adsorbs the moisture in the air which was indicated by the broad band at 3300  $\text{cm}^{-1}$  and 1500-1747  $\text{cm}^{-1}$  in PE [66-68]. The band around 3300  $\text{cm}^{-1}$  was due to the hydroxyl group (-OH). The band around 1500-1747  $\text{cm}^{-1}$  present the oxygen based groups, which contain carbonyl groups absorption (C=O stretch) in the range of 1750-1600  $\text{cm}^{-1}$  and COO- asymmetrical stretching at 1645  $\text{cm}^{-1}$  [67, 68]. These additional peaks illustrated the functionalization of the PE film surface after Ar plasma. Hence the water contact angle of PE sample decreased from 110°-10° after Ar plasma treatment due to the formation of polar groups like hydroxyl group and other oxygen based groups. The results indicated the Ar plasma could increase the hydrophilicity of PE surfaces [67, 69].

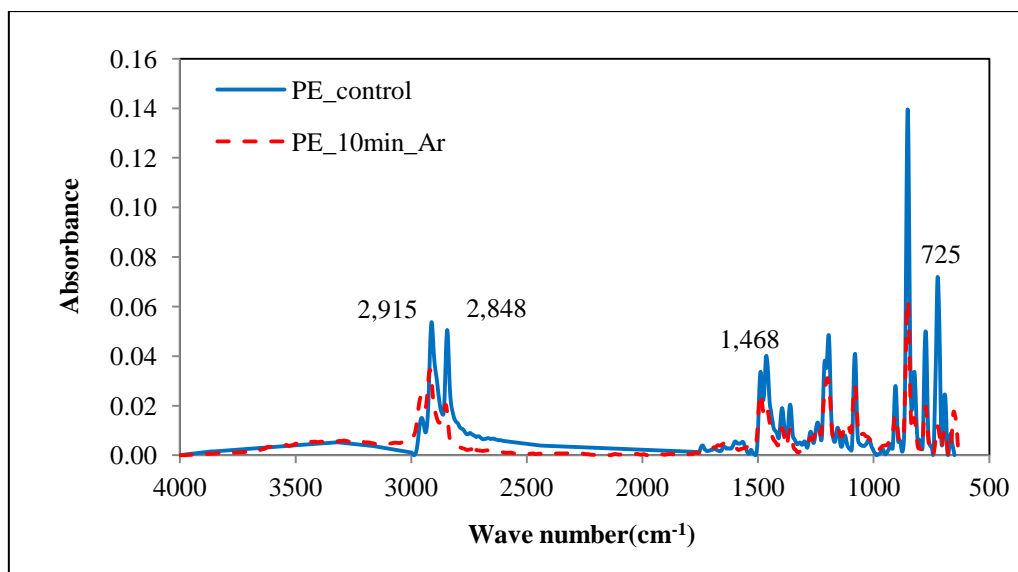


**Figure 4.21** FTIR spectra of PE films in the range from  $600 \text{ cm}^{-1}$  to  $4000 \text{ cm}^{-1}$

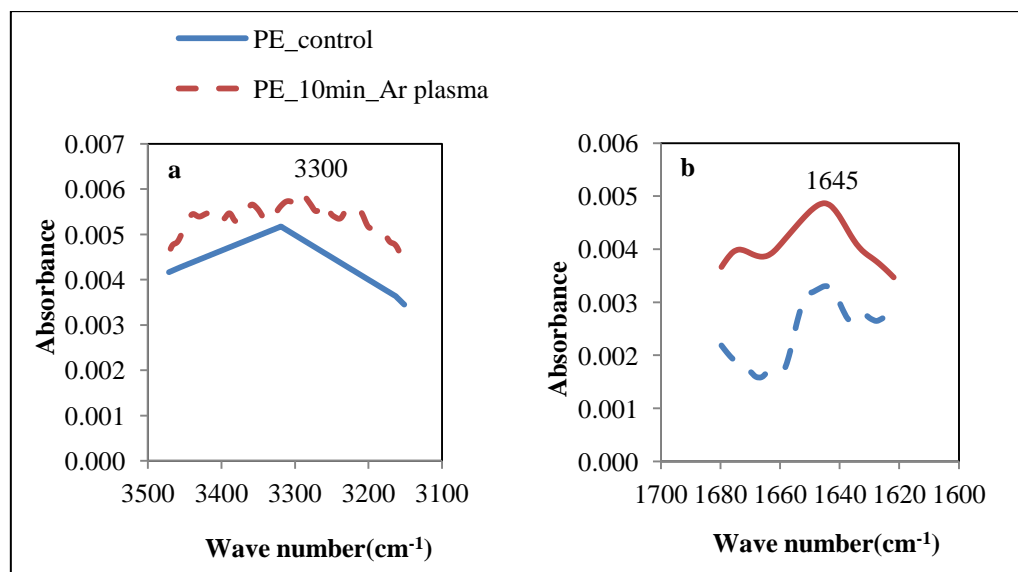


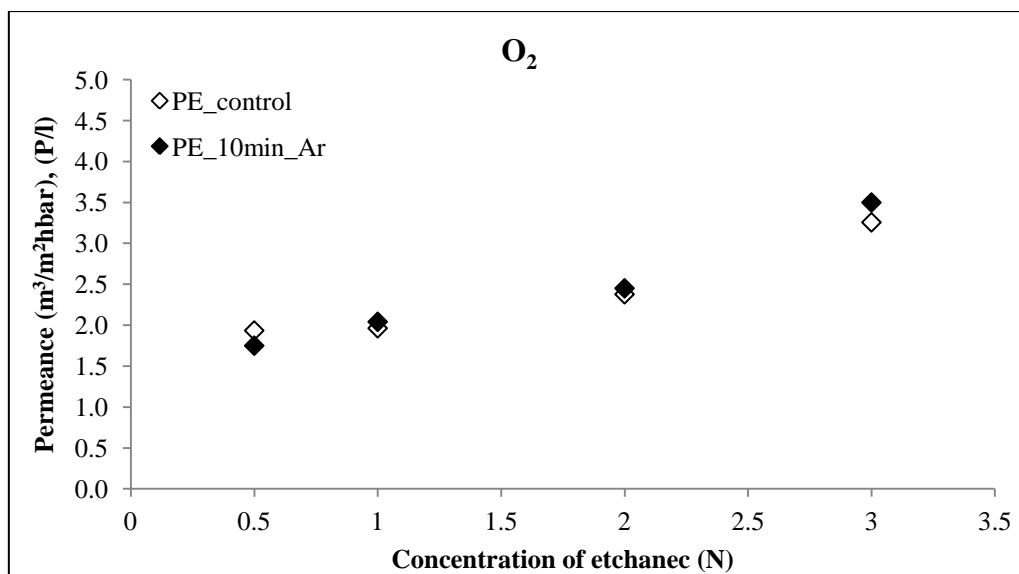
**Figure 4.22** FTIR spectra of PE films in the range from  $3100 \text{ cm}^{-1}$  to  $3500 \text{ cm}^{-1}$  (a) and  $1600 \text{ cm}^{-1}$  to  $1700 \text{ cm}^{-1}$  (b).

### 4.6.3 The effect of Ar plasma treatment on gas separation

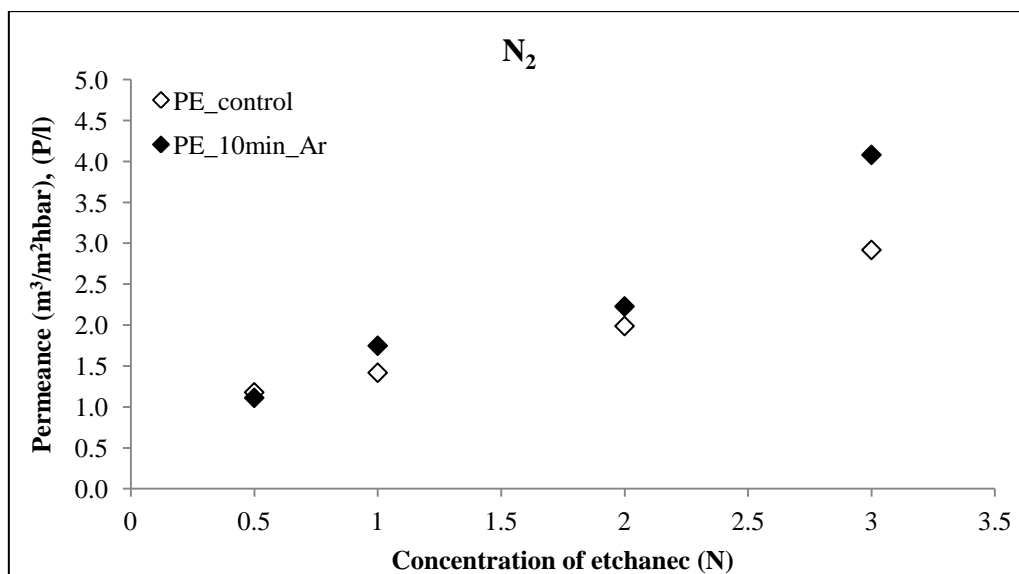
PE membranes were prepared by nuclear track etching method. Gas permeation through the untreated and treated PE membranes by Ar plasma was investigated under the effect of conditions for chemical processes such as concentration of etchant, etching time and etching temperature. These results were shown in Figure 4.23-4.28. The effect of conditions for chemical processes was studied under gas pressure at 3 bar. For study of concentration of etchant effect, PE film was etched in 0.5-3 N  $K_2Cr_2O_7$  in  $H_2SO_4$  (40% W/W) at 25 °C for 1 min. For study of etching time effect, PE film was etched in 2 N  $K_2Cr_2O_7$  in  $H_2SO_4$  (40% W/W) at 25 °C for 1-10 min. For study of etching temperature effect, PE film was etched in 2 N  $K_2Cr_2O_7$  in  $H_2SO_4$  (40% W/W) at 25-60 °C for 10 min. The effects of conditions for chemical processes were shown in Figures 4.23-4.28. The results obtained suggest that they played a major role in increment the gases permeance. The gases permeance of  $O_2$ ,  $N_2$ ,  $CO_2$  and  $CH_4$  increased with increasing concentration of etchant, etching time and etching temperature. When the concentration of etchant increased from 0.5- 3 N, they were increased from 1.9- 3.3, 1.2- 2.9, 2.3-3.7 and 1.1- 3.2  $m^3/m^2hbar$  for  $O_2$ ,  $N_2$ ,  $CO_2$  and  $CH_4$  (Figures 4.23), respectively. While, the etching time increased from 1-10 min, they were increased from 2.4- 4.4, 2.0- 4.3, 2.6-4.6 and 1.8-4.1  $m^3/m^2hbar$  for  $O_2$ ,  $N_2$ ,  $CO_2$  and  $CH_4$  (Figures 4.24), respectively. Moreover, the etching temperature increased from 25-60 °C, they were increased from 4.4-8.9, 4.3-8.8, 4.6-9.0 and 4.1-8.8  $m^3/m^2hbar$  for  $O_2$ ,  $N_2$ ,  $CO_2$  and  $CH_4$  (Figures 4.25), respectively. The increment of concentration of etchant, etching time and etching temperature affected enlarges the latent tracks, which were generated during exposure of fission fragment. Therefore, they lead to the increasing pore size, which result in increased gases permeance. However, the surface modification of PE membranes by Ar plasma did not show any significant difference in the gases permeance. This indicated the interaction effects between polar functional groups of treated membranes and polar gases were not present. Therefore, the gas permeation through the track- etched PE membranes caused by diffusivity more than the solubility [21]. The diffusivity of gases based on their sizes, normally represented by their kinetic diameters. The kinetic diameters of  $O_2$ ,  $N_2$ ,  $CH_4$  and  $CO_2$  were 3.34,

3.68, 3.30 and 3.82 °A (Table 2.2), respectively. So that gases permeance decreased with the increasing kinetic diameters of gases (Figures 4.23-4.25).

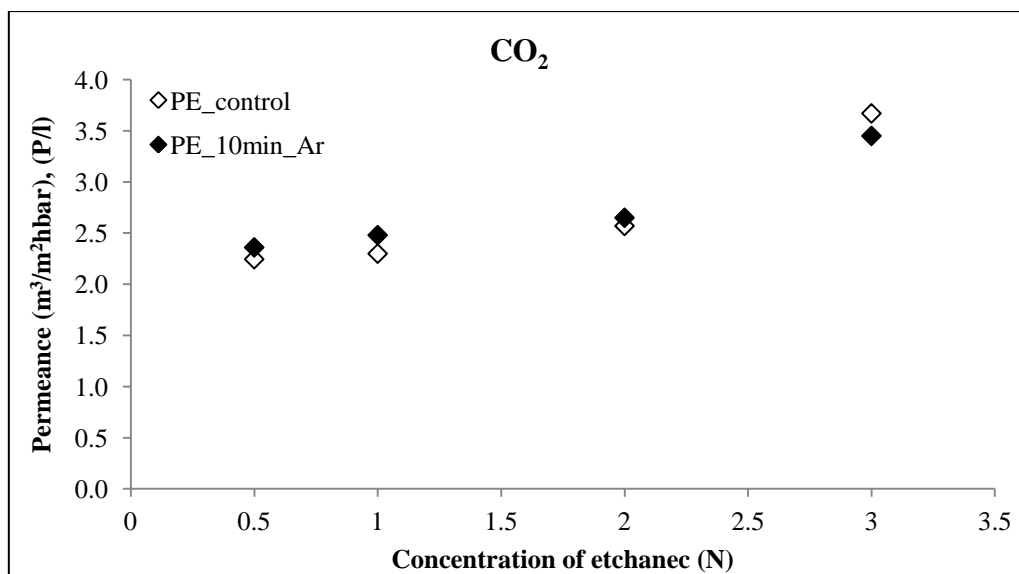
The effect of conditions for chemical processes on gas separation was shown in Figure 4.26-4.28. In mild etching conditions, gas selectivity was found to increase. However, it decreased in high etching conditions. When concentration of etchant etching time and etching temperature increased, the gases permeance increased. Finally, the equal permeance of each gas as result in selectivity did not occur. The maximum selectivity under the concentration of etchant was 1.6 and 2.0 for O<sub>2</sub>/N<sub>2</sub> and CO<sub>2</sub>/CH<sub>4</sub> (Figures 4.26), respectively, which obtained at 0.5 N, 25 °C and 1 min of etching time. For etching time, the maximum selectivity of O<sub>2</sub>/N<sub>2</sub> and CO<sub>2</sub>/CH<sub>4</sub> was 1.2 and 1.4 (Figures 4.27), respectively, which obtained at 2 N, 25 °C and 1 min of etching time. For etching temperature (2 N, 25-60 °C and 10 min of etching time), membranes could not separate these gases (Figures 4.28).



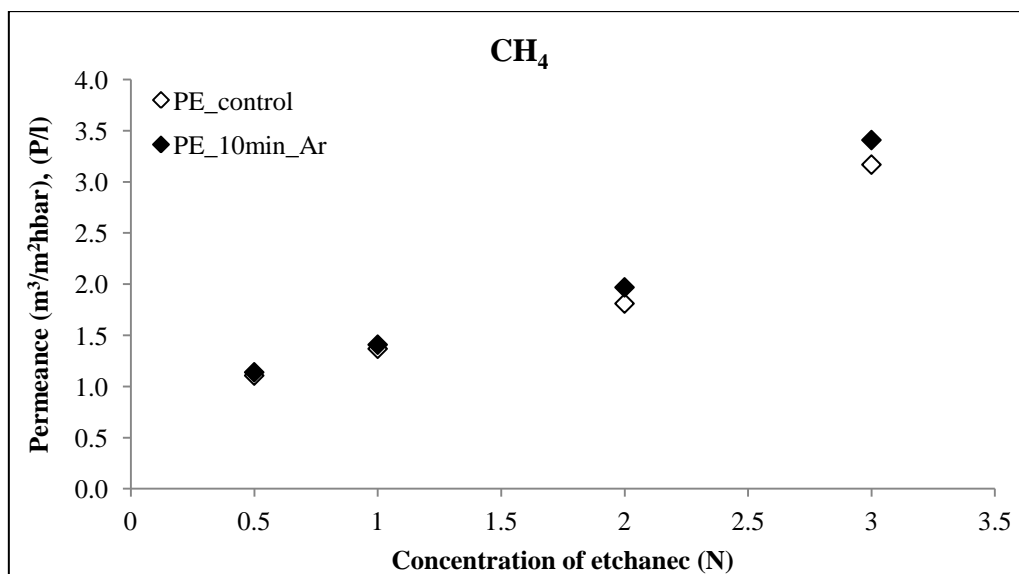
(a)



(b)

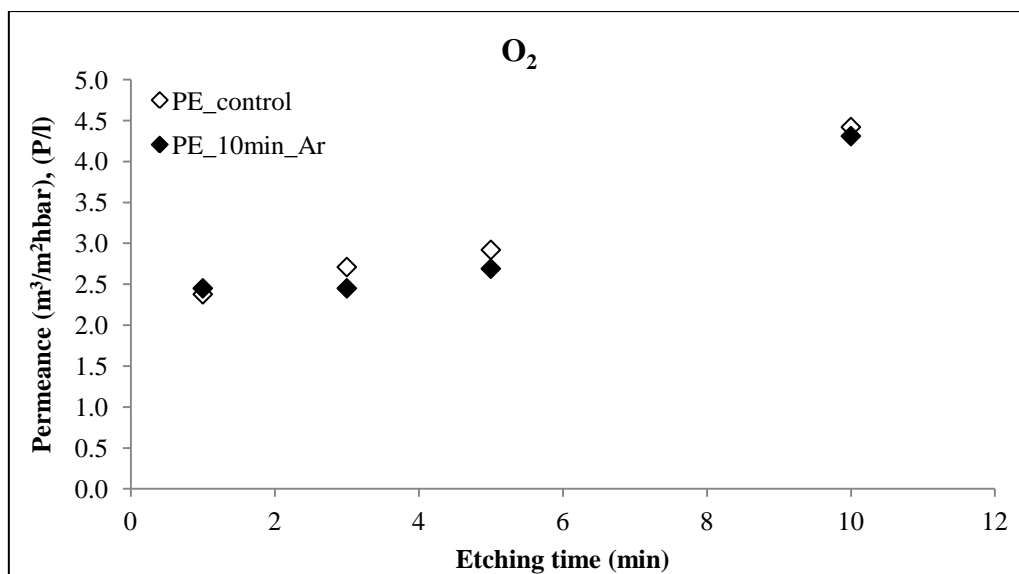


(c)

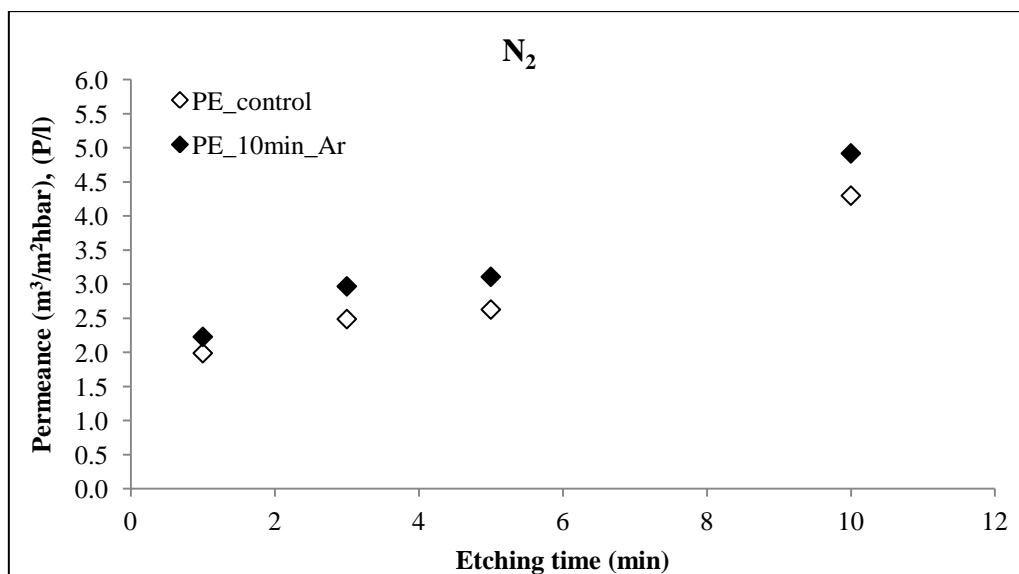


(d)

**Figure 4.23** Graph of permeation of O<sub>2</sub> (a), N<sub>2</sub> (b), CO<sub>2</sub> (c), and CH<sub>4</sub> (d) vs. concentration of etchant for the untreated and treated membrane by Ar plasma.

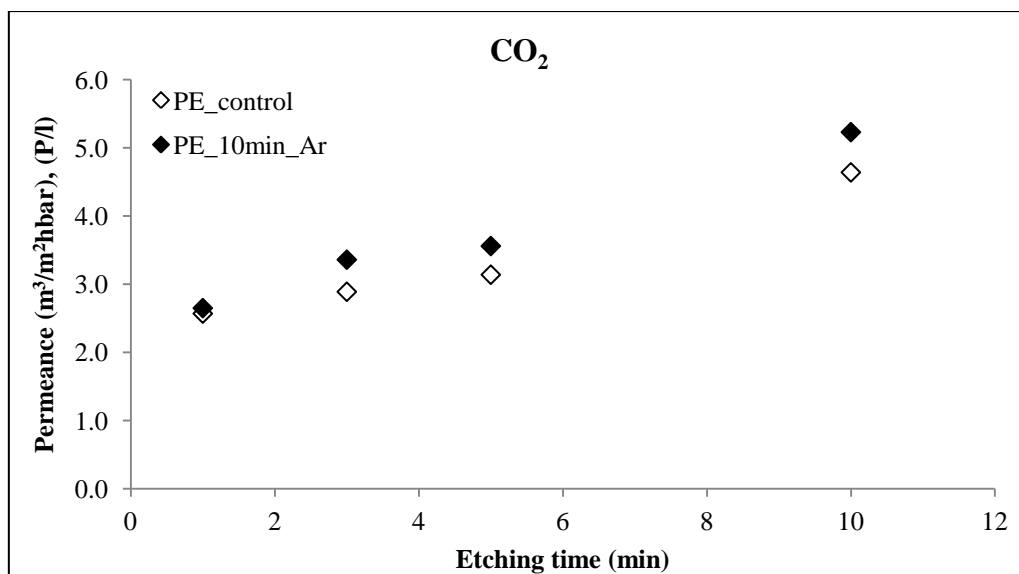


(a)

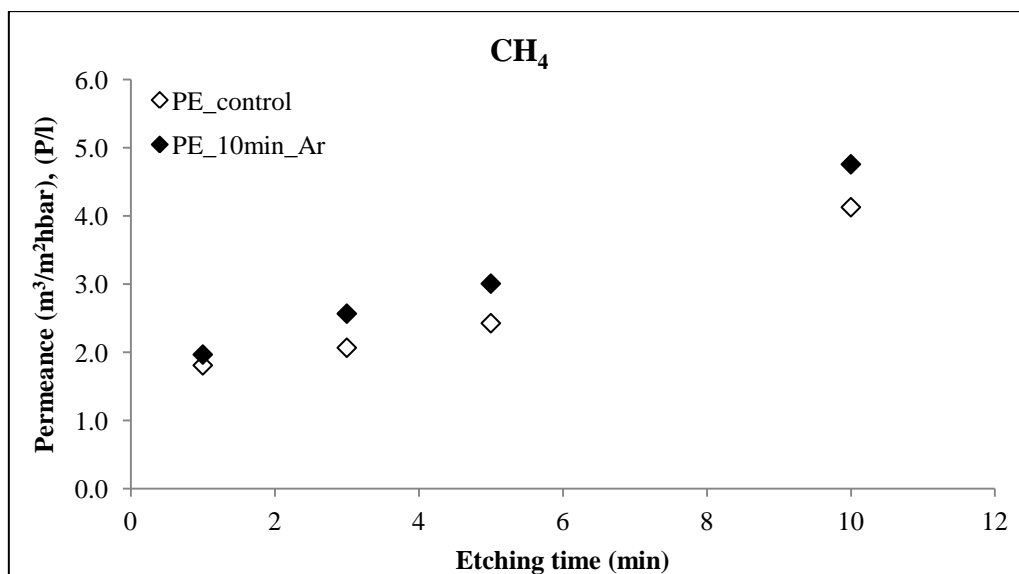


(b)



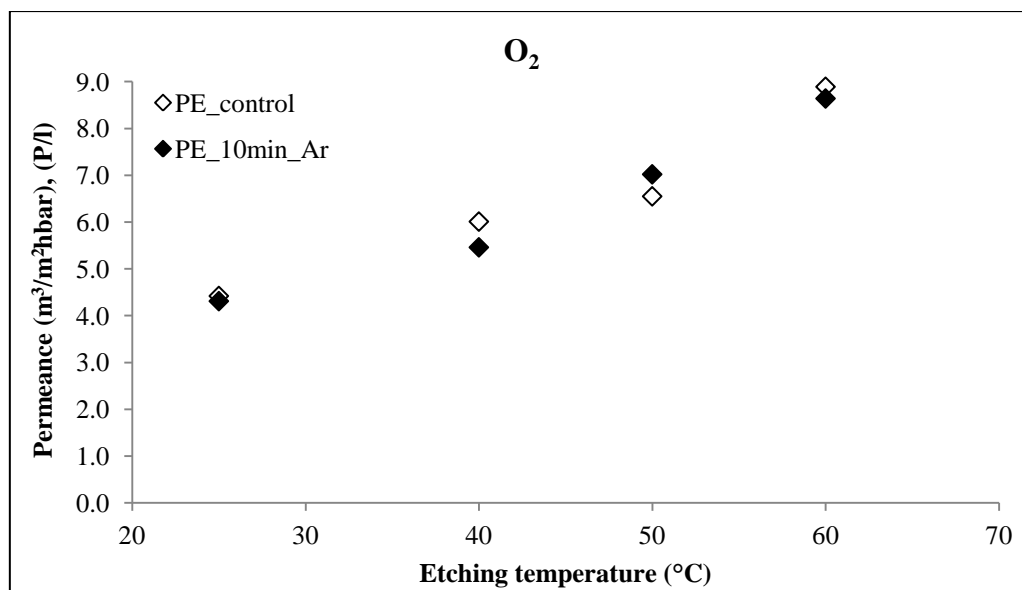


(c)

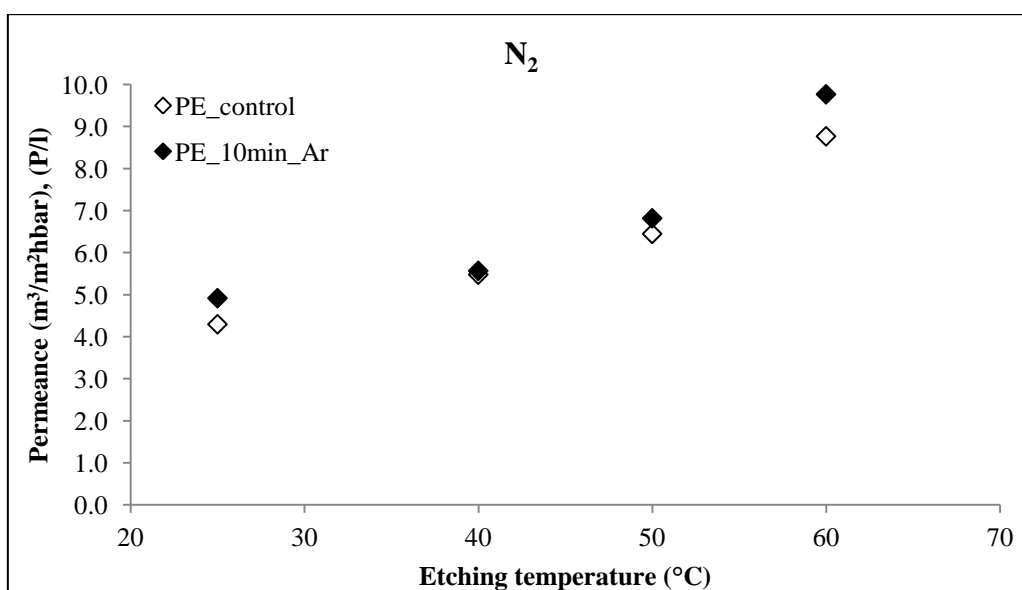


(d)

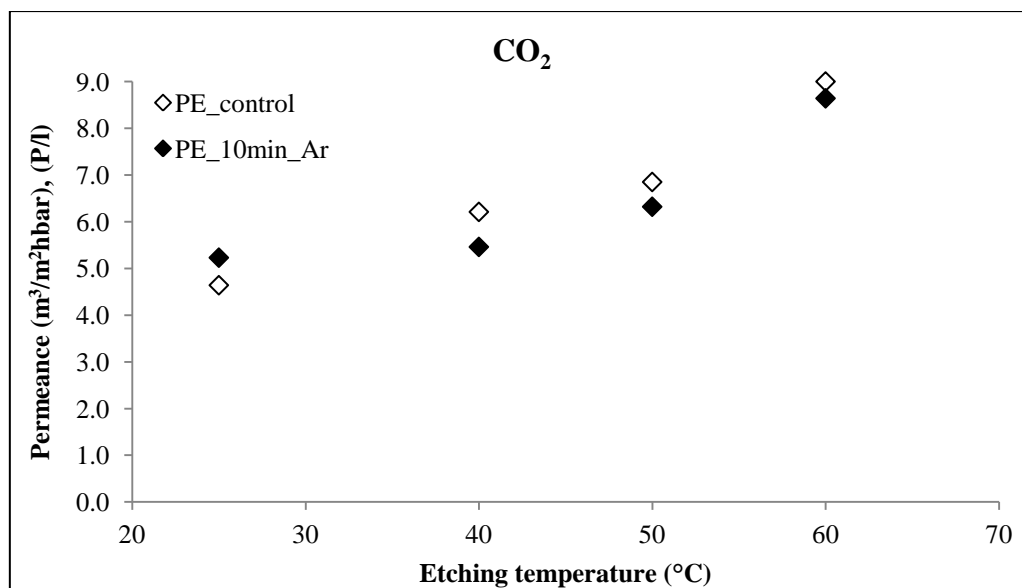
**Figure 4.24** Graph of permeation of O<sub>2</sub> (a), N<sub>2</sub> (b), CO<sub>2</sub> (c), and CH<sub>4</sub> (d) vs. etching time for the untreated and treated membrane by Ar plasma.



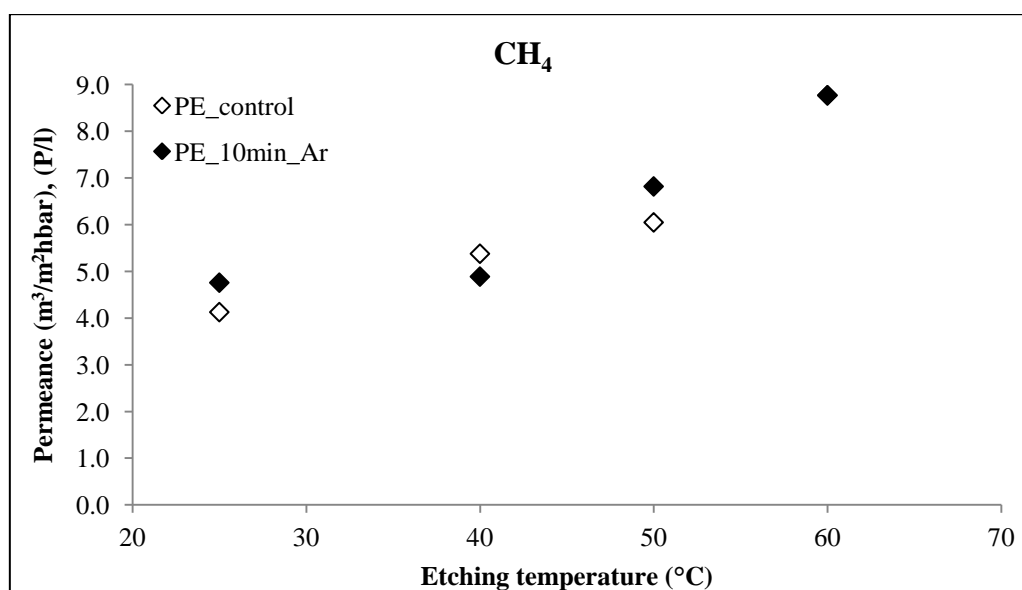
(a)



(b)

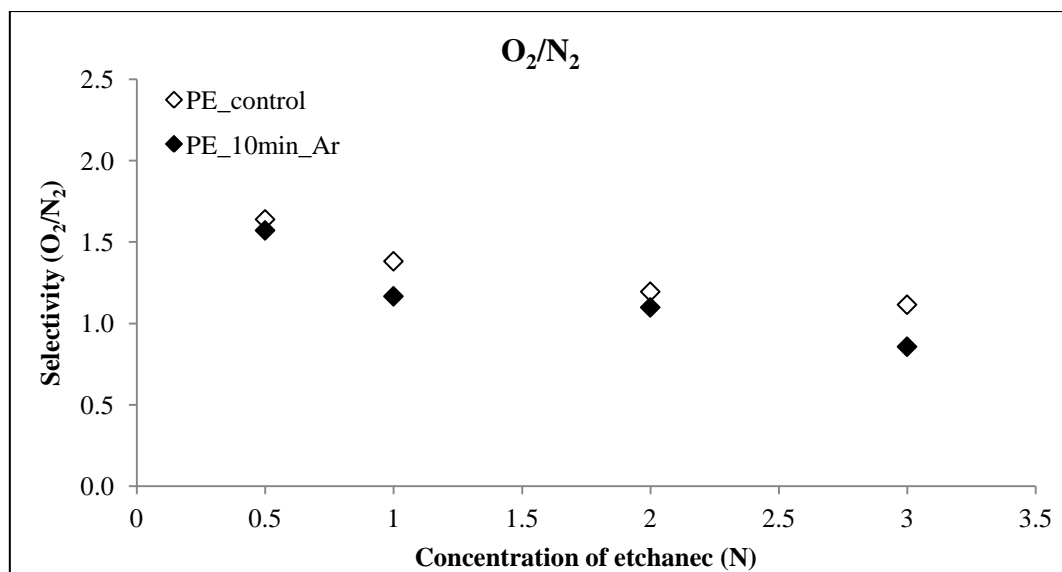


(c)

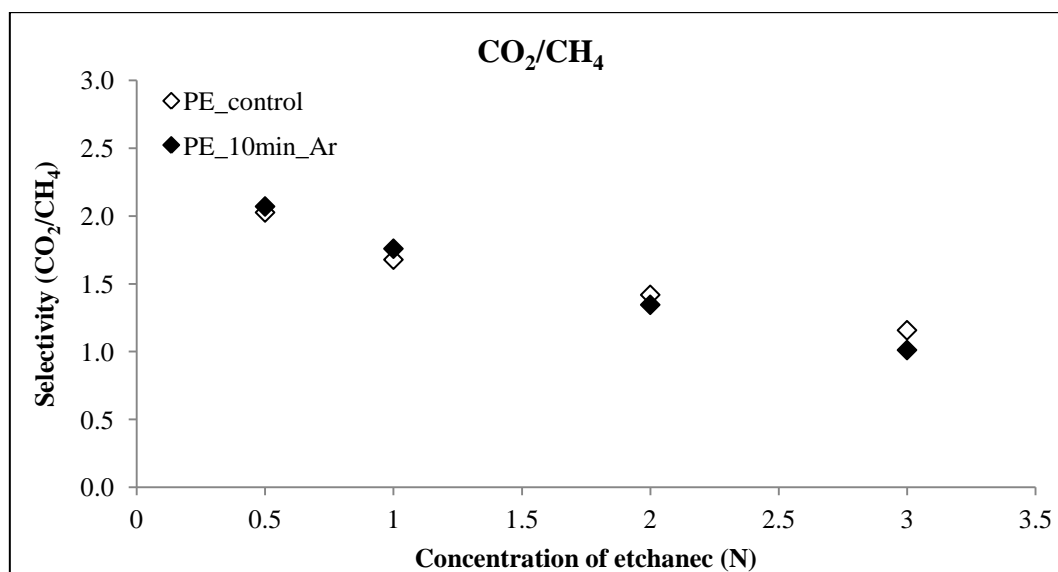


(d)

**Figure 4.25** Graph of permeation of O<sub>2</sub> (a), N<sub>2</sub> (b), CO<sub>2</sub> (c), and CH<sub>4</sub> (d) vs. etching temperature for the untreated and treated membrane by Ar plasma.

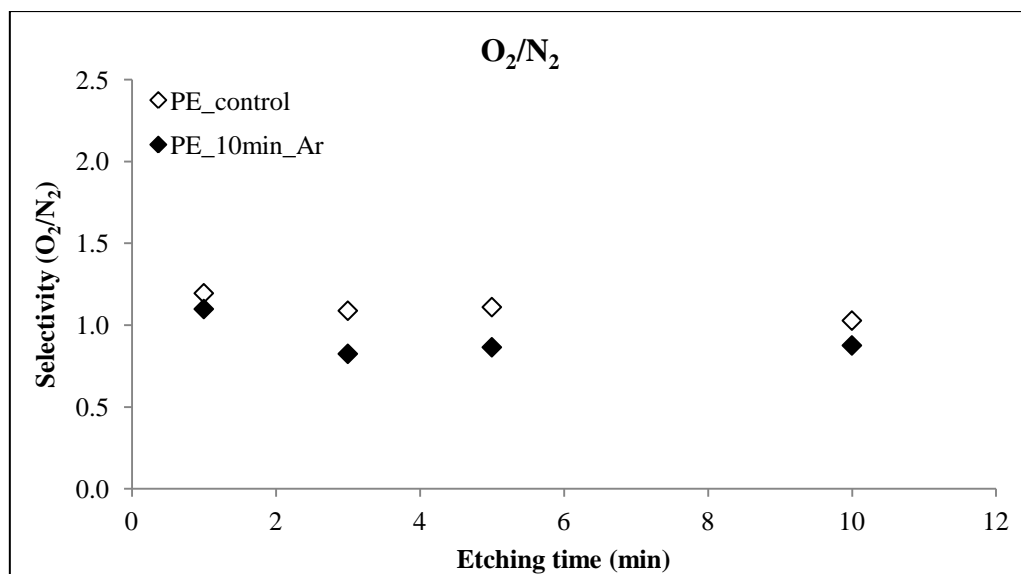


(a)

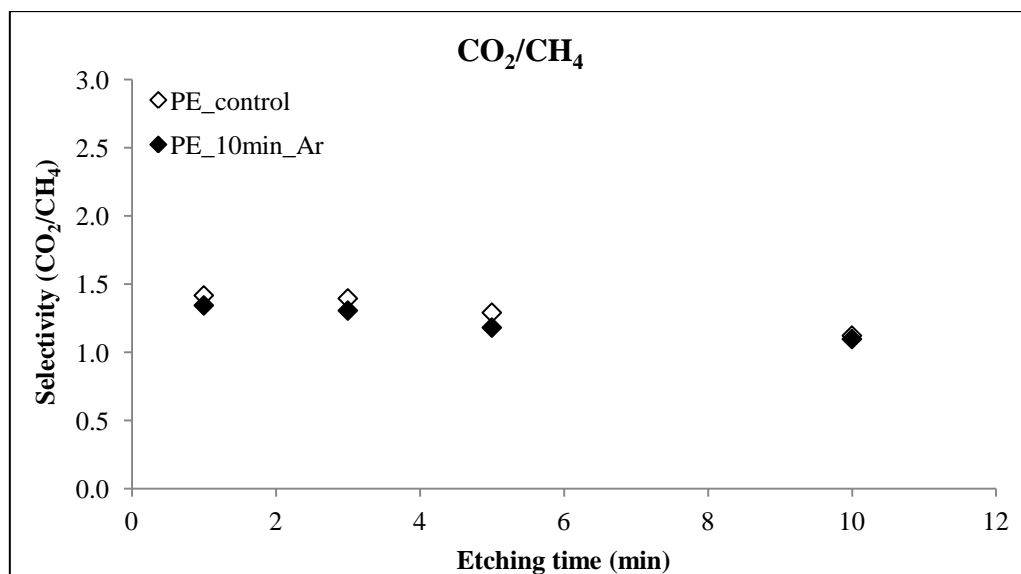


(b)

**Figure 4.26** Graph of selectivity vs. concentration of etchant for the untreated and treated membrane by Ar plasma; (a)  $O_2/N_2$  and (b)  $CO_2/CH_4$ .

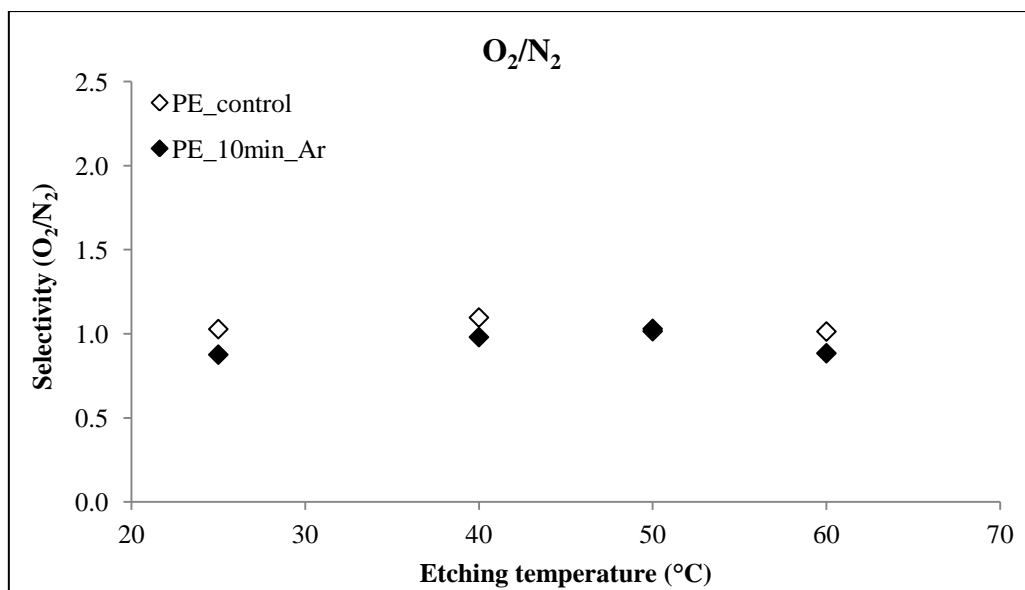


(a)

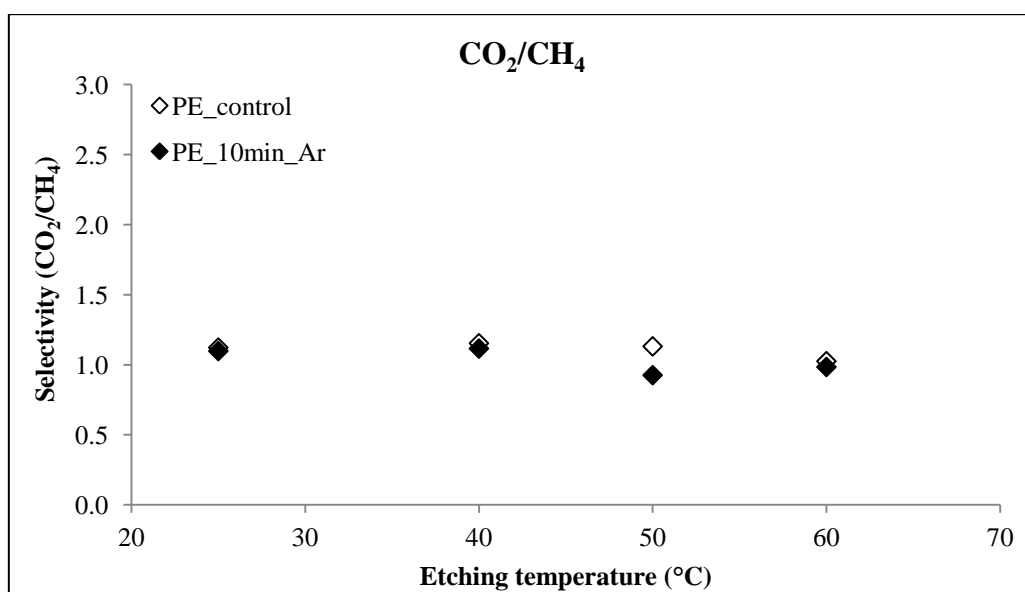


(b)

**Figure 4.27** Graph of selectivity vs. etching time for the untreated and treated membrane by Ar plasma; (a)  $O_2/N_2$  and (b)  $CO_2/CH_4$ .



(a)



(b)

**Figure 4.28** Graph of selectivity vs. etching temperature for the untreated and treated membrane by Ar plasma; (a)  $O_2/N_2$  and (b)  $CO_2/CH_4$ .

## Chapter 5

### Conclusion

#### 5.1 Conclusion

Asymmetric polysulfone membranes prepared by phase inversion method using acetone as non-solvent in polymeric solution. For membranes surface modification by UV irradiation, the result showed that UV irradiation can improve polar group such as hydroxyl and carbonyl groups on the membrane surface. These polar groups affect gases permeation in such as O<sub>2</sub> permeation decreased by 2.5 times compared to the untreated membrane. In contrast, the permeation of N<sub>2</sub>, CH<sub>4</sub> and CO<sub>2</sub> were increased by 1.8, 2.6 and 4.2 times greater than that of the untreated membranes, respectively. This effect might be due to dipole–quadrupole interaction between polymer matrix and gas molecules. These permeations affect gases selectivity. The O<sub>2</sub>/N<sub>2</sub> selectivity decreases after UV irradiation. In contrast, the CO<sub>2</sub>/CH<sub>4</sub> selectivity increases. The maximum selectivity of CO<sub>2</sub>/CH<sub>4</sub> and O<sub>2</sub>/N<sub>2</sub> was found on prepared membrane by concentration of 25% PSF when the applied pressure was selected to be 3 bar. The maximum of CO<sub>2</sub>/CH<sub>4</sub> selectivity was 6.4 which increased about 3 times compared to the untreated membranes. However, the maximum O<sub>2</sub>/N<sub>2</sub> selectivity was 7.5 belonging to the untreated membranes which was greater than the treated membranes by 4.9 times. For Ar plasma modification, the result shows that it has effected on membrane similar to UV irradiation but lower. After Ar plasma treatment, O<sub>2</sub> permeation was decreased to 1.4 times of the untreated membrane while permeation of N<sub>2</sub>, CH<sub>4</sub> and CO<sub>2</sub> were increased to 1.4, 1.8 and 2.4 times of the untreated membranes, respectively. These permeations affect O<sub>2</sub>/N<sub>2</sub> and CO<sub>2</sub>/CH<sub>4</sub> selectivity, the O<sub>2</sub>/N<sub>2</sub> selectivity decreases while the CO<sub>2</sub>/CH<sub>4</sub> selectivity increases after Ar plasma treatment. Considering the polymer concentration of 25% and pressure of 3 bar, the CO<sub>2</sub>/CH<sub>4</sub> and O<sub>2</sub>/N<sub>2</sub> selectivity were 4.3 and 3.8 respectively, which increased about 2 times and decreased about 2 times of the untreated membranes, respectively.

PE membranes were prepared by nuclear track etching method. The effect of conditions for chemical processes was studied under gas pressure at 3 bar. The results obtained, suggest that the gases permeance of O<sub>2</sub>, N<sub>2</sub>, CO<sub>2</sub> and CH<sub>4</sub> increased with increasing concentration of etchant, etching time and etching temperature. When the concentration of etchant increased from 0.5- 3 N, permeance were increased from 1.9- 3.3, 1.2- 2.9, 2.3-3.7 and 1.1-3.2 m<sup>3</sup>/m<sup>2</sup>hbar for O<sub>2</sub>, N<sub>2</sub>, CO<sub>2</sub> and CH<sub>4</sub>, respectively. While, the etching time increased from 1-10 min, permeance were increased from 2.4- 4.4, 2.0- 4.3, 2.6-4.6 and 1.8-4.1 m<sup>3</sup>/m<sup>2</sup>hbar for O<sub>2</sub>, N<sub>2</sub>, CO<sub>2</sub> and CH<sub>4</sub>, respectively. Moreover, the etching temperature increased from 25-60 °C, permeance were increased from 4.4-8.9, 4.3-8.8, 4.6-9.0 and 4.1-8.8 m<sup>3</sup>/m<sup>2</sup>hbar for O<sub>2</sub>, N<sub>2</sub>, CO<sub>2</sub> and CH<sub>4</sub>, respectively. The increment of concentration of etchant, etching time and etching temperature affected increasing pore size, which result in increased gases permeance. UV irradiation lightly affects surface of PE film so it was not studied for surface modification. Ar plasma treatment affects increase hydrophilicity of PE film more than UV irradiation. However, it did not show any significant difference in the gases permeance. This indicated the interaction effects between polar functional groups of treated membranes and polar gases were not present. Therefore, the gas permeation caused by the different of molecular sizes of gases and pressure. The gas selectivity decreased when concentration of etchant, etching time and etching temperature increased. The maximum selectivity under the concentration of etchant was 1.6 and 2.0 for O<sub>2</sub>/N<sub>2</sub> and CO<sub>2</sub>/CH<sub>4</sub> respectively, which obtained at 0.5 N, 25 °C and 1 min of etching time. For etching time, the maximum selectivity of O<sub>2</sub>/N<sub>2</sub> and CO<sub>2</sub>/CH<sub>4</sub> was 1.2 and 1.4, respectively, which obtained at 2 N, 25 °C and 1 min of etching time. For etching temperature, membranes cannot separate these gases.

In conclusion, asymmetric PSF membranes prepared by phase inversion method and modified by UV irradiation have polar group on the membrane surface. The polar membrane which was hydrophilic is most suitable for CO<sub>2</sub>/CH<sub>4</sub> separation. However, the untreated PSF membrane which was hydrophobic is suitable for O<sub>2</sub>/N<sub>2</sub> separation. For PE membrane prepared by nuclear track etching method and etched in aforementioned conditions is not suitable for gas separation.



## 5.2 Suggestion

1. Membranes polarity is a significant effect in gas separation membranes systems. Membrane with polar functional group is hydrophilic. Polar membrane is suitable for CO<sub>2</sub>/CH<sub>4</sub> separation. Although the nature of polysulfone membrane is hydrophobic, a surface modification can improve its hydrophobicity. In this thesis, membrane was modified by plasma treatment and UV-ray irradiation. However, there are many methods for surface modification including ozone treatment and gamma-ray irradiation.

2. In this thesis, Ar was used for membrane surface modification in plasma system. However, there are several gases can improve hydrophobicity of membrane such as N<sub>2</sub>, CO<sub>2</sub>, O<sub>2</sub> and NH<sub>3</sub>.

3. Similar method should be applied for some particular polymers for the gas separation membranes production such as poly (ethylene terephthalate), polypropylene, poly (vinylidene fluoride) and polyimide.

## References

- [1] I.G. Wenten, Songklanakarín J. Sci. Technol., 24 (2002) 1009-1024.
- [2] F. Liu, N.A. Hashim, Y. Liu, M.R.M. Abed, K. Li, Journal of Membrane Science, 375 (2011) 1-27.
- [3] A.F. Ismail, N. Ridzuan, S.A. Rahman, Songklanakarín J. Sci. Technol., 24 (Suppl.) (2002) 1025-1043.
- [4] A.L. Kohl, R.B. Nielsen, Gulf Publishing Company, Houston, Texas, (1985).
- [5] R. Abedini, A. Nezhadmoghadam, Petroleum & Coal, 52 (2010) 69-80.
- [6] R.E. Kesting, A.K. Fritzsche, John Wiley & Sons Inc, Canada, (1993).
- [7] Y. Zhang, J. Sunarso, Shaomin Liu, R. Wang, Int. J. Greenh. Gas. Con., 12 (2013) 84-107.
- [8] R. Xing, W.S.W. Ho, Journal of the Taiwan Institute of Chemical Engineers, 40 (2009) 654-662.
- [9] M.R. Othman, S.C. Tan, S. Bhatia, Microporous and Mesoporous Materials, 121 (2009) 138-144.
- [10] S. Modarresi, M. Soltanieh, S.A. Mousavi, I. Shabani, Journal of Applied Polymer Science, 124 (2012) E199-E204.
- [11] K.S. Kim, K.H. Lee, K. Cho, C.E. Park, J. Membr. Sci. , 199 (2002) 135-145.
- [12] B. Jaleh, P. Parvin, P. Wanichapichart, A. P. Saffar, A. Reyhani, Appl. Surf. Sci., 257 (2010) 1655-1659.
- [13] M. Nystrom, P. Jarvinen, J. Membr. Sci. , 60 (1991) 275-296.
- [14] K.K. Hsu, S. Nataraj, R.M. Thorogood, P.S. Puri, J. Membr. Sci., 79 (1993) 1-10.
- [15] S.H. Choi, M.K. Lee, S.J. Oh, J.K. Koo, J. Membr. Sci. , 221 (2003) 37-46.
- [16] N.N. Rupiasih, P.B. Vidyasagar, Polym. Degrad. Stabil., 93 (2008) 1300-1307.
- [17] M. I. Vazquez, R. de Lara, P. Galán, J. Benavente, Colloid Surface A, 256 (2005) 245-251.
- [18] M. Zhang, Q.T. Nguyen, Z. Ping, J. Membr. Sci. , 327 (2009) 78-86.
- [19] M. Bryjak, I. Gancarz, G. Pozniak, W. Tylus, Eur Polym J., 38 (2002) 717.
- [20] B. Kaeselev, P. Kingshottb, G.r. Jonsson, Desalination, 146 (2002).
- [21] Y. Yampolskii, I. Pinnau, B. Freeman, John Wiley & Sons Ltd, The Atrium, Southern Gate, Chichester, West Sussex PO19 8SQ, England, (2006).

- [22] R.W. Baker, John Wiley & Sons Ltd, The Atrium, Southern Gate, Chichester, West Sussex PO19 8SQ, England, (2004).
- [23] A.F. Ismail, P.Y. Lai, *Sep. Purif. Technol.*, 40 (2004) 191–207.
- [24] C.A. Scholes, S.E. Kentish, G.W. Stevens, *Recent Pat. Chem. Eng.*, 1 (2008) 52-66.
- [25] M.A. Aroon, A.F. Ismail, M.M. Montazer-Rahmati, T. Matsuura, *Sep. Purif. Technol.*, 72 (2010) 194-202.
- [26] H. Lin, B.D. Freeman, *J. Membr. Sci.*, 239 (2004) 105-117.
- [27] A.F. Ismail, B.C. Ng, W.A.W. Abdul Rahman, *Sep. Purif. Technol.*, 33, (2003) 255-272.
- [28] H. Strathmann, L. Giorno, E. Drioli, *Intrumente on membrane technology*, University of Calabria, Italy, (2006).
- [29] S.S. Madaeni, P. Moradi, *J. Poly Sc.*, 121 (2011) 2157-2167.
- [30] W.J. Lee, D.S. Kim, J.H. Kim, *Koreano chem. eng.*, 17 (2000) 143-148.
- [31] S.S. Madaeni, A. Rahimpour, J. Barzin, 9th Iranian Chemical Engineering Congress, Iran University of Science and Technology 23-25 November, 2004., (2004) 4309-4314.
- [32] P. T. P. Aryanti, Khoiruddin, I.G. Wenten, *Journal of Water Sustainability*, 3 (2013) 85-96.
- [33] P. Apel, *Radiat. Meas.*, 34 (2001) 559-566.
- [34] D. Holliday, R. Resnick, J. Walk, (2005) 1197-1202.
- [35] R.L. Fleischer, P.B. Price, R.M. Walker, (1975) 3-34.
- [36] Y.K. Vijay, N.K. Acharya, S. Wate, D.K. Avasthi, *Int. J. Hydrogen Energ.*, 29 (2004) 515-519.
- [37] N. K. Acharya, V. Kulshrestha, K. Awasthi, R. Kumar, A. K Jain, M. Singh, D. K. Avasthi, Y. K. Vijay, *Vacuum*, 81 (2006) 389-393.
- [38] V. Kulshrestha, N. K. Acharya, K. Awasthi, R. Nathawat, M. Singh, Y. K. Vijay, *Micron*, 38 (2007) 326-329.
- [39] I. M. Yamazaki, R. Paterson, L.P. Geraldo, *J. Membr. Sci.*, 118 (1996) 239-245.
- [40] X. He, Z. Sun, C. Wan, *Radiat. Meas.*, 41 (2006) 112-113.
- [41] J. Kaewsaneee, Degree of Master of Science in Physics, Faculty of Science, King Mongkut's University of Technology Thonburi, (2005).

- [42] A. Thongphud, Degree of Master of Science in Physics, Faculty of Science, King Mongkut's University of Technology Thonburi, (2005).
- [43] P. Makphon, W. Ratanatongchai, S. Chongkum, S. Tantayanon, T. Supaphol, J. Appl. Polym. Sci. , 101 (2006) 982-990.
- [44] Y. S. Bae, O.K. Farha, J.T. Hupp, R.Q. Snurr, J. Mater. Chem., 19 (2009) 2131-2134.
- [45] S. H. Chen, W. H. Chuang, A. A. Wang, R.C. Ruaan, J.Y. Lai, J.Membr. Sci., 124 (1997) 273-281.
- [46] D. M. D'Alessandro, B.Smit, J.R. Long, Angew. Chem. Int. Ed. , 49 (2010) 6058 - 6082.
- [47] W.J. Koros, J. Polym. Sci. Part B: Polym. Phys. Ed., 23 (1985) 1611-1628.
- [48] V.I. Bondar, B.D. Freeman, I. Pinnua, J Polym Sci: Polym Phys, 37 (1999) 2463-2475.
- [49] M. Sadeghi, M.A. Semsarzadeh, H. Moadel, J.Membr. Sci., 331 (2009) 21-30.
- [50] M.L. Steen, L. Hymasa, E.D. Havey, N.E. Capps, D.G. Castner, E.R. Fisher, J.Membr. Sci. , 188 (2001) 97.
- [51] I. Gancarz, G.PozÂniak, M. Bryjak, Eur Polym J., 35 (1999) 1419.
- [52] S.H. Chen, T.H. Wu, R.C. Ruaan, J.Y. Lai, Journal of Membrane Science 141 (1998) 255-264.
- [53] K.S. Kim, K.H. Lee, K. Cho, C.E. Park, J.Membr. Sci., 199 (2002) 135-145.
- [54] D.S. Wavhal, E.R. Fisher, J.Membr. Sci. , 209 (2002) 255.
- [55] P. Wanichapichart, R. Sungkum, W. Taweepreda, M. Nisoa, Surf. Coat. Tech., 203 (2009) 2531-2535.
- [56] R. Xing, W.S. W. Ho, J. Taiwan. Inst. Chem. E., 40 (2009) 654-662.
- [57] Y. S. Bae, C.H. Lee, Carbon., 43 (2005) 95-107.
- [58] S. Nir, S. Adams, R. Rein, J. of chemical physics, 59 (1997) 3341-3355.
- [59] I.M. Smallwood, J. Wley & Sons, New York (1996) 171,217.
- [60] K.S. Kim, K.H. Lee, K. Choa, C.E. Park, J.Membr. Sci., 199 (2000).
- [61] P. Wanichapichart, W. Bootluck, P. Thopan, L.D. Yu, Nuclear Instruments and Methods in Physics Research Section B: Beam Interactions with Materials and Atoms, 326 (2014) 195-199.

- [62] M.G. Yan, L.Q. Liu, Z.Q. Tang, L. Huang, W. Li, J. Zhou, J.S. Gu, X.W. Wei, H.Y. Yu, *Chem. Eng. J.*, 145 (2008) 218-224.
- [63] A. Lazea, L.I. Kravets, B. Albu, C. Ghica, G. Dinescu, *Surface and Coatings Technology*, 200 (2005) 529-533.
- [64] D. Klepac, M. Scetar, G. Baranovi, K. Galic, S. Valic, *Radiat. Phys. Chem.*, 97 (2014) 304-312.
- [65] I. A. F., L. J. Y., *Sep. Purif. Technol.*, 33 (2003) 127-143.
- [66] L. S. Shi, L. Y. Wang, Y. N. Wang, *Eur. Polym. J.* , 42 (2006) 1625-1633.
- [67] H. Liu, Y. Pei, D. Xie, X. Deng, Y. X. Leng, Y. Y. Jin, N. Huang., *Appl. Surf. Sci.*, 256 (2010) 3941-3945.
- [68] S. Guruvenket, G. M. Rao, M. Komath, A.M. Raichur, *Appl. Surf. Sci.*, 236 (2004) 278-284.
- [69] N. Patra, J. Hladik, M. Pavlatová, J. Militký, L. Martinová, *Polym. Degrad. Stabil.*, 98 (2013) 1489-1494.

## **Appendix**

## Paper

Sutthisa Konruang, Thawat Chittrakarn, Suksawat Sirijarakul “Surface modification of asymmetric polysulfone membrane by UV irradiation”. *Jurnal Teknologi (Sciences & Engineering)* 70:2 (2014) 55–60.

### Surface Modification of Asymmetric Polysulfone Membrane by UV Irradiation

Sutthisa Konruang<sup>a</sup>, Thawat Chittrakarn<sup>a,b</sup>, Suksawat Sirijarakul<sup>a,b,c\*</sup>

<sup>a</sup>Department of Physics, Faculty of Science, Prince of Songkla University, Songkhla 90112, Thailand

<sup>b</sup>Membrane Science and Technology Research Center, Prince of Songkla University, Songkhla 90112, Thailand

<sup>c</sup>Thailand Center of Excellence in Physics, Commission on Higher Education, 328 Si Ayutthaya Road, Bangkok 10400, Thailand

\*Corresponding author: suksawat.s@psu.ac.th

#### Article history

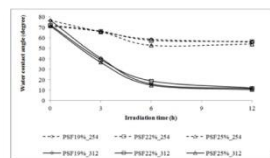
Received :1 November 2013

Received in revised form :

1 June 2014

Accepted :30 June 2014

#### Graphical abstract



#### Abstract

The effects of ultraviolet (UV) irradiation for surface modification of hydrophobic asymmetric polysulfone membranes have been investigated. The asymmetric polysulfone (PSF) membranes were prepared by phase inversion method using 19%-25% of PSF in two solvents, viz. dimethylacetamide (DMF) and Acetone (Ac) collectively. The surface of asymmetric polysulfone membranes were modified by UV ray with 254 and 312 nm wavelength. Chemical and physical properties of the untreated and the treated membranes were characterized. Scanning electron microscope (SEM) was used to determine asymmetric structure of polysulfone membranes. Contact angle device was used to analyze the effect of UV ray treatment on hydrophilicity of membranes surface. Polar functional groups introduced by UV irradiation were examined using FTIR. The water flux was measured under a pressure of 500 kPa to 2,500 kPa with a feed temperature of 25°C. It was shown that asymmetric polysulfone membranes were produced and the UV ray treatment significantly alters the hydrophilicity of membranes surface indicated by the reduction of water contact angle with increasing treatment time. The FTIR analysis showed the formations of polar functional groups such as hydroxyl and carbonyl groups. Consequently, the surface of asymmetric polysulfone membranes was changed from hydrophobic to hydrophilic by UV irradiation leading to the enhancement of the water flux.

**Keywords:** Surface modification; asymmetric polysulfone membrane; UV irradiation; water flux; hydrophilicity

© 2014 Penerbit UTM Press. All rights reserved.

#### 1.0 INTRODUCTION

Polysulfone were widely used in the preparation of asymmetric membranes with different pore sizes in the skin layer [1]. Among many methods, phase separation was the common method for fabrication of flat sheet asymmetric membranes [2]. Aroon *et al.* [2] prepared asymmetric polysulfone membranes using a mixture of a more volatile solvent (THF) and less volatile solvent (NMP) instead of one single nonvolatile solvent. They found that the skin layer is thicker and less defects. This was due to a volatile solvent can rapidly evaporate from the outermost surface of the membrane during polymer casting, which results in higher polymer concentration in the upper layer of the membrane lead to delayed liquid-liquid demixing and as a result, a dense skin layer with less defects and pin-holes was prepared. Acetone is a more volatile solvent with has boiling point 56°C, while boiling point of THF is 66°C.<sup>3</sup> It mean acetone more rapidly evaporate than THF so that it is possible to prepare asymmetric membranes with dense skin layer using acetone [2, 4-6]. Madaeni *et al.* [5] found that addition of acetone in to polymeric solution consist of PSF

and DMAc cause a decline in flux and an improvement in the retention of protein. In the same condition, Aryanti *et al.* [6] reported humic acid rejection increase with acetone concentration increase. This is confirmed that acetone could improve dense membrane.

Although polysulfone (PSF) has been widely used as a membrane material due to its high performance engineering thermoplastic, which resists degradation, low cost, excellent thermal, chemical and mechanical properties [7]. However, hydrophobicity of PSF membranes limits its wider application. Therefore, numerous investigations have been focused on the modification of PSF membranes to impart hydrophilicity to their structure [8-9]. There are many methods to modify the membrane surface such as plasma treatment, ozone treatment, ion beam treatment, gamma-rays or UV irradiations.

The plasma processes can alter the physico-chemical properties of the polymer surface. It improves polymer wettability, permeability, conductivity, adhesion or biocompatibility [10]. However, it resulted in only transient hydrophilicity with contact angle changes within 24 h of plasma

treatment, only the outer membrane surface was modified [11] and it difficult to control the chemical structure of the plasma treated polymer. Ozone is known to change the chemical structure of polymer membranes. It is anticipated that ozone-treated polymer membranes can show more stable properties, compared to plasma-treated membranes, due to ozone treatment which can change the bulk properties of the polymer while the plasma process only changes the surface properties of the polymer [12]. Ion beam irradiation has long been recognized as an effective method for the modification of diverse materials [13]. It can improve polymer properties such as surface hardness, resistance to mechanical wearing and chemical erosion, and conductivity [14]. With appropriate choice of irradiation conditions (i.e. ion type and energy), energetic ions modify the surface layer of materials within a well-defined depth [15]. It is known that many important physical and chemical properties of polymers can be modified with gamma-rays irradiation [16]. It has been reported that it can change electrochemical characterization (salt permeability, ionic permselectivity and electrical resistance) of cellophane membranes [17]. However, these methods are expensive and difficult to perform.

Many studies about the effects of these methods on several types of polymers have been reported. But the information about the effects UV irradiation on microporous PSF membrane especially, is scarce. However, it has been reported that it increased flux and the hydrophilicity of the membranes.<sup>18</sup> Compared with other surface modification techniques such as plasma treatment, ozone treatment, ion beam treatment, and gamma-rays irradiation, UV irradiation has distinct advantages over other techniques due to its simplicity, inexpensive and widespread industrial applications [19].

The objectives of this research were preparation asymmetric polysulfone membranes and surface modification by UV irradiation. The asymmetric polysulfone membranes were prepared by a phase inversion process using acetone as volatile solvent. The effect of acetone on the morphology was investigated by SEM. The UV ray with 254 and 312 nm wavelength and power 2000 and 360  $\mu\text{w}/\text{cm}^2$ , respectively, was used for the treated membranes. Also, the effect of UV irradiation on hydrophilicity of membranes and was studied using contact angle device, FTIR and dead-end filtration techniques by comparing the results with the untreated membranes.

## 2.0 EXPERIMENTAL

### 2.1 Materials

Polysulfone (Udel P-3500) resin was supplied by Sovay (China). N,N-dimethylacetamide (DMAc) and Acetone (Ac) were used as solvents for PSF membrane and supplied by Sigma-Aldrich Co. (USA) and Guangdong Guanghua Chemical Factory Co., Ltd. (China), respectively. Tap water at room temperature (25°C) was used as a coagulation medium during phase-inversion process.

### 2.2 Preparation of Asymmetric Flat Sheet Membranes

PSF resin was dried in an oven at about 80°C for 24 h to remove humidity before use. PSF was dissolved in solvents of DMAc and Ac different concentrations (Table 1). The solutions were mixed at 60°C for 24 h and placed in an ultrasonic water bath to remove air bubbles. Each solution was cast on a clean glass plate. The thin polymer sheet was immersed in the coagulation bath for 24 h. During the phase inversion process, the exchange between the solvent and nonsolvent lead to the formation of the asymmetric

PSF membrane. The wet membranes were dried at room temperature for 24 h before being used.

**Table 1** Membranes with different dope solution compositions and UV irradiation conditions

Sample	PS F (%)	DMAc (%)	Ac (%)	UV ray wavelength (nm)	Irradiation time (h)
PSF19%_0h	19	54	27	-	0
PSF22%_0h	22	52	26	-	0
PSF25%_0h	25	50	25	-	0
PSF19%_3h_254	19	54	27	254	3
PSF22%_3h_254	22	52	26	254	3
PSF25%_3h_254	25	50	25	254	3
PSF19%_6h_254	19	54	27	254	6
PSF22%_6h_254	22	52	26	254	6
PSF25%_6h_254	25	50	25	254	6
PSF19%_12h_254	19	54	27	254	12
PSF22%_12h_254	22	52	26	254	12
PSF25%_12h_254	25	50	25	254	12
PSF19%_3h_312	19	54	27	312	3
PSF22%_3h_312	22	52	26	312	3
PSF25%_3h_312	25	50	25	312	3
PSF19%_6h_312	19	54	27	312	6
PSF22%_6h_312	22	52	26	312	6
PSF25%_6h_312	25	50	25	312	6
PSF19%_12h_312	19	54	27	312	12
PSF22%_12h_312	22	52	26	312	12
PSF25%_12h_312	25	50	25	312	12

\*The ratio of DMAc and Ac was fixed at 2:1 (wt/wt)

### 2.3 UV Irradiation

The UV ray source (VILBER LOURMAT, VI-215.MC) with 254 and 312 nm wavelength of 2000 and 360  $\mu\text{w}/\text{cm}^2$ , respectively, was used for the membranes treatment. Dried PSF membranes of 2  $\text{cm}^2$  were irradiated by UV ray in air at room temperature for 3–12 h (Table 1).

### 2.4 Membrane Characterizations

#### 2.4.1 Scanning Electron Microscopy (SEM)

Membrane thickness and porous substructure of the untreated and the treated membrane morphology were determined by a scanning electron microscopic (SEM) technique. For cross-sections analysis, the samples were frozen in liquid nitrogen and fractured followed by gold sputtering before scanning on a scanning electron microscope (FEI, Quanta 400) with potentials of 20 kV under magnifications ranging from 1,000x to 5,000x.

#### 2.4.2 Fourier Transform Infrared Spectrometer (FTIR)

Fourier Transform Infrared Spectrometer (FTIR: Bruker, EQUINOX 55) was used to investigate changes in functional groups of the membranes. The membrane was scanned at 400–4000  $\text{cm}^{-1}$  wave numbers.



### 2.4.3 Water Contact Angles

Water contact angle of PSF membranes was measured using a contact angle device (Dataphysics, COCA 15 ED) immediately after the UV irradiation.

### 2.4.4 Water Flux and Hydraulic Permeability Coefficient ( $L_p$ )

Dead-end filtration method was used to characterize the water flux of the untreated and the treated membranes. A piece of circular membrane of 6 cm diameter was immersed in ethanol (70%) for around 3 min before being used as a filter. Water flux measurement was made by placing a membrane in a dead end filtration unit, using applied pressures between 0.5 and 2.5 MPa. The water flux  $J$  ( $L/m^2h$ ) was calculated and the slope of the graph between corresponding fluxes and applied pressures was used to deduce the membrane hydraulic permeability coefficient ( $L_p$ ), using the Hagen–Poiseuille equation,  $J = L_p \Delta P$  [20].

## 3.0 RESULTS AND DISCUSSION

### 3.1 Scanning Electron Microscopy (SEM)

The morphology of the prepared membranes was investigated by SEM. The formation of thick skin layer on sponge-like support was shown in Figure 1. This structure was asymmetric membranes structures [21]. This was in accordance with result determined by Aroon *et al.* [2] The skin layer was thicker and less defect due to a volatile solvent (acetone) can rapidly evaporate from the outermost surface of the membrane during polymer casting, which results in higher polymer concentration in the upper layer of the membrane lead to delayed liquid–liquid demixing and as a result, a dense skin layer with less defects and pin-holes was prepared.

The asymmetric polysulfone membranes prepared by different polymer concentrations (19%-25%) shown similar surface morphology. The surface morphology of PSF 25% was shown in Figure 2. No surface pores could be observed on membrane surface, even at magnifications of 5000. This indicated that the diameter of surface pores were less than  $200 \text{ \AA}$  [7]. Furthermore, it also showed the macro-voids of sponge-like support reduce at higher polymer. The formation of this structure is due to higher resistance for exchange of solvent and nonsolvent for more concentrated polymer. This results in liquid–liquid demixing. This produces a membrane with thicker skin layer and denser support [2, 22]. This is confirmed that acetone could improve dense membrane. The surface morphology of prepared membranes was shown Figure 2.

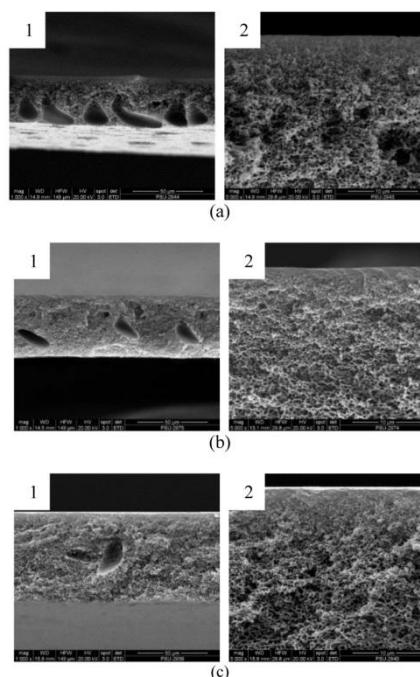


**Figure 1** SEM micrographs of the membranes prepared by different polymer concentrations; (1)  $\times 1,000$  (2)  $\times 5,000$  (a) PSF19%\_0h, (b) PSF22%\_0h and (c) PSF25%\_0h

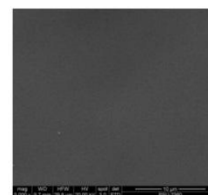
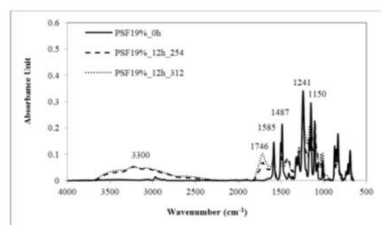


**Figure 2** SEM micrographs of asymmetric polysulfone membrane surface prepared by 25% of polymer concentrations (PSF25%\_0h.)

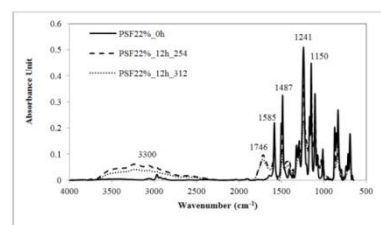
### 3.2 Fourier Transform Infrared Spectrometer (FTIR)

Figure 3 shows the FTIR spectra of the treated membranes by UV ray with 254 and 312 nm wavelength for 12 h, compared to the untreated membranes. Based on the spectral change, there is not much difference in each PSF concentrations. The PSF consists of a backbone made up of diaryl sulfone (Ar-SO<sub>2</sub>-Ar), diaryl ether (Ar-O-Ar) groups showed strong bands at 1150 and 1241  $\text{cm}^{-1}$ , respectively. The bands at 1487 and 1585  $\text{cm}^{-1}$  belong to the vibration of the aromatic (C=C) in PSF molecule [7]. However, the intensities of the peak at 1150, 1241, 1487 and 1585  $\text{cm}^{-1}$  decreased after UV irradiation, while new broad peaks arose around 3300  $\text{cm}^{-1}$  and near 1746  $\text{cm}^{-1}$ . The peaks appeared around 3300 and 1746  $\text{cm}^{-1}$  are ascribed to the stretching vibration of hydroxyl (-OH) group and carbonyl (C=O) group, respectively. The appearance of the peaks around 3300 and 1746  $\text{cm}^{-1}$  by UV irradiation indicates that the carbons in methyl group

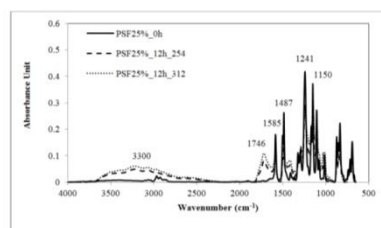
and in benzene ring of PSF were attacked and oxidized by UV ray to form carbonyl (C=O) group and hydroxyl (-OH) group [12]. Due to carbonyl and hydroxyl group were polar functional group so resulting in an increase of the hydrophilic property of the membrane [23]. In addition, it was found that the UV ray with 312 nm wavelength affected carbonyl and hydroxyl functional group of the treated membranes more than 254 nm wavelength.



(a)



(b)



(c)

**Figure 3** Comparison of FTIR spectra of the untreated and the treated membrane by two UV ray wavelengths (a) PSF19%, (b) PSF 22% and (c) PSF 25%

### 3.3 Water Contact Angle

The water contact angles on the membrane surface of the treated membranes are shown in Figure 4 in comparison to the untreated ones. For the untreated, they were reduced to 76°, 72° and 71° while the polymer concentration was increased to 19%, 22%, and 25%, respectively. However, those of the treated membranes reduced greatly after UV irradiation. In addition, the 312 nm UV wavelength affected the water contact angles of the treated membranes greater than the 254 nm wavelength because the increment of polar functional groups on membranes surface by 312 nm UV greater than the 254 nm wavelength. This result was confirmed with FTIR. The angles reduced from 71°–76° to about 18°–15°, after 6 h of 312 nm ray treatment and being stable about 10°–12° after 12 h of the treatment. Using 254 nm wavelength,

they were about 52°–59° after 6 h treatment and became stable about 52°–56° after 12 h treatment. The results indicate that the UV irradiation increased the hydrophilicity of PSF membranes [24].

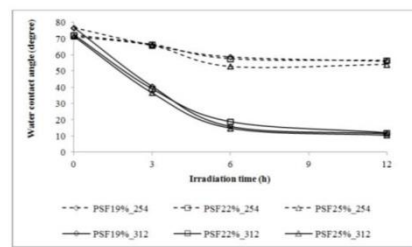


**Figure 4** Water contact angles studies vs irradiation time treated membranes by two UV ray wavelengths

Further experiment was carried out by varying the time after membrane irradiation was made and shown in Figure 5. The treated membranes by 312 nm UV wavelength for 12 h were selected for this study because it more affected on membranes surface. A change in water contact angle with time was observed. The contact angle for the treated membranes increased rapidly up to 1 week. They increased from 30° to 70°, from 25° to 35° and from 15° to 25° while the irradiation time was increased to 3, 6 and 12 h, respectively. They remained rather steady after this treatment. For a membrane which was irradiated for 3 h, the water contact angle increased nearly equal to the untreated membranes within 2–4 weeks after the irradiation. It indicated that hydrophilicity gained by short irradiation time is not stable; the effect can be smaller and even disappear completely, namely “hydrophobic recovery” [25]. However, hydrophobic recovery decreased when irradiation time increased. Moreover, the polymer concentration affect water contact angle slightly at the same irradiation time.

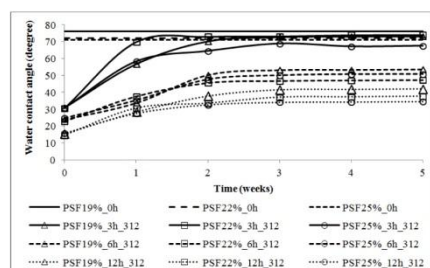
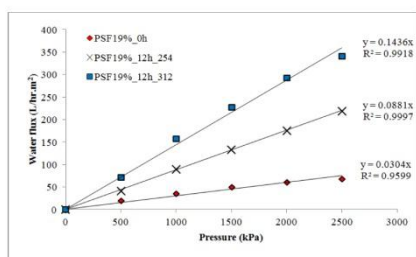


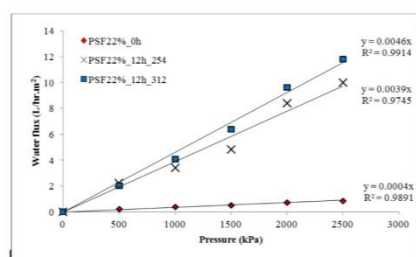
**Figure 5** Variation of water contact angles of the treated membranes by the UV ray with 312 nm wavelength (0-12h) vs storage time

### 3.4 Water Flux

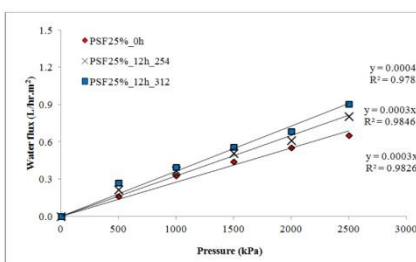
The water fluxes of the untreated and the treated membranes of different mixtures are shown in Figure 6. The treated film by UV ray 12 h was selected for this study because the contact angle shows minimum value at this condition. The results show the increased water flux with increased applied pressure, but the water flux was reduced with increased polymer concentration.



(a)



(b)



(c)

**Figure 6** Permeate of water flux vs driver pressure of untreated and treated membranes by two UV ray wavelengths (a) PSF19%, (b) PSF22% and (c) PSF25%

This is due to the increase in thickness with increased polymer concentration. Although the membrane thickness was controlled in casting process, the different polymer concentration casts the different membrane thickness after the loss of a volatile solvent from a casting solution in evaporation process [2, 22]. This results in smaller diffusion of water molecules through the membrane. In addition, the water fluxes of the treated membranes higher than the untreated membranes in overall polymer concentration. However, it was found that the UV ray with 312 nm wavelength affected water fluxes of the treated membranes more than 254 nm wavelength. This is due to the UV ray with 312 nm wavelength affected polar functional group of the treated membranes more than 254 nm wavelength. The water fluxes of the treated membranes by UV ray with 312 nm wavelength were 3.4, 12.9 and 0.3 times of the untreated membrane for polymer concentrations of 19%, 22%, and 25%, respectively. While water fluxes of the treated membranes by UV ray with 254 nm wavelength were 1.6, 11.0 and 0.2 times of the untreated membrane for polymer concentrations of 19%, 22%, and 25%,

respectively. This result confirms that the hydrophilicity of membranes increased after the UV irradiation. Due to UV ray produced polar functional group on membranes surface which according to Nyström *et al.* [18]. Table 2 shows the hydraulic permeability coefficient ( $L_p$ ) of the untreated and the treated membranes. It should be noted that the UV ray could increase  $L_p$  in the membranes. Hence UV irradiation increased hydrophilicity of the asymmetric polysulfone membranes.

**Table 2** Hydraulic permeability coefficient ( $L_p$ ) of the untreated and the treated membrane by UV ray for 12 h

Sample	$L_p \times 10^{-13} \text{ (ms}^{-1}\text{Pa}^{-1}\text{)}$
PSF19%_0h	84.21
PSF22%_0h	1.11
PSF25%_0h	0.83
PSF19%_12h_254	244.04
PSF22%_12h_254	10.80
PSF25%_12h_254	0.83
PSF19%_12h_312	397.77
PSF22%_12h_312	12.74
PSF25%_12h_312	1.11

#### 4.0 CONCLUSION

Asymmetric polysulfone membrane was prepared by phase inversion technique using acetone as volatile solvent. This structure was illustrated by SEM. The membrane surface was changed from hydrophobic to hydrophilic by UV irradiation. The optimum UV irradiation time was 12 h, UV ray 312 nm wavelength. Polar functional groups such as hydroxyl and carbonyl group were introduced to the skin of membrane surface and confirmed by FTIR and contact angle measurement. This study indicates that UV irradiation could increase the hydrophilicity of the polysulfone membrane.

#### Acknowledgement

This work was supported by the Higher Education Research Promotion and National Research University Project of Thailand, Office of the Higher Education Commission. The author would like to thank Assoc. Prof. Dr. Pikul Vanichapichart (Physics Department, Faculty of Science, Prince of Songkla University) for her kind advice and assistance.

#### References

- [1] Blanco, J. F., Sublet, J., Nguyen, Q. T., Schaezel, P. 2006. Formation and Morphology Studies of Different Polysulfones-based Membranes Made By Wet Phase Inversion Process. *J Membr. Sci.* 283: 27–37.
- [2] Aroon, M. A., Ismail, A. F., Montazer-Rahmati, M. M., Matsuura, T. 2010. Morphology and permeation Properties of Polysulfone Membranes for Gas Separation: Effects of Non-solvent Additives and Co-solvent. *Sep. Purif. Technol.* 72: 194.
- [3] Smallwood, I. M. 1996. *Handbook of Organic Solvent Properties*. John Wiley & Sons, New York.
- [4] Lee, W. J., Kim, D. S., Kim, J. H. 2000. Preparation and Gas Separation Properties of Asymmetric Polysulfone Membranes by a Dual Bath Method. *Korean J Chem. Eng.* 17(2):143–148.
- [5] Madaeni, S. S., Rahimpour, A., Barzin, J. 2004. Effect of Acetone on Morphology and Performance of Polysulfone Ultrafiltration Membranes for Milk Concentration. *9th National Iranian Chemical Engineering Congress*, Tehran, Iran. 4309–4314.
- [6] Aryanti, P. T. P., Khoiruddin, W. G. 2013. Influence of Additives on Polysulfone-Based Ultrafiltration Membrane Performance during Peat Water Filtration. *J Water Sustainability* 3(2): 85–96.
- [7] Ismail, A. F., Ng, B. C., Abdul Rahman, W. A. W. 2003. Effects of Shear Rate and Forced Convection Residence Time on Asymmetric

- Polysulfone Membranes Structure and Gas Separation Performance. *Sep. Purif. Technol.* 33(3): 255–272.
- [8] Wayhal, D. S., Fisher, E. R. 2005. Modification of Polysulfone Ultrafiltration Membranes by CO<sub>2</sub> Plasma Treatment. *Desalination*. 172: 189–205.
- [9] Kim, K. S., Lee, K. H., Cho, K., Park, C. E. 2002. Surface Modification of Polysulfone Ultrafiltration Membrane by Oxygen Plasma Treatment. *J Membr. Sci.* 199: 135–145.
- [10] Bryjak, M., Gancarz, I., Pozniak, G. & Tylus, W. 2002. Modification of Polysulfone Membranes 4. Ammonia Plasma Treatment. *Eur Polym. J.* 38: 717–726.
- [11] Steen, M. L., Hymasa, L., Havey, E. D., Capps, N. E., Castner, D. G. & Fisher, E. R. 2001. Low Temperature Plasma Treatment of Asymmetric Polysulfone Membranes for Permanent Hydrophilic Surface Modification. *J Membr. Sci.* 188: 97–114.
- [12] Choi, S-H., Lee, M-K., Oh, S-J., Koo, J-K. 2003. Gas Sorption and Transport of Ozone-treated Polysulfone. *J Membr. Sci.* 221: 37–46.
- [13] Chennamsetty, R., Escobar, L., Xu, X. 2006. Characterization of Commercial Water Treatment Membranes Modified Via Ion Beam Irradiation. *Desalination*. 188: 203.
- [14] Xu, G., Hibino, Y., Suzuki, Y., Kurotobi, K., Osada, M., Iwaki, M., Kaibara, M., Tanihara, M., Imanishi, Y. 2000. Oxygen Ion Implantation at 20 to 2000 keV into Polysulfone for Improvement of Endothelial Cell Adhesion. *Colloid Surface B.* 19(3): 237–247.
- [15] Ikonich, J. B., Xua, X., Colemana, M., Simpson, P. J. 2003. Impact of Ion Beam Irradiation on Microstructure and Gas Permeance of Polysulfone Asymmetric Membranes. *J Membr. Sci.* 214 (1): 143–156.
- [16] Rupiasih, N. N., Vidyasagar, P. B. 2008. Comparative Study of Effect of Low and Medium Dose Rate of  $\Gamma$  Irradiation on Microporous Polysulfone Membrane Using Spectroscopic and Imaging Techniques. *Polym. Degrad. Stabil.* 93(7): 1300–1307.
- [17] Vazquez, M. I., Lara, R., Galan, P., Benavente, J. 2005. Modification of Cellophane Membranes by  $\gamma$ -radiation: Effect of Irradiation Doses on Electrochemical Parameters. *J Membr. Sci.* 256(1–2): 202–208.
- [18] Nystrom, M., Jarvinen, P. 1991. Modification of Polysulfone Ultrafiltration Membranes with UV Irradiation and Hydrophilicity Increasing Agents. *J Membr. Sci.* 60(2–3): 275–296.
- [19] Zhang, M., Nguyen, Q. T., Ping, Z. 2009. Hydrophilic Modification of Poly (Vinylidene Fluoride) Microporous Membrane. *J Membr. Sci.* 327(1–2): 78–86.
- [20] Wanichapichart P., Kaewnoparat S., Phud-hai W., and Buaking K. 2003. Characteristic of Filtration Membranes Produced by Acetobacter xylinum. Songklanakarin *J Sci. Technol.* 24(Suppl.): 855–862.
- [21] Ismail, A. F., Ridzuan N., Rahman, S. A. 2002. Latest Development on Membrane Formation for Gas Separation. Songklanakarin. *J. Sci. Technol.* 24(Suppl.): 1025–1043.
- [22] Madaeni, S. S., Moradi, P. 2011. Preparation and Characterization of Asymmetric Polysulfone Membrane for Separation of Oxygen and Nitrogen Gases. *J Polym. Sci.* 121: 2157.
- [23] Kim, K. S., Lee, K. H., Choa, K., Park, C. E. 2000. Preparation and Characterization of Asymmetric Polysulfone Membrane for Separation of Oxygen and Nitrogen Gases. *J Membr. Sci.* 199: 135.
- [24] Kaeselev, B., Kingshottb, P., Jonsson, G. 2002. Influence of the surface Structure on the Filtration Performance of UV-modified PES Membranes. *Desalination*. 146: 265–271.
- [25] Yan, M. G., Liu, L. Q., Tang, Z. Q., Huang, L. Li, W., Zhou, J., Gu, J. S., Wei, X. W. and Yu, H. Y. 2008. Plasma Surface Modification of Polypropylene Microfiltration Membranes and Fouling by BSA Dispersion. *Chem. Eng. J.* 145: 218–224.

## Submitted manuscript

### UV-ray treatment of polysulfone membranes on O<sub>2</sub>/N<sub>2</sub> and CO<sub>2</sub>/CH<sub>4</sub> separation performance

Sutthisa Konruang<sup>a</sup>, Suksawat Sirijarukul<sup>a,b,c\*</sup>, Pikul Wanichapichart<sup>a,b,c</sup>, Liangdeng Yu<sup>d</sup>

and Thawat Chittrakarn<sup>a,b\*</sup>

<sup>a</sup> Department of Physics, Faculty of Science, Prince of Songkla University, Songkhla 90112, Thailand

<sup>b</sup> Membrane Science and Technology Research Center, Prince of Songkla University, Songkhla 90112, Thailand

<sup>c</sup> Thailand Center of Excellence in Physics, Commission on Higher Education, 328 Si Ayutthaya Road, Bangkok 10400, Thailand

<sup>d</sup> Department of Physics & Materials Science, Faculty of Science, *Chiang Mai University*, Chiang Mai 50200, Thailand

\* Correspondence to: Suksawat Sirijarukul (E-mail: suksawat.s@psu.ac.th)

Thawat Chittrakarn (E-mail: tawat.c@psu.ac.th)

### ABSTRACT

Ultraviolet (UV) irradiation on polysulfone (PSF) membranes was studied to improve the gas separation property. Membranes of 19-25% PSF content were prepared by the phase inversion method and the membrane surface was modified using UV ray of 312 nm wavelength and 360  $\mu\text{w}/\text{cm}^2$  power. Measurements of gas permeation were conducted using pure carbon dioxide (CO<sub>2</sub>), methane (CH<sub>4</sub>), oxygen (O<sub>2</sub>) and nitrogen (N<sub>2</sub>) gasses under 3-8 bar pressure at 25 °C. Fourier transform infrared spectrometer (FTIR) revealed that polar functional groups of hydroxyl and carbonyl were introduced by the UV irradiation. The water contact angle of the treated membrane was reduced from 70°-75° to 10°-12° after 12 h of UV exposure. Scanning electron microscopic (SEM) observation showed that the dense skin layer increased as increasing the polymer concentration. After the UV treatment, permeation of O<sub>2</sub> decreased from 0.4-3.4 to 0.2-2.3  $\text{m}^3/(\text{m}^2\text{hbar})$ , while that of N<sub>2</sub>, CO<sub>2</sub> and CH<sub>4</sub>

increased for all pressures used from 0.1-1.7 to about 0.1-3.4 m<sup>3</sup>/(m<sup>2</sup>hbar), depending on the applied pressure and the PSF content. As a consequence, the selectivity ratio of O<sub>2</sub>/N<sub>2</sub> decreased from 1.9-7.8 to 0.6-1.5, while that of CO<sub>2</sub>/CH<sub>4</sub> increased from 0.9-2.6 to 1.1-6.1. Moreover, the O<sub>2</sub>/N<sub>2</sub> and CO<sub>2</sub>/CH<sub>4</sub> of the untreated and the treated membranes decreased with increased pressure and increased with increased polymer concentration.

**KEYWORDS:** Gas separation, Polysulfone (PSF) membrane, UV Ray treatment, FTIR, Gas selectivity ratio

## INTRODUCTION

Recently, polymeric membrane technology has been increasingly attractive to scientists in gas separation task. Generally, increased concentration of carbon dioxide (CO<sub>2</sub>) in the atmosphere is a major contributor to the global warming. Not only being released from every day vehicles, CO<sub>2</sub> is also commonly found in natural gas streams, biogas from anaerobic digestion, flue gas from fossil fuel combustion, and product of coal gasification with pipeline specifications below 2% (in USA).[1] It is classified as an acid gas, similar to H<sub>2</sub>S and SO<sub>2</sub>, and required several steps to take to be removed from the gas streams. In many industrial processes, such as natural gas sweetening, biogas upgrading, oil recovery enhancement and landfill gas purification, a mixture of carbon dioxide and methane (CH<sub>4</sub>) has commonly remained as waste. Separation of CO<sub>2</sub> from CH<sub>4</sub> can benefit to both environment and energy recovery aspects. Separation and sequestration of CO<sub>2</sub> by pumping and storing deeply underground is a feasible approach of dealing with the greenhouse gas emissions.[2]

Another gas separation is separation of nitrogen and oxygen from air or oxygen enrichment.[3] Enriched oxygen generation from air mixture is an important process for hospitals, as well as for the effectiveness of combustion systems and green house gas emissions.[4] Therefore, effective techniques for the separations have attracted great interest from workers in many laboratories.

The conventional processes for gas separation are absorption, adsorption and cryogenic distillation.[5] These conventional methods usually involve substantially complicated equipment, higher energy consumption and capital cost,[6, 7] whereas

membrane gas separation does have advantages in its energy efficiency, simple process design, modular design permitting easy expansion, compactness and light weight, low labor intensiveness, low maintenance, low cost and environmental friendliness. In addition, gas separation membrane units are smaller than other types of plants, potentially beneficial to offshore gas-processing.[7, 8]

High gas permeability and selectivity are always desirable for polymeric membranes. In most cases, an increase in gas permeability often causes a decrease in gas selectivity. Asymmetric membranes of a highly selective thin layer on top were known as a high performance membrane type.[5, 9] However, the gas transport property of polymeric membranes depended on physical-chemical interaction between the various gas species and the polymer molecules.[6] A difficulty for gas separation process falls on the fact that the gas molecules to be separated are relatively small. Also, the differences do exist in the membrane material properties and electronic properties such as polarizability and quadrupole moment of the gases.[10] In addition, membrane modification with polarity addition to the surface is of interest to improve absorption and adsorption properties for gas separation.

There are many methods to modify the membrane surface such as plasma treatment and UV irradiations. Kim *et al.* (2002)[11] and Jaleh *et al.* (2010)[12] reported changes from hydrophobicity to hydrophilicity in polymeric membranes after oxygen plasma treatment. However, this technique has a very short lifetime effect, having hydrophobicity recovery within hours, which was explained as due to migration of short uncrosslinked chains to the surface.[13] An equally effective method for the surface modification is an exposure of a membrane to UV irradiation. Nystrom and Pia Jarvinen (1991)[14] reported increases in flux and hydrophilicity of polysulfone (PSF) membranes after UV irradiation. In addition, Hsu *et al.* (1993)[15] revealed that UV irradiation on poly trimethylsilyl propyne (PTMSP) membranes resulted in an improvement of O<sub>2</sub>/N<sub>2</sub> selectivity from 1.4 to approximately 4 after the treatment. The information about the membrane surface modification by UV irradiation is rather scarce, although the technique has distinct advantages over others due to its simplicity, inexpensiveness and widespread industrial applications.[16]

This paper reports on the surface modification of PSF asymmetric membranes by UV ray irradiation to investigate its effects on CO<sub>2</sub>/CH<sub>4</sub> and O<sub>2</sub>/N<sub>2</sub> separations.

## EXPERIMENTAL

### Preparation of asymmetric flat sheet membranes

Polymeric solution in this study consisted of polysulfone (PSF: Udel P-3500) supplied by Solvay (China). N,N-dimethylacetamide (DMAc) and Acetone (Ac) were used as solvents for PSF membrane and supplied by Sigma–Aldrich Co. (USA) and Guangdong Guanghua Chemical Factory Co., Ltd. (China), respectively. Tap water was used as a coagulation medium. PSF resin was dried in an oven at temperature about 80 °C for 24 h to remove humidity before being used. Asymmetric polysulfone flat sheet membranes were prepared by casting using solution consisting of polysulfone (polymer), DMAc (less volatile solvent) and Ac (more volatile solvent) of various concentrations (Table 1), while the ratio of DMAc and Ac was fixed at 2:1 (wt/wt). The solutions were mixed at 60 °C for 24 h and placed in an ultrasonic water bath to remove air bubbles. Casting was carried out on a clean glass plate at an ambient atmosphere (25°C and 85% relative humidity). The thin polymer sheet was immersed in a coagulation bath at 25 °C and remained there for 24 h. The wet membranes were dried at room temperature for 24 h before being used.

TABLE 1. The composition of PSF membranes according to the PSF content.

Sample	PSF (wt.%)	DMAc (wt.%)	Ac (wt.%)
PSF19%	19	54	27
PSF22%	22	52	26
PSF25%	25	50	25

\*The ratio of DMAc and Ac was fixed at 2:1 (wt/wt)

Three pieces of dried PSF membranes in the form of squares with area approximately 2 cm<sup>2</sup> were irradiated by UV radiation in air at room temperature within basement. The exposure area was 20 cm<sup>2</sup>. Membranes were exposed to UV source (VILBER LOURMAT, VI-215.MC) by keeping the distance between the source and sample holder constant at 3 cm where the light intensity was measured to of 360 μw/cm<sup>2</sup> all position on the sample holder. Membranes were exposed in varied times such as 3 h, 6 h and 12 h. The control (0 h) was placed in the box without humidity.



### Membrane characterizations

The permeation performance of PSF membranes were evaluated by two parameters: the permeability ( $P$ ) and the selectivity ( $\alpha$ ). Gas permeation measurements were conducted by using a gas permeation unit as shown in figure 1. PSF membranes were cut into circle area of  $3.14 \text{ cm}^2$  and mounted in the gas permeation unit. The testing temperature was room temperature ( $25^\circ\text{C}$ ). The testing pressure was controlled from 3 to 8 bar and the testing gases were  $\text{O}_2$ ,  $\text{N}_2$ ,  $\text{CO}_2$  and  $\text{CH}_4$ . The feed gas was fed into the up-side and the permeating gas was at the down-side of the membrane. The gas flow rate ( $Q$ ) was determined by bubble flow meters. The pure gas permeance ( $P/l$ ) of the membrane was calculated by the following equation :[17]

$$\left(\frac{P}{l}\right) = \frac{Q}{A\Delta P} \quad (1)$$

where  $\Delta P$  is the pressure difference across the membrane,  $A$  is the membrane effective surface area and  $l$  is the membrane skin thickness. Each membrane was determined 3 times for each gas and the results were presented in average. The selectivity ( $\alpha$ ) was defined by: [1, 17]

$$\alpha_{ij} = \frac{(P/l)_i}{(P/l)_j} \quad (2)$$

where  $(P/l)_i$  and  $(P/l)_j$  are the permeances of gases  $i$  and  $j$ , respectively. The reported values were the average of 3 times measurements.

The membrane morphology was examined by scanning electron microscopy (SEM: FEI, Quanta 400) using 20 kV voltage potentials. In cross-section studies, membrane samples were fractured in liquid nitrogen and coated with gold before scanning. A Fourier transform infrared spectrometer (FTIR: Bruker, EQUINOX 55) was used to investigate changes in functional groups of the membranes after UV ray irradiation. Water contact angle of the membranes was measured using a contact angle device (Dataphysics, OCA 15 EC) immediately after the UV treatment and also after leaving them at room temperature for 4 weeks for studying the hydrophobic recovery of the treated membranes. The membrane surface topography was observed using an atomic force microscope (AFM) operated in the tapping-mode scanning. The membrane sample was prepared into  $1 \times 1\text{-cm}^2$  size for the AFM scanning and scanned in a  $30 \times 30\text{-}\mu\text{m}^2$  area.

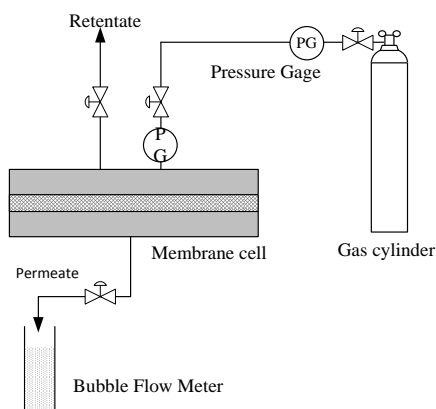
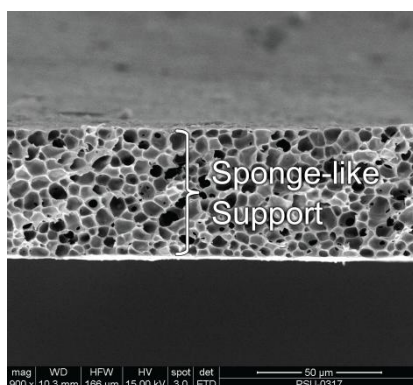


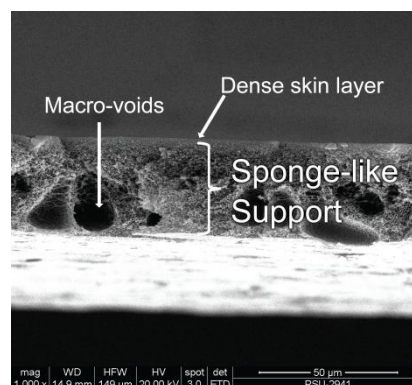
FIGURE 1. Schematic view of the experimental setup.

## Results and Discussion

The formation of dense skin layer was investigated by SEM and shown in figure 2. Acetone is a more volatile solvent. It can rapidly evaporate from the outermost surface of the membrane during polymer casting, which results in higher polymer concentration in the upper layer of the membrane lead to delayed liquid–liquid demixing and as a result, a dense skin layer with less defects and pin-holes was prepared [18]. The asymmetric membranes were prepared. And the dense skin layer increased and the macro-voids of sponge-like support decreased with increasing the polymer concentration, and it is consistent with the results of Madaeni and Moradi.[19]



(a)



(b)

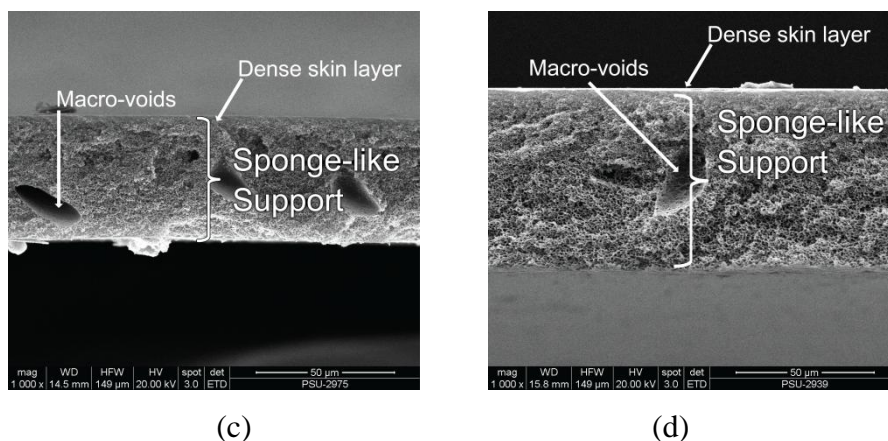
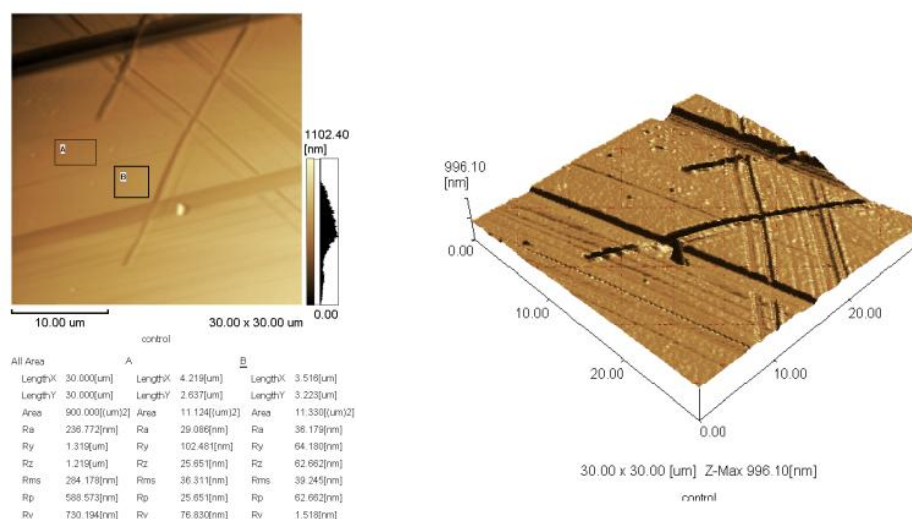
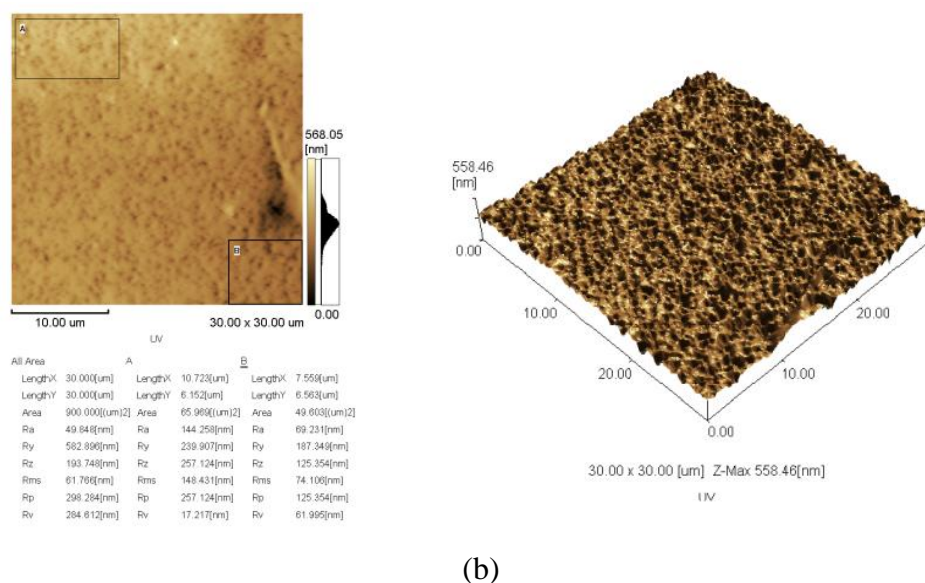


FIGURE 2. SEM micrographs of PSF membranes prepared without and with acetone (a) 20% PSF (without acetone), (b) 19% PSF, (c) 22% PSF and (d) 25% PSF

The AFM scanning found the membrane surface roughness increased significantly after the UV irradiation compared with the control, as shown in figure 3. AFM images obtained suggest that chains scission and crosslink have occurred simultaneously in the irradiated membranes by UV radiation. [20]



(a)



(b)

FIGURE 3. AFM images of (a) untreated (control) and (b) 12-hrs UV-treated membranes (22% PSF).

The water contact angles on the untreated and the treated membranes by UV irradiation are shown in Table. 2. For the untreated membranes, they were  $71^{\circ}$ - $76^{\circ}$ . After 6 h of UV irradiation, they were reduced to  $14^{\circ}$ - $18^{\circ}$  and stabilized at  $10^{\circ}$ - $11^{\circ}$  after 12-h irradiation. Apparently, these membranes possess similar contact angles regardless of the polymer content. This result indicates that hydrophilicity of the PSF membranes was increased by UV irradiation.

TABLE 2. Water contact angle of PSF membranes against irradiation time. Data was averaged from 3 experiments.

Irradiation time(h)	Water contact angle (degree)		
	19% PSF	22% PSF	25% PSF
0	76.5±0.2	72.1±1.8	71.4±3.4
3	40.4±2.0	38.9±0.1	36.5±2.7
6	15.9±0.5	18.8±1.3	14.8±0.4
12	11.5±0.5	11.9±0.8	10.4±1.0

In addition, the hydrophobic recovery was observed after the irradiated membranes were left in storage for several periods of time. This is indicated by changes in the contact angle with time as shown in figure 4. The hydrophobic recovery of the 3-h treated membranes occurred rapidly within one week after

treatment ending. The contact angle increased from 30° to 70°, fairly equal to that of the untreated membranes. It is interesting to point out that for the 6h and 12h UV irradiation, the contact angle gradually increased from 25° to 35° and from 15° to 25°, respectively and this took place for 4 weeks. This result indicated that the membrane hydrophilicity could not be achieved for a short irradiation period of time. Moreover, it was noted that the irradiated membranes of greater polymer content exhibited smaller contact angles in all cases, and the hydrophobic recovery seemed to be inhibited.

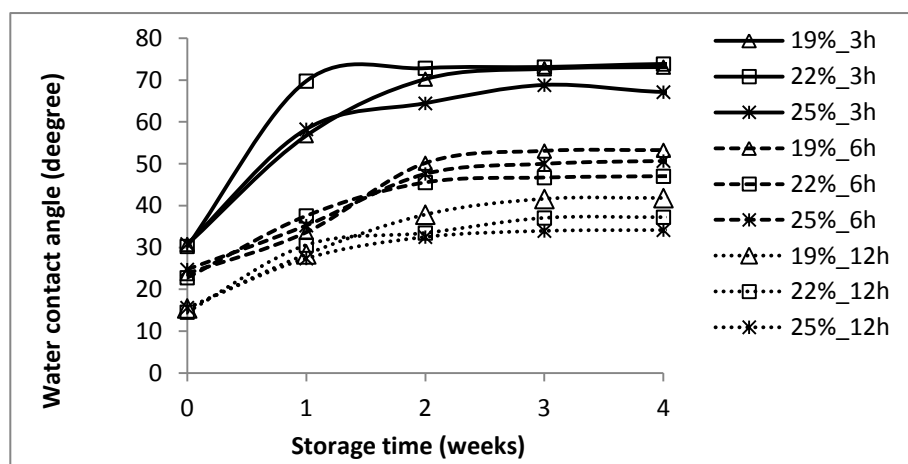


FIGURE 4. The changes in water contact angles on the UV treated membranes against storage time.

The FTIR spectra of the UV-treated membranes compared to the control are shown in figure 5 which though describes functional groups of only the greatest PSF containing membrane, since all membranes showed similar spectral peaks. The PSF consists of a backbone made up of diaryl sulfone (Ar-SO<sub>2</sub>-Ar) and diaryl ether (Ar-O-Ar) groups which show strong bands at 1150 and 1241 cm<sup>-1</sup>, respectively. The bands at 1487 and 1585 cm<sup>-1</sup> belong to the vibration of the aromatic (C=C) in the PSF molecule [17]. There are two new peaks appearing round 3300 and 1746 cm<sup>-1</sup> which should belong to the stretching vibration of hydroxyl (-OH) and carbonyl (C=O) groups, respectively. Since they are polar functional groups [11], this indicates that polar functional groups were introduced to the PSF membrane by UV ray irradiation, leading to increasing of hydrophilicity. This is confirmed by contact angle

measurements and consistent with the result of Kim et al.,[11] who modified the surface of PSF membrane by oxygen plasma treatment.

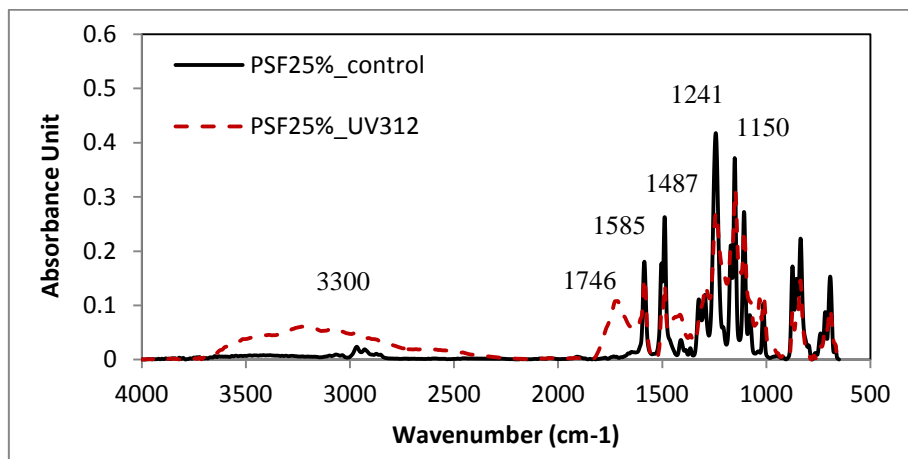
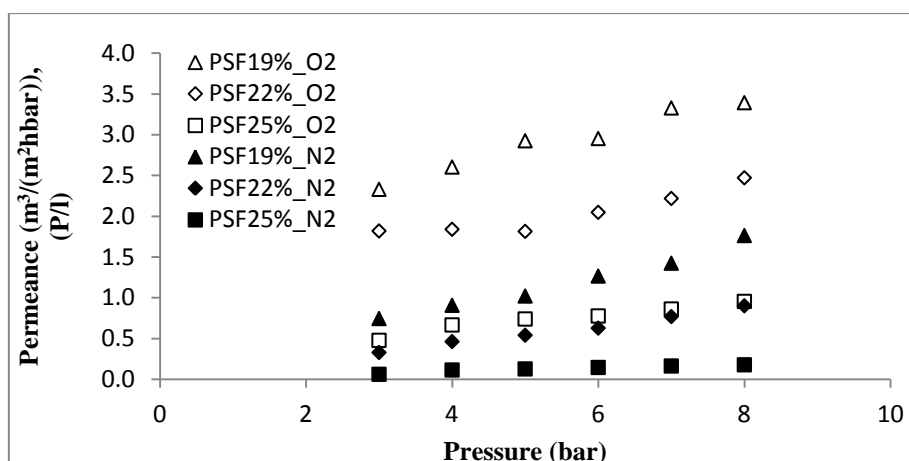
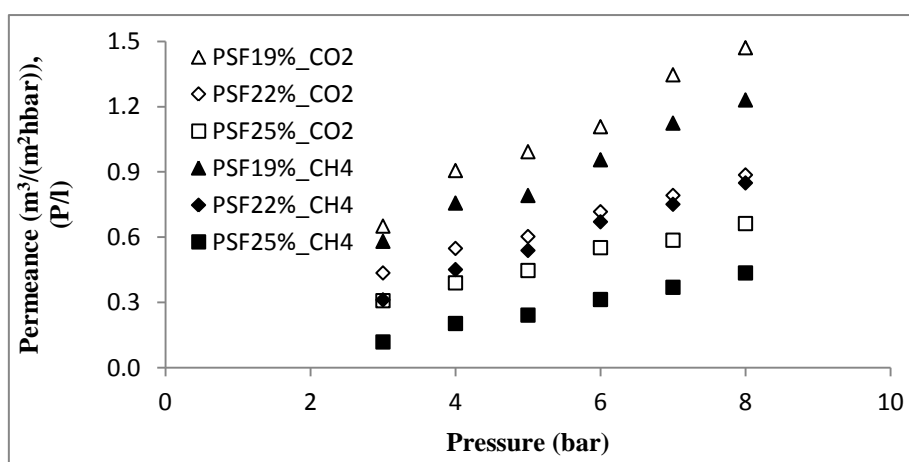


FIGURE 5. Comparison of FTIR spectra of the untreated and treated membrane by UV ray.

The permeance of four gases through the PSF membrane of different polymer concentration was investigated using equation (1), and the results are illustrated in figure 6. It can be seen that the permeance of all gases ( $O_2$ ,  $N_2$ ,  $CO_2$  and  $CH_4$ ) increased with the increase of pressure and decreased with the increase of polymer concentration from 19% to 25% due to the increased in the dense skin layer and membrane thickness resistance against gas diffusion. However,  $O_2$  and  $CO_2$  permeance was greater compared respectively to  $N_2$  and  $CH_4$ , respectively due to  $O_2$  and  $CO_2$  molecules are smaller than  $N_2$  and  $CH_4$  molecule, respectively. The molecular size of gas is considered from kinetic diameters which shown in Table 3.



(a)



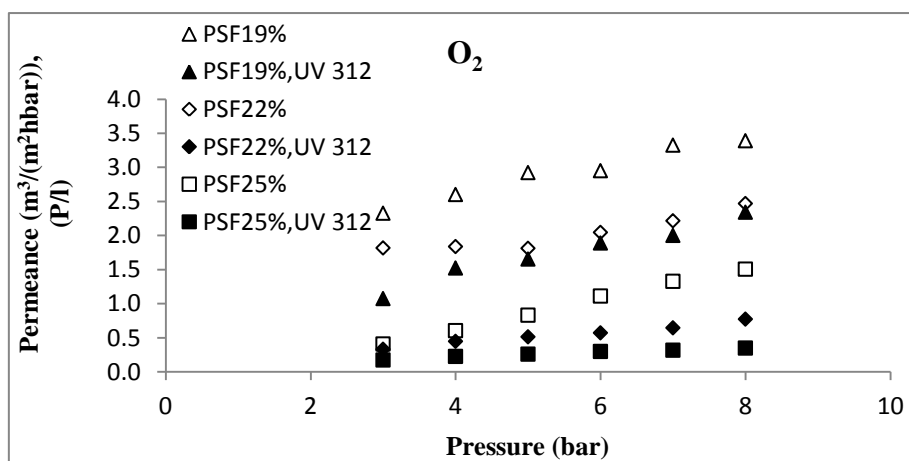
(b)

FIGURE 6. Permeation of O<sub>2</sub> and N<sub>2</sub> (a) and CO<sub>2</sub> and CH<sub>4</sub> (b) through several untreated PSF membranes

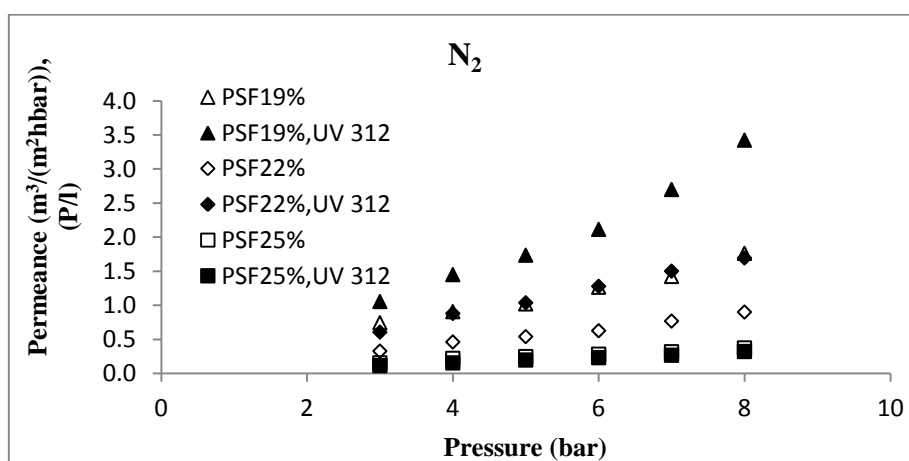
TABLE 3. Comparison of structural, physical, and electronic parameters of gas molecules.

Molecule	Kinetic Diameter (°A) [6]	Structure[21]	Quadrupole moment [10 <sup>-40</sup> Cm <sup>2</sup> ] [21]	Polarizability [10 <sup>-40</sup> J <sup>-1</sup> C <sup>2</sup> m <sup>2</sup> ]
O <sub>2</sub>	3.46	linear	1.3	1.57 [22]
N <sub>2</sub>	3.64	linear	4.7	1.97[21]
CO <sub>2</sub>	3.30	linear	13.4	2.93[21]
CH <sub>4</sub>	3.80	tetrahedral	0	2.89[21]

The effect of UV irradiation on gas permeation through membranes is shown in figure 7. From contact angle result, the 12 h UV treated was the optimum condition. So The 12 h UV treated membranes was selected for this study. The result showed that O<sub>2</sub> permeation was decreased while permeation of N<sub>2</sub>, CO<sub>2</sub> and CH<sub>4</sub> was increased after UV irradiation. It may be due to gas molecules permeate through the membrane by quadrupole–dipole interactions between the gas molecules and polar segments of membrane.[1] UV irradiation improved hydrophilicity and polar group of membrane which confirmed by contact angle (Table 2) and FTIR analysis.

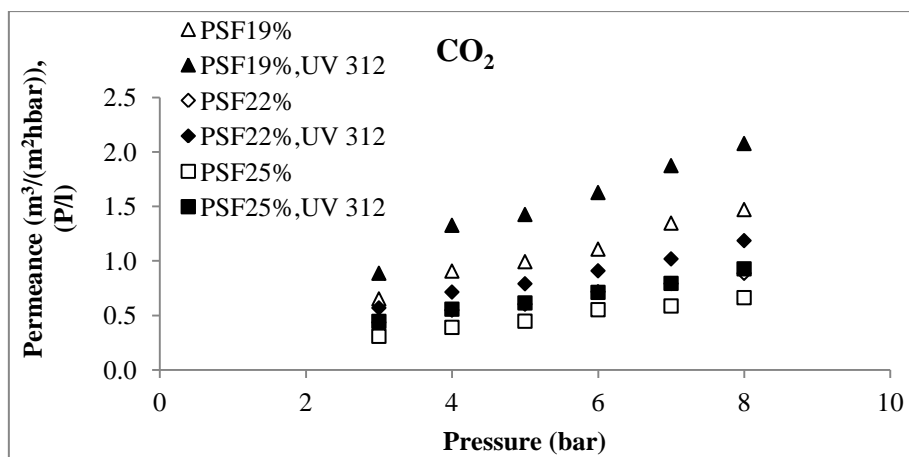


(a)

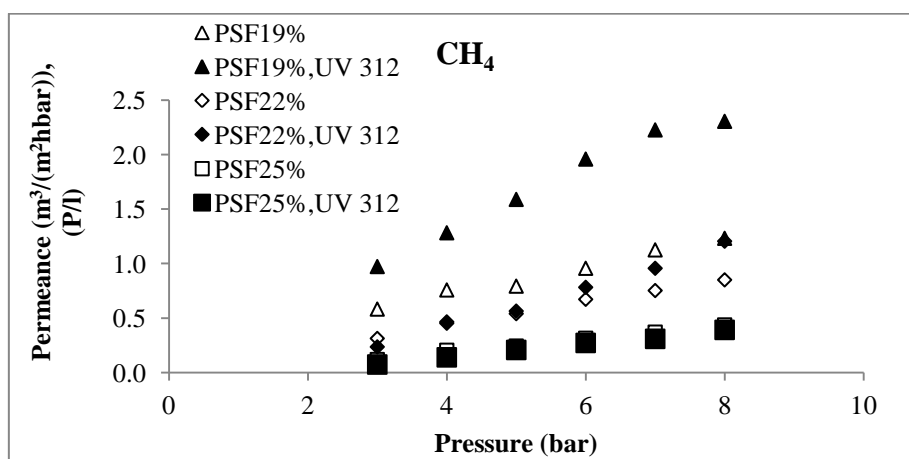


(b)





(c)

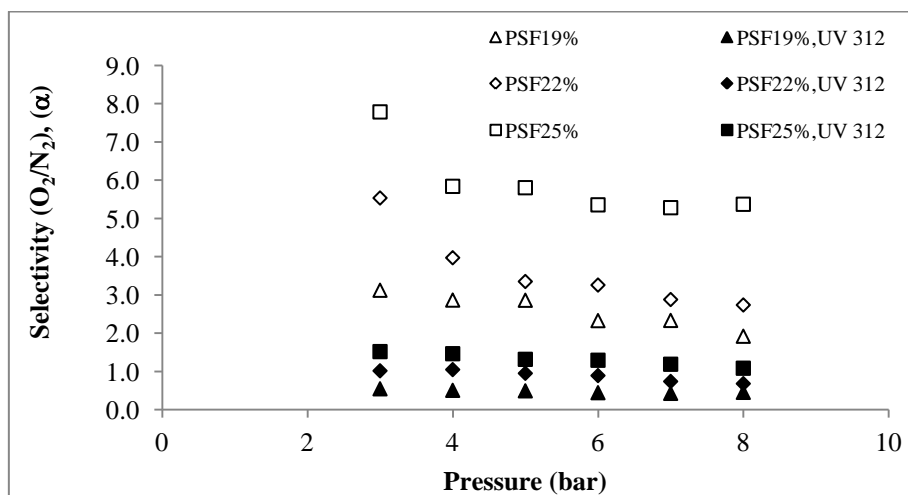


(d)

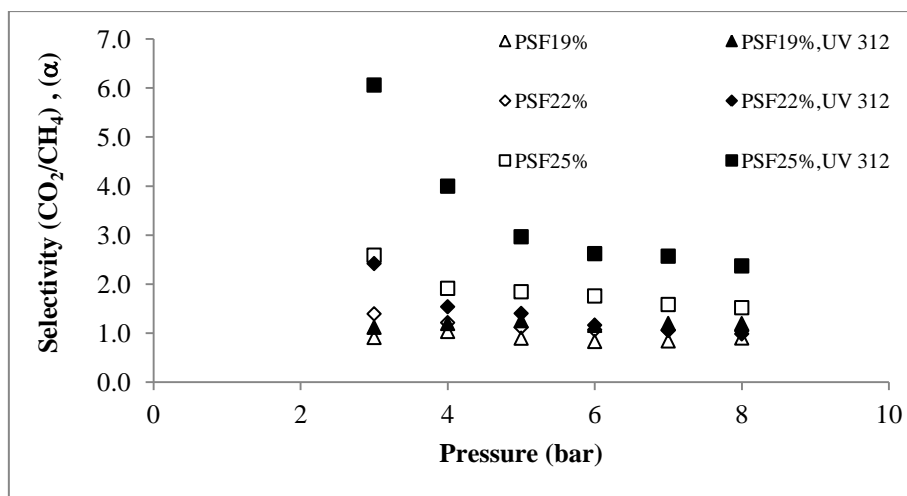
FIGURE 7. Comparison of O<sub>2</sub> (a), N<sub>2</sub> (b), CO<sub>2</sub> (c), and CH<sub>4</sub> (d) permeation through the untreated and treated membrane by UV ray.

Therefore, the highly polar groups in the treated membranes should be more attractive to CO<sub>2</sub>, N<sub>2</sub>, and CH<sub>4</sub> because the CO<sub>2</sub> molecule has high quadrupole moment (see Table 3) with a high polarizability while the N<sub>2</sub> and CH<sub>4</sub> have high polarizability leads to more permeance. However, the O<sub>2</sub> has low quadrupole moment and polarizability lead to a repellent from polar membrane and hence smaller gas permeation was evidenced. This permeation affects O<sub>2</sub>/N<sub>2</sub> and CO<sub>2</sub>/CH<sub>4</sub> selectivity of membranes because selectivity is a proportion of 2 gas permeation. Therefore, O<sub>2</sub> permeance divide by N<sub>2</sub> permeance following equation (2) and using data from figure 7 (a-b) become O<sub>2</sub>/N<sub>2</sub> selectivity which shown in figure 8 (a). In the same way,

$\text{CO}_2/\text{CH}_4$  selectivity which shown in figure 8 (b) was calculated by this method using data from figure 7 (c-d). The result shown that  $\text{O}_2/\text{N}_2$  selectivity decreases while  $\text{CO}_2/\text{CH}_4$  selectivity increases after UV irradiation. The permeance of  $\text{O}_2$  through the treated membranes decreases, while that of  $\text{N}_2$  increased lead to a decreasing in  $\text{O}_2/\text{N}_2$  selectivity. In the case of  $\text{CO}_2$  and  $\text{CH}_4$ , both permeances increase after UV irradiation but  $\text{CO}_2$  permeance was greater due to the greater quadrupole moment (table 3). It should be also pointed out that the selectivity decreased with increased pressure and increased when the polymer concentration increased from 19 to 25%. Due to the formation of a dense skin layer in higher polymer content membranes with less macro-voids (in figure 2) lowered diffusion of gas molecules through the membrane.



(a)



(b)

FIGURE 8. Selectivity of the untreated and treated membrane by UV ray for O<sub>2</sub>/N<sub>2</sub> (a) and CO<sub>2</sub>/CH<sub>4</sub> (b).

To confirm polar segments of the membrane, the surface properties of polysulfone membranes were examined by contact angle measurement (Dataphysics, OCA 15 EC). With the contact angles of formamide and ethylene glycol, the surface energy, polar component and dispersive component of polysulfone membrane was calculated from SCA20 software. The results were shown in Table 4. The surface free energy increased mainly due to the increase of polar component and dispersive component decreased after UV irradiation. This result was consistent with surface modification of PSF membrane by oxygen plasma treatment of Kim et. al., [11]. This indicates UV affected the polar component which affect to gas permeation of PSF membranes.

TABLE 4. Surface free energy of the untreated and treated PSF membrane.

Sa mpl e	Untreated membranes			Treated membranes		
	Surface energy	Dispersive component	Polar component	Surface energy	Dispersive component	Polar component
19%	34.91	30.20	4.21	83.58	0.83	82.76
22%	31.35	18.08	13.27	84.92	0.79	84.14
25%	36.48	31.37	5.11	84.06	0.94	83.12

## CONCLUSIONS

This study found that the UV ray of 312 nm wavelength, 360  $\mu\text{w}/\text{cm}^2$  powers affected the polar component which affect to gas permeation of PSF membranes. The UV irradiation decreased  $\text{O}_2/\text{N}_2$  selectivity but increased  $\text{CO}_2/\text{CH}_4$  selectivity of the membranes. Hence, separation of  $\text{CO}_2$  from  $\text{CH}_4$  could be improved only if permanent hydrophilicity of the treated membranes was achieved and could be improved further by increasing polymer content of the membrane.

## ACKNOWLEDGEMENTS

This work was supported by the Higher Education Research Promotion and National Research University Project of Thailand, Office of the Higher Education Commission and the Thailand Center of Excellence in Physics, Physics Department Faculty of Science Prince of Songkla University, and Chiang Mai University.

## REFERENCES AND NOTES

- [1] R. Xing, W.S. W. Ho, J. Taiwan. Inst. Chem. E., 40 (2009) 654-662.
- [2] H. Yang, Z. Xu, M. Fan, R. Gupta<sup>1</sup>, R.B. Slimane, A.E. Bland, I. Wright<sup>5</sup>, J. Environ. Sci., 20 (2008) 14-27.
- [3] P. Li, H. Z. Chen, T.S. Chung, J.Membr. Sci., 434 (2013) 18-25.
- [4] P. Li, F.H. Tezel, Micropor. Mesopor. Mater., (2007) 94-101.
- [5] Y. S. Bae, O.K. Farha, J.T. Hupp, R.Q. Snurr, J. Mater. Chem., 19 (2009) 2131-2134.
- [6] C.A. Scholes, S.E. Kentish, G.W. Stevens, Recent Pat. Chem. Eng., 1 (2008) 52-66.
- [7] Y. Zhang, J. Sunarso, Shaomin Liu, R. Wang, Int. J. Greenh. Gas. Con., 12 (2013) 84-107.
- [8] R. Abedini, A. Nezhadmoghadam, Pet. Coal., 52 (2010) 269-280.
- [9] S. H. Chen, W. H. Chuang, A. A. Wang, R.C. Ruaan, J.Y. Lai, J.Membr. Sci., 124 (1997) 273-281.
- [10] D. M. D'Alessandro, B.Smit, J.R. Long, Angew. Chem. Int. Ed. , 49 (2010) 6058 - 6082.
- [11] K.S. Kim, K.H. Lee, K. Cho, C.E. Park, J.Membr. Sci. , 199 (2002) 135-145.

- [12] B. Jaleha, P. Parvin, P. Wanichapichart, A. Pourakbar Saffar, A. Reyhani, *Appl. Surf. Sci.*, 257 (2010) 1655-1659.
- [13] H. Hillborg, J.F. Ankner, U.W. Gedde, G.D. Smith, H.K. Yasuda, K. Wikstrom, *Polymer.*, 41 (2000) 6851-6863.
- [14] M. Nystrom, P. Jarvinen, *J.Membr. Sci.* , 60 (1991) 275-296.
- [15] K.K. Hsu, S. Nataraj, R.M. Thorogood, P.S. Puri, *J.Membr. Sci.*, 79 (1993) 1-10.
- [16] M. Zhang, Q. T. Nguyen, Z. Ping, *J.Membr. Sci.*, 327 (2009) 78-86.
- [17] A.F. Ismail, B.C. Ng, W.A.W. Abdul Rahman, *Sep. Purif. Technol.*, 33, (2003) 255-272.
- [18] M.A. Aroon, A.F. Ismail, M.M. Montazer-Rahmati, T. Matsuura, *Sep. Purif. Technol.*, 72 (2010) 194-202.
- [19] S.S. Madaeni, P. Moradi, *J.Poly Sc.*, 121 (2011) 2157-2167.
- [20] N.N. Rupiasih, *OJOPM.*, 3 (2013) 12-18.
- [21] Y. S. Bae, C.H. Lee, *Carbon.*, 43 (2005) 95-107.
- [22] S. Nir, S. Adams, R. Rein, *J. of chemical physics*, 59 (1997) 3341-3355.

## Proceeding 1

S. Konruang, S. Sirijarukul, W. Taweepreeda and T. Chittrakarn. Preparation of polysulfone nanofiltration membranes using dry/wet phase-inversion process. Membrane Science and Technology 2011 (MST 2011), 24 - 26 August 2011, Nanyang Technological University (NTU), Singapore.



**Preparation of polysulfone nanofiltration membranes using the dry/wet phase-inversion process**S. Konruang<sup>a,\*</sup>, S. Sirijarakul<sup>a</sup>, W. Taweepreeda<sup>b</sup> and T. Chitrakarn<sup>a</sup><sup>a</sup>*Department of Physics, Prince of Songkla University, Songkhla, Thailand*<sup>b</sup>*Polymer Science Programme, Prince of Songkla University, Songkhla, Thailand*\*: [5210230008@email.psu.ac.th](mailto:5210230008@email.psu.ac.th)

Polysulfone nanofiltration membranes were prepared using the dry/wet phase-inversion process with the same coagulation bath. The 20% of polysulfone (PSF) in five different compositions of solutions (i.e. DMF:DMAc / 80:0, 60:20, 40:40 20:60 and 0: 80 wt. %) were cast on a glass plate. PSF nanofiltration membranes were characterized by both contact angle device and scanning electron microscope (SEM). The water flux measurement was conducted successively under a pressure from 100 kPa to 500 kPa with a feed temperature of 25 °C. The results suggest that the PSF nanofiltration membranes in PSF:DMF:DMAc solution with the respective amounts of 20 wt.%, 40 wt.% and 40 wt.%, has the highest water contact angle of 94 degree and the lowest water flux of 0.10 L/m<sup>2</sup>h and 0.29 L/m<sup>2</sup>h at 100 kPa and 500 kPa, respectively. These results were consistent with the SEM micrographs that showed the lowest pores surface density.

Keywords: Polysulfone, water contact angle, water flux

## Proceeding 2

S. Konruang, S. Sirijarukul, T. Chitrakarn and W. Taweepreda. Hydrophilicity modification of polysulfone membrane by UV ray treatment. Siam Physics Congress 2012 (SPC2012), 9-12 May 2012, Phra Nakhon Si Ayutthata, Thailand.







## Hydrophilicity Modification of Polysulfone Membrane by Ultraviolet Ray Treatment

S. Konruang<sup>1\*</sup>, S. Sirijarukul<sup>1</sup>, T. Chitrakarn<sup>1</sup> and W. Taweepreeda<sup>2</sup>

<sup>1</sup>Department of Physics, Prince of Songkla University, Songkhla, Thailand

<sup>2</sup>Polymer Science Programme, Prince of Songkla University, Songkhla, Thailand

\*Corresponding author. E-mail: 5210230008@email.psu.ac.th

### Abstract

The effects of Ultraviolet (UV) ray on hydrophilicity of polysulfone membranes have been studied. Polysulfone (PSF) membranes were prepared using the phase-inversion process with the same coagulation bath. The solutions consisting of 19% - 25% of PSF, dimethylacetamide (DMF) and acetone (Ac) were cast on a glass plate. To improve surface hydrophilicity, the prepared PSF membranes were treated by UV ray. The UV ray source with 254 nm wavelength and power 2mW/cm<sup>2</sup> was used for treated membranes. Dried PSF membranes in the form of squares were irradiated by UV ray in air at room temperature for 3-12 hr. The hydrophilicity of untreated and treated membranes was characterized by contact angle device. The membrane surface was determined by scanning electron microscope (SEM). The filtration performance of untreated and treated membranes was examined in a dead-end cell, using distilled water. The water flux measurement was conducted successively under a pressure from 500 kPa to 2,000 kPa with a feed temperature of 25 °C. The surfaces of the modified membranes were chemically characterized using Fourier Transform Infrared Spectrometer (FTIR). The results show that the water contact angle decreased with increasing irradiation time. After 12 hr of treatment, the water contact angle reduced from 71°–76° to about 50°–60°, while the water flux of the treated membranes increased. Results of contact angle measurements and filtration tests indicated that UV ray was effective for hydrophilicity improvement of the PSF membranes surface. The formations of new peaks corresponding to hydroxyl and carboxyl groups in FTIR spectra confirmed hydrophilicity improvement of membrane surface by UV ray treatment. Results of SEM scanning also showed changes in membrane surfaces after modification.

**Keywords:** UV Ray Treatment, Polysulfone Membranes, Hydrophilicity, Water Flux, Water Contact Angle

### Introduction

There are many methods to modify the membrane surface in order to increase water transport across these membranes, such as plasma treatment (Yu *et al.*, 2005, Gancarz *et al.*, 2002, Jaleh *et al.*, 2010), ion beam treatment (Ilconich *et al.*, 2003, Dworeckiet al., 2004, Chennamsetty *et al.*, 2006), gamma-rays irradiation and UV irradiation (Yu *et al.*, 2010, Vazquez *et al.*, 2005, Rahimpour *et al.*, 2008).

The plasma processes can improve polymer wettability, permeability, conductivity, adhesion or biocompatibility (Bryjaket *et al.*, 2002). However, it resulted in only transient hydrophilicity with contact angle changes within 24 h of plasma treatment (Steen *et al.*, 2001).

Ion beam irradiation can improve polymer properties such as surface hardness, resistance to mechanical wearing and chemical erosion, and conductivity with appropriate choice of irradiation conditions (Xu *et al.*, 2000). Gamma-rays irradiation can modify physical and chemical properties of polymers (Rupiasih and Vidyasagar, 2008). It has been reported that it can change electrochemical

characterization of cellophane membranes (Vazquez *et al.*, 2005). However, both methods are expensive and difficult to operation.

The effect of UV irradiation on microporous membrane has been reported that it increased flux and the hydrophilicity of the membranes (Nystrom and Jarvinen, 1991). Comparing with other surface modification techniques, UV irradiation has distinct advantages over other techniques due to its simplicity, inexpensive and widespread industrial applications (Zhang *et al.*, 2009). In this study the prepared PSF membranes were modified using UV irradiation. The modification results were tested by filtration experiments with different pressure. The hydrophilicities of the modifications were tested with contact angle measurements. Moreover, the UV ray irradiation effects were studied using SEM and FTIR.

### Materials and Methods

#### Materials

PSF (PSF :Udel 3500 LCD MB) was supplied by Sovay (China). N,N-dimethylacetamide (DMAc) and acetone (Ac) were used as solvents for PSF



membrane and supplied by Fluka Riedel-deHaën. Tap water was used as a coagulation medium during phase-inversion process.

#### Preparation of asymmetric flat sheet membranes

PSF membranes were prepared by the wet phase inversion technique. The polymer solution was cast on glass plate by film applicator from the PSF solution which consists of DMAc and Ac with different concentrations of polymer specified in Table 1. The membranes were immersed in the coagulation bath of distilled water for to remove the remaining solvent. The wet membranes were dried at room temperature.

**Table 1:** Casting solution composition and film casting condition.

Sample	PSF (wt.%)	DMAc (wt.%)	Ac (wt.%)
PSF19%	19	54	27
PSF22%	22	52	26
PSF25%	25	50	25

\*The ratio of DMAc and Ac was fixed at 2:1 (wt/wt)

#### Ultraviolet Ray Treatment

The UV ray source (VI-215.MC) with 254 nm wavelength and power 2mw/cm<sup>2</sup> was used for treated membranes. Dried PSF membranes were irradiated by UV ray in air at room temperature for 3-12 hr.

#### Membrane Characterizations

##### Water contact angles

Water contact angles of the untreated and the treated membranes were measured by a contact angle device (Dataphysics, COCA15ED). The measurement was carried out immediately after the UV ray treatment.

##### Water flux

The water flux of untreated and treated membranes was characterized by dead-end filtration method. Water flux measurement was made by placing a membrane in the dead-end filtration unit, using applied pressures between 0.5 and 2.5 MPa. The water flux  $J$  (L/m<sup>2</sup>hr) was calculated using equation below (Bhongsuwan, 2002)

$$J = \frac{\text{volume of permeate (L)}}{\text{membrane area (m}^2\text{)} \times \text{time (hr)}} \quad (1)$$

##### Scanning electron microscopy (SEM)

The morphologies of the untreated and the treated membrane were determined by a SEM technique. For cross-sections analysis, the samples were frozen in liquid nitrogen and fractured before scanning on a SEM (FEI, Quanta 400) with potentials of 20 kV under magnifications ranging from 1,000x to 50,000x.

Fourier Transform Infrared Spectrometer (FTIR)

FTIR (Bruker, EQUINOX 55) was used to investigate changes in functional groups of the membranes. The membrane was scanned at 400–4000 cm<sup>-1</sup> wave numbers.

## Results and Discussion

### Water contact angle

The water contact angles of the untreated and the treated membranes were shown in Figure 1. The water contact angles of untreated membranes were 71–76°. After irradiated by UV ray irradiation, the water contact angles of treated membranes reduced from 71°–76° to about 55°, after 12 hr of treatment. The results indicate prepared membranes increase in hydrophilicity after the UV ray treatment.

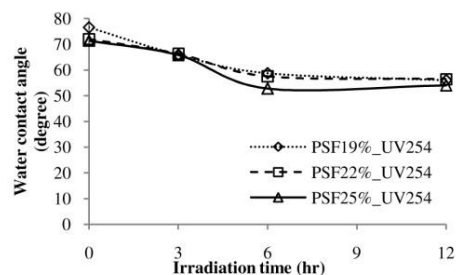


**Figure 1.** The water contact angles of treated membranes with the UV ray treatment for 0 – 12 hr.

### Water Flux

The water fluxes of the untreated and the treated membranes prepared by different polymer concentration were shown in Figure 2. The membranes prepared by 19%–25% of PSF were irradiated by UV ray for 12 hr before tested. The results show the water fluxes of treated membranes higher than untreated membranes in all conditions. This result confirms that the hydrophilicity of membranes increased after the UV ray treatment.

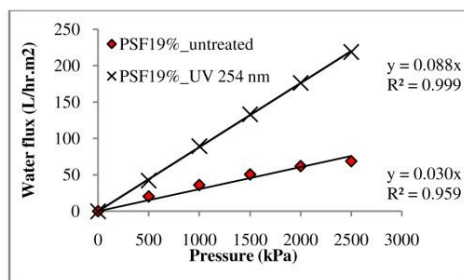
In addition, the water flux decreased with the increasing polymer concentration.

### Scanning Electron Microscopy (SEM)

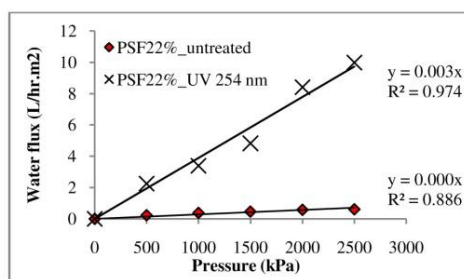
The SEM of the cross-sectional of the membrane was studied by SEM. The results show the thick skin layer increased with the increasing of polymer concentration. Furthermore, the macro-voids of sponge-like support reduced at the higher polymer concentration (Figure 3). The thicknesses of skin layer were 1.74, 1.93, and 2.73 μm for polymer concentrations of 19%, 22%, and 25%, respectively. This is consistent with the water flux in which the thicker the skin layer, the lower water flux was obtained under the same pressure.

The surface structures of the untreated and the treated membranes by UV ray for 12 hr were shown in Figure 4. It was observed that the surface structure of the treated membranes changed as compared to

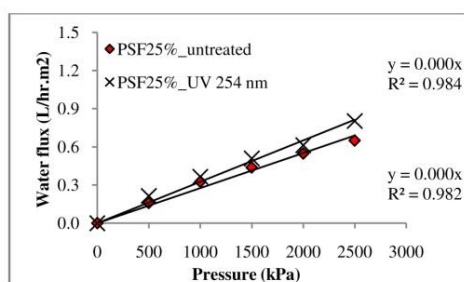
the untreated membranes. The treated membranes show more roughness. It is accepted that the increasing hydrophilicity of membranes was due to the surface roughness, which enhanced water absorption (Wanichapichart, 2009). This is consistent with the water contact angle and the water flux.



(a) PSF 19%

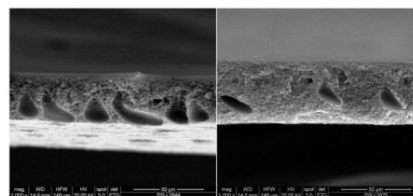


(b) PSF 22%

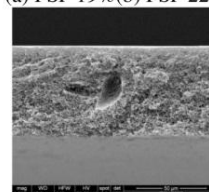


(c) PSF 25%

**Figure 2.** The water flux of untreated and treated membranes by UV ray for 12 hr with different concentration of polymer.

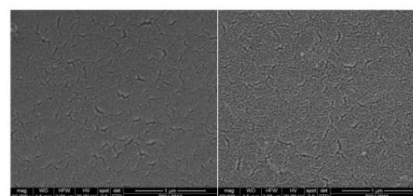


(a) PSF 19% (b) PSF 22%



(c) PSF 25%

**Figure 3.** SEM micrographs of the membranes prepared by different polymer concentrations.



(a) untreated membranes (b) UV treated membranes  
**Figure 4.** Comparison of SEM micrographs of untreated and treated membranes by UV ray for 12 hr.

#### Fourier Transform Infrared Spectrometer (FTIR)

The FT-IR spectra of untreated and treated membranes were shown in Figure 5. Based on the spectral change, there is no difference in each PSF concentration. The result showed that the new broad peaks arose around 3300  $\text{cm}^{-1}$  and near 1746  $\text{cm}^{-1}$ . The PSF consists of a backbone made up of diarylsulfone (Ar-SO<sub>2</sub>-Ar), diaryl ether (Ar-O-Ar) groups showed strong bands at 1150 and 1241  $\text{cm}^{-1}$ , respectively. (Ismail *et al.*, 2003). The peaks appeared around 3300 and 1746  $\text{cm}^{-1}$  are ascribed to the stretching vibration of hydroxyl (-OH) group and carbonyl (C=O) group, respectively. The appearance of these peaks by UV ray treatment indicates that the carbons in methyl group and in benzene ring of PSF were attacked and oxidized by UV ray to form carbonyl (C=O) group and hydroxyl (-OH) group (Choi *et al.*, 2003). This indicated the higher number of water molecules surrounding the membrane (Wanichapichart *et al.*, 2010), resulting in the increasing of the hydrophilic property of the membrane.

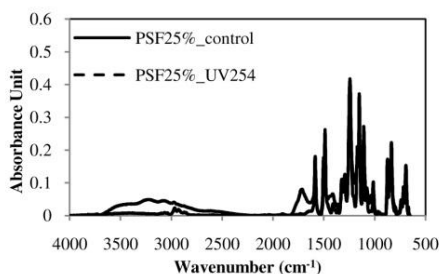


**Figure 5.** Comparison of FTIR spectra of untreated and treated membrane by UV ray for 12 hr.

### Conclusions

The surface of PSF membrane was modified by the UV ray irradiation. The results show that the water contact angle decreased with the increasing of UV ray irradiation time and the water flux increased after UV ray irradiation. From SEM micrographs, the treated membranes show more roughness surface after UV ray irradiation. This is due to the membrane surface hydrophilicity increasing since the hydrophilic functional groups were introduced on the surface of hydrophobic PSF membrane by UV ray treatment. These were confirmed by FT-IR spectrometer. However, the water flux decreased as polymer concentration increased. The SEM micrographs show the thick skin layer increased and the macro-voids of sponge-like support decreased at the higher polymer concentration. This results in lower diffusion of water molecules through the membrane.

### Acknowledgments

We would like to thank the National Research University Project of Thailand's Office of the Higher Education Commission and Graduate School of Prince of Songkla University for financial support. We thank Thailand Center of Excellence in Physics, Membrane Science and Technology Research Center and Department of Physics, Faculty of Science, Prince of Songkla University for permission to using scientific and workshop equipment.

### References

1. D. S. Wavhal, and E. R. Fisher, "Modification of polysulfone ultrafiltration membranes by CO<sub>2</sub> plasma treatment", *Desalination* **172** (2005) 189.
2. M. Bryjak, I. Gancarz, G. Pozniak and W. Tylus, "Modification of polysulfone membranes 4. Ammonia plasma treatment", *European Polymer Journal*. **38** (2002) 717.
3. M. L. Steen, L. Hymas, E. D. Havey, N.E. Capps, D. G. Castner, and E. R. Fisher, "Low temperature plasma treatment of asymmetric polysulfone membranes for permanent hydrophilic surface modification", *J. Membr. Sci.* **188** (2001)97.
4. M. Nystrom, and P. Jarvinen, "Modification of polysulfone ultrafiltration membranes with UV irradiation and hydrophilicity increasing agents", *J. Membr. Sci.* **60** (1991) 275.
5. H. Y. Yu, Y. J. Xie, M. X. Hu, J. L. Wang, S. Y. Wang, and Z. K. Xu, "Surface modification of polypropylene microporous membrane to improve its antifouling property in MBR: CO<sub>2</sub> plasma treatment", *J. Membr. Sci.* **254** (2005) 219.
6. I. Gancarz, G. Pozniak, M. Bryjak, and W. Tylus, "Modification of polysulfone membranes 5. Effect of n-butylamine and allylamine plasma", *European Polymer Journal* **38** (2002)1937.
7. B. Jaleh, P. Parvin, P. Wanichapichart, A. PourakbarSaffar, and A. Reyhani, "Induced super hydrophilicity due to surface modification of polypropylene membrane treated by O<sub>2</sub> plasma", *Applied Surface Science* **257** (2010) 1655.
8. J. B. Ilconich, X. Xu, M. Coleman, and P.J. Simpson, "Impact of ion beam irradiation on microstructure and gas permeance of polysulfone asymmetric membranes", *J. Membr. Sci.* **214** (2003) 143.
9. K. Dworecki, M. Drabik, T. Hasegawa, and S. Wasik, "Modification of polymer membranes by ion implantation", *Nuclear Instrumenta and Methods in physics Research* **B225** (2004)483.
10. R. Chennamsetty, I. Escobar, and X. Xu, "Characterization of commercial water treatment membranes modified via ion beam irradiation", *Desalination* **188** (2006)203.
11. H. Y. Yu, J. Zhou, J. S. Gu, and S. Yang, "Manipulating membrane permeability and protein rejection of UV-modified polypropylene macroporous membrane", *Membr. Sci.* **364** (2010)203.
12. A. Rahimpour, S.S. Madaeni, A.H. Taheri, and Y. Mansourpanah, "Coupling TiO<sub>2</sub> nanoparticles with UV irradiation for modification of polyethersulfone ultrafiltration membranes", *J. Membr. Sci.* **313** (2008)158.
13. G. Xu, Y. Hibino, Y. Suzuki, Y. Suzuki, K. Kurotobi, M. Osada, M. Iwaki, M. Kaibara, M. Tanihara, and Y. Imanishi, "Oxygen ion implantation at 20 to 2000 keV into polysulfone for improvement of endothelial cell adhesion", *Colloids Surf. B: Biointerfaces*. **19** (2000)237.
14. N. N. Rupiasih, and P.B. Vidyasagar, "Comparative study of effect of low and medium dose rate of g irradiation on microporous polysulfone membrane using spectroscopic and imaging techniques", *Polymer Degradation and Stability* **93** (2008) 1300.
15. M. Zhang, Q. T. Nguyen, and Z. Ping, "Hydrophilic modification of poly(vinylidene fluoride) microporous membrane", *J. Membr. Sci.* **327** (2009) 78.



Siam Physics Congress SPC2012  
*Past, Present and Future of Physics* 9-12 May 2012

16. D. Bhongsuwan<sup>1</sup>, T. Bhongsuwan, and J. N. Suwan, "Construction of a dead-end type micro to R.O. membrane test cell and performance test with the laboratory made and commercial membranes", *Songklanakarin J. Sci. Technol.* **24** (2002)999.
17. S. H. Choi, M. K. Lee, S. J. Oha, and J. K. Koo, "Gas sorption and transport of ozone-treated polysulfone", *J. Membr. Sci.* **221** (2003) 37.
18. A.F. Ismail, B.C. Ng, and W.A.W. Abdul Rahman, "Effects of shear rate and forced convection residence time on asymmetric polysulfone membranes structure and gas separation performance", *Sep. Purif. Technol.* **33** (2003), 255.

## VITAE

**Name** Miss Sutthisa Konruang

**Student ID** 5210230008

### **Educational Attainment**

Degree	Name of Institution	Year of Graduation
Bachelor of Science (Physics)	Thaksin University	2005
Master of Science (Physics)	Prince of Songkla University	2009

### **Scholarship Awards during Enrolment**

The Higher Education Research Promotion and National Research University Project of Thailand.

### **List of Publication and Proceedings**

Sutthisa Konruang, Thawat Chittrakarn, Suksawat Sirijarukul “Surface modification of asymmetric polysulfone membrane by UV irradiation”. *Jurnal Teknologi (Sciences & Engineering)* 70:2 (2014) 55–60.

S. Konruang, S. Sirijarukul, W. Taweepreeda and T. Chittrakarn. Preparation of polysulfone nanofiltration membranes using dry/wet phase-inversion process. *Membrane Science and Technology 2011 (MST 2011)*, 24 - 26 August 2011, Nanyang Technological University (NTU), Singapore.

S. Konruang, S. Sirijarukul, T. Chittrakarn and W. Taweepreeda. Hydrophilicity modification of polysulfone membrane by UV ray treatment. *Siam Physics Congress 2012 (SPC2012)*, 9-12 May 2012, Phra Nakhon Si Ayutthata, Thailand.